THE CHEMICAL SPECIATION OF CHROMIUM IN SEAWATER BY CATHODIC STRIPPING VOLTAMMETRY

RAVINDLALL RAMJUTTUN

INFORMATION TO USERS

This manuscript has been reproduced from the microfilm master. UMI films the text directly from the original or copy submitted. Thus, some thesis and dissertation copies are in typewriter face, while others may be from any type of computer printer.

The quality of this reproduction is dependent upon the quality of the copy submitted. Broken or indistinct print, colored or poor quality illustrations and photographs, print bleedthrough, substandard margins, and improper alignment can adversely affect reproduction.

In the unlikely event that the author did not send UMI a complete manuscript and there are missing pages, these will be noted. Also, if unauthorized copyright material had to be removed, a note will indicate the deletion.

Oversize materials (e.g., maps, drawings, charts) are reproduced by sectioning the original, beginning at the upper left-hand corner and continuing from left to right in equal sections with small overlaps.

Photographs included in the original manuscript have been reproduced xerographically in this copy. Higher quality 6" x 9" black and white photographic prints are available for any photographs or illustrations appearing in this copy for an additional charge. Contact UMI directly to order.

Bell & Howell Information and Learning
300 North Zeeb Road, Ann Arbor, MI 48106-1346 USA
800-521-0600

UMI®

THE CHEMICAL SPECIATION OF CHROMIUM IN SEAWATER BY CATHODIC STRIPPING VOLTAMMETRY

Ravindlall Ramjuttun

A thesis submitted to the School of Graduate Studies
in partial fulfilment of the requirements for the degree of
Doctor of Philosophy

Department of Chemistry
Memorial University of Newfoundland

December 1997

St John's
Newfoundland

To my mother .....

ABSTRACT

Chromium has an interesting ecotoxic role in aquatic environments, where it occurs in two different oxidation states, Cr(III) and Cr(VI). While Cr(III) is considered an essential nutrient, Cr(VI) is toxic and carcinogenic. Hence it is important to monitor the concentrations of the individual Cr species in natural waters.

This thesis describes the development, optimization and application of a new voltammetric method for the determination of Cr species in aqueous environmental samples, with particular reference to seawater. This method is based on the Square Wave Cathodic Stripping Voltammetry (CSV) of a Cr-Xylenol Orange (XO) complex preceeded by its adsorptive preconcentration on a hanging mercury drop electrode. The catalytic reduction of nitrate ions in the vicinity of the electrode is utilized to enhance the sensitivity of the method. Stable reduction peaks are obtained for both Cr(VI) and Cr(III) species. The formation of the adsorbed analyte complexes derived from Cr(VI) and Cr(III) is dependent on the deposition potential used for the preconcentration and this forms the basis for the speciation of Cr. Hence the need for lengthy sample pretreatment steps is precluded from the analytical procedure.

Under optimized conditions, sensitivities greater than 1.8 μA $(\mu g/L)^{-1}$ min^{-1} (90 nA nM^{-1} min^{-1}) can be achieved, making the method adequate for the determination of Cr at the concentration levels prevalent in all types of natural waters. For 60 s preconcentration times, detection limits for Cr(VI) and Cr(III) are respectively 1.2 and 1.8 ng/L in distilled, deionized water. The method is virtually free from interferences and is applicable to Cr analysis in seawater as well as in surface waters and has been applied to the determination of Cr speciation in the N.W. Atlantic Ocean.

Results of experiments aimed at elucidating the electrode processes involved in the deposition and reduction of the analyte complex suggest that the adsorbed complex is Cr^{III}-XO. This complex is formed on the surface of the electrode by the reaction between nascent Cr species and adsorbed XO. The analytical signal is the current obtained when this complex is reduced to Cr^{II}-XO.

ACKNOWLEDGEMENTS

I would like to express my sincere gratitude to the following people:

Dr Niall Gogan, my supervisor, for his constant guidance and support throughout the duration of this work.

Dr Bob Helleur and Dr Chris Parrish, members of my supervisory committee, for their useful comments and criticisms.

Dr John Green of the Biology Dept. for his friendship and help during my stay in St. John's.

Dr Tony Dickinson and Ms Colleen Clarke of MUN's International Office.

All fellow graduate students and friends in the Chemistry Dept.

I would like to thank the Canadian International Development Agency (CIDA) and the Memorial University of Newfoundland (MUN) for their financial support through the CIDA/MUN Marine Science Scholarship Programme.

Thanks are also due to the Chemistry Dept. of MUN for partial financial support through a Teaching Assistantship and for providing all necessary resources in the completion of this research programme.

Finally I would like to thank the University of Mauritius for granting me leave during the duration of this work.

TABLE OF CONTENTS

LIST OF TABLES

LIST OF FIGURES

LIST OF ABBREVIATIONS

AAS	Atomic Absorption Spectrometry
ADDC	Ammonium diethyldithiocarbamate
Bis-Tris	bis[2-Hydroxyethyl]iminotris[hydroxymethyl]methane
CSV	Cathodic Stripping Voltammetry
CV	Cyclic Voltammetry
DOM/DOC	Dissolved Organic Matter/Carbon
DP(V)	Differential Pulse (Voltammetry)
DPCA	Diphenylcarbazide
DTPA	Diethylenetriaminepentaacetic acid
E_λ	Switching potential in cyclic voltammetry
E_s	Square wave scan increment
E_p	Reduction peak potential
$E_{1/2}$	Half-wave potential
$E_{p,a}$	Anodic peak potential in cyclic voltammetry
$E_{p,c}$	Cathodic peak potential in cyclic voltammetry
EDTA	Ethylenediaminepentaacetic acid
E_{dep}	Deposition potential
E_{SW}	Square wave amplitude
f	Square wave frequency
HA/FA	Humic Acid/Fulvic Acid
HEPES	*N*-2-Hydroxyethylpiperazine-*N'*-2-ethanesulphonic acid
HMDE	Hanging Mercury Drop Electrode
i_p	Magnitude of reduction peak current

$i_{p,a}$	Anodic peak current in cyclic voltammetry
$i_{p,c}$	Cathodic peak current in cyclic voltammetry
ICP-AES	Inductively Coupled Plasma-Atomic Emission Spectrometry
ICP-MS	Inductively Coupled Plasma-Mass Spectrometry
IOC	Intergovernmental Oceanographic Commission
LS(V)	Linear Sweep (Voltammetry)
PIPES	piperazine N,N'-bis[2-ethanesulphonic acid]
SDS	Sodium dodecyl sulphate
SW(V)	Square Wave (Voltammetry)
t_{dep}	Deposition time
TTHA	Triethylenetetraaminepentaacetic acid
TX-100	Triton X-100, polyethylene glycol tert-octylphenyl ether
XO	Xylenol Orange

CHAPTER 1

INTRODUCTION

1.1 TRACE METALS IN THE MARINE ENVIRONMENT

A large proportion of pollutants introduced in the environment by anthropogenic activities ultimately reach the oceans and seas as precipitation, surface run-offs or through the direct discharge of effluents. While in the long term, aquatic microorganisms break down organic pollutants, metals are a cause for concern in these environments because they are non-biodegradable and because of their toxic effects on marine life and, through the food chain, on human health. A study of the behaviour of metals in the marine environments can provide an understanding of the biological and geochemical cycling of these metals. These cyclings regulate the concentrations and bioavailability of the elements in these environments.

The considerable interest and apprehension about the role and fate of trace metals in marine environments is the result of several catastrophic events, the most tragic of which is probably the case of mercury poisoning at Minamata Bay in Japan. This event also highlighted the need for the measurement of the chemical speciation of toxic elements rather than the total element concentrations: mercury was initially not suspected as the cause of what is now

known as Minamata disease because the known symptoms of inorganic mercury poisoning were not seen. It was only during a second outbreak of the disease that it was recognized that methylmercury species were responsible for Minamata disease[1]. It is now recognized that both the bioavailability and toxicity of trace elements are critically dependent on the specific chemical form of the element. Measurement of the total concentration of any trace element therefore provides very little information about its bioavailability or toxicity.

The availability of reliable and sensitive analytical techniques is of paramount importance to the study of the chemical behaviour of trace metals in the environment. Trace metals in seawater are present at concentrations that range down to the picomolar levels. The development of analytical techniques that can reliably measure these concentrations is a major challenge which is made even more formidable by the need for speciation analysis. It is no surprise therefore that there is a huge literature base dealing with the occurrence and analysis of trace elements in seawater. Several books and reviews have treated the progress made in our understanding of trace element chemistry in seawater and natural waters [1-5]. There have also been books [6, 7] and numerous reviews [8-17] specifically dealing with the speciation of trace elements in the environment.

---

[1] An extremely readable account of Minamata disease is given in *'Environmental Chemistry'* by Nigel J. Bunce. Wuerz Publishers, Winnipeg, 1994.

Over the last 15-20 years, there has been a revolution in the existing data regarding the distributions and chemical behaviour of trace elements in natural waters, particularly seawater. This revolution has been brought about by the realisation that any analytical methodology has to account for the risks of contamination as well as analyte losses involved during the sampling and sample handling steps. Thus clean techniques have been developed and adopted for the collection, preservation, storage and analysis of water samples for trace analysis. This, coupled with the advent of extremely sensitive techniques, has resulted in concentrations of trace elements in seawater being shown to be factors of 10 to 1000 times lower than those previously accepted [18]. This in turn has led to a demand for more accurate data to be generated at lower concentrations. Thus, the focus of this thesis is to develop a reliable and sensitive method for the determination of species of one of the biogeochemically important trace metals in seawater: chromium.

1.2 CHROMIUM

Chromium occurs principally in nature as the extremely stable mineral chromite, $FeO.Cr_2O_3$ [19]. In most soils and bedrocks, it is similarly immobilized in the trivalent state; however, the environmental concentrations of chromium are significantly in excess of the natural mobilization of the element by weathering processes. This is because chromium and its compounds have widespread industrial applications, resulting in large quantities of the element being discharged in the environment.

Chromium enters the environment mainly as leachings from sanitary landfills and as industrial effluents from, for example, electroplating and tanning industries, from dyeing, pigment production and steel industries. It can also enter the drinking water distribution system from the corrosion inhibitors used in water pipes. Due to these factors, human exposure to chromium is unavoidable. In view of its paradoxical roles as an essential micronutrient as well as a known carcinogen, there is much concern about the occurrence, fate and effects of chromium in the environment. References [20, 21] give a comprehensive account of the chemistry of chromium with respect to its sources, uses and effects on aquatic and terrestrial biota and humans.

Chromium occurs mainly in the trivalent or the hexavalent oxidation states in the environment. Chromium (III) is considered to be an essential nutrient [20, 21]. It

is established that an organo-chromium complex of uncertain structure, synthesized from adsorbed Cr(III), helps activate insulin [22]. Deficiency of this complex through lack of Cr(III) in the diet results in glucose intolerance and reduced efficiency of insulin. On the other hand, Cr(VI) has been shown to have toxic effects on the biological system. Exposure to Cr(VI) can lead to skin lesions, lung disease and various forms of cancer. The carcinogenic effect of Cr(VI) has been attributed to its ability to migrate through cell membranes as CrO_4^{2-} and the highly oxidizing nature of this ion. It has been proposed [23] that Cr(V), an intermediate in the reduction of Cr(VI), forms a Cr(V)-DNA complex. Further reduction of Cr(V) to Cr(III) leads to irreversible changes to the DNA structure.

1.3 CHROMIUM IN THE MARINE ENVIRONMENT

The chromium concentrations encountered in natural waters are very low; concentrations vary from 0.1 to 0.3 µg/L in seawater [23. 24] and from 0.3 to 6 µg/L in unpolluted surface waters [23].

The study of the chemical speciation of chromium in natural waters has been a topic of great interest for almost 40 years (see for example ref [25]. The speciation studies have almost exclusively focused on the distribution of chromium between Cr(III) and Cr(VI).

On the basis of thermodynamic calculations, Elderfield [26] predicted that at pH 8.1 in seawater, chromium should exist almost exclusively as Cr(VI) species, mainly as CrO_4^{2-} with minor amounts of $HCrO_4^-$, and H_2CrO_4 and $Cr_2O_7^{2-}$. Any Cr(III) occuring under these conditions should be present to 85% as $Cr(H_2O)_4(OH)_2^+$, 13.5% as $Cr(OH)_4^-$ and $Cr(H_2O)_5(OH)^{2+}$ as a minor species. Considering only the dominant Cr(III) species, the redox equilibrium is assumed to be controlled by

$$CrO_4^{2-} + 2H_2O + 6H^+ + 3e \rightleftharpoons Cr(H_2O)_4(OH)_2^+ .$$

and the equilibrium ratio of dissolved Cr is given by [27]

$$\log [Cr(VI)]/[Cr(III)] = 6pH + 3pE - 66.1.$$

Hence, taking the pH of seawater to be 8.1 and using the theoretical value of pE=12.5 for water in equilibrium with atmospheric oxygen [26], the ratio of Cr(VI) to Cr(III) should be $\sim 10^{20}$. If the pE is 6.5, consistent with the assumption that the redox level of seawater is controlled by the O_2/H_2O_2 couple and $[H_2O_2]$=0.1 μM [28], this ratio falls to 100.

In practice, however, Cr(VI):Cr(III) ratios ranging from less than 1 to 70 have been reported [27]. Several reasons have been put forward to explain the observed discrepancies between the calculated values and the experimental data. These include the kinetic stability of Cr(III) which makes oxidation very slow and the possible removal of Cr(VI) by organic matter in natural waters. Both these factors would result in a higher relative concentration of Cr(III). However, nowadays the consensus is that the analytical data does not truly reflect the actual situation in the original sample because of deficiencies in the analytical methodologies used [29]. Many sampling and analytical techniques actually disturb the equilibria in solution. The realization that the sampling, storage and analysis of trace metals in environmental samples requires extreme precautions to overcome possible contamination has cast doubt over much available trace metal data, including the available data on chromium in seawater. New data are therefore called for.

1.4 ANALYTICAL METHODS FOR CHROMIUM

There is a prolific literature dealing with the determination and speciation of chromium in various matrices. Virtually all the standard methods for metal analysis methods have been employed for the determination of chromium, ranging from the relatively simple and cheap spectrophotometric methods to chromatographic and nuclear methods. A literature search shows that just during the period 1992-1997, there have been almost 100 papers relating to the determination of chromium in environmental samples. While this is an indication of the amount of interest in the determination of chromium, it also underlines the fact that no single method has gained universal acceptance as a standard method. The reason for this lies in the difficulties that have to be overcome in the establishment of a reliable method. The extremely low concentrations of chromium in seawater mean that there are very few applicable techniques with sufficient sensitivity and selectivity. Even with the most sensitive technique available, the analyte needs to be preconcentrated for the determination of chromium species. Very often the Cr(III) and Cr(VI) species need to be physically separated before the analysis. Preconcentration/ separation methods that have been employed for the determination of chromium in seawater have been based on coprecipitation [30-38], solvent extraction [39-42], ion-exchange and sorbent extraction [29, 43-53], and electrodeposition [54, 55]. These sample pretreatment steps are often very time consuming and liable to introduce

errors (speciation change, analyte loss, contamination) in the analytical data. This is probably why during recent years there has been a shift in emphasis towards on-line flow-injection methods for the separation and preconcentration of chromium species.

Following the sample pretreatment steps, detection of the chromium species has been achieved by uv-vis spectrophotometry [53, 56-59], chemiluminescence [47, 51, 60], flame and electrothermal atomic absorption spectrometry [29, 33, 35, 36, 38, 39, 41, 43, 44, 46, 49, 50, 52, 54, 55, 61-66], ICP-AES [48, 67-69], ICP-MS [45, 70-74], neutron activation analysis [30], X-ray fluorescence [32, 37] and isotope dilution mass spectrometry [75, 76]. An electron capture detector has also been used for detection in a gas chromatographic method for chromium [42].

In addition to the methods listed above, electrochemical methods have also been employed for the determination of chromium in natural waters, including seawater. These methods are discussed in Section 1.6.

In spite of the multitude of existing methods for the determination of chromium, it is interesting to note that very few have actually been employed for the analysis of chromium in seawater. Methods that have been employed for the determination of chromium in seawater are shown in Table 1.1. Except for the methods with on-line separation and preconcentration of the species [29, 43],

the pretreatment steps are time consuming, laborious and prone to contamination during for example, the filtration and centrifugation steps.

Table 1.1: Non-electrochemical methods for the determination of chromium in seawater.

Separation/preconcentration method	Mode of Detection	Detection limit	Reference
Cr(VI) extracted with Aliquat-336 in toluene at pH 2. Cr(III) extracted as above but at pH 6-8 and in the presence of > 1 M thiocyanate.	Flameless AAS	Cr(VI): 0.01 µg/L Cr(III): 0.03 ug/L	39
Cr(III) coprecipitated with $Fe(OH)_3$ at pH 8. Both Cr species coprecipitated with aerial oxidation of $Fe(OH)_2$. Cr(VI) by difference.	Flameless AAS	1 ng/L	33
Cr(III) coprecipitated with $Fe(OH)_3$ at pH 8.5 then Cr(VI) from same solution with $Co(PDC)_2$* at pH 4. Precipitates collected as thin films.	XRF	0.1 µg/L	32
Cr(III) coprecipitated with $Fe(OH)_3$ at pH 8. Both Cr species coprecipitated with bismuth oxide at pH 8. Cr(VI) by difference.	Flameless AAS	not mentioned	31
Cr(VI) coprecipitated with $PbSO_4$ at pH 3.5. Cr(III) not determined.	Flameless AAS	0.3 µg/L	35

Table 1.1 (continued)

Separation/preconcentration method	Mode of Detection	Detection limit	Reference
Cr(VI) coprecipitated with $Pb(PDC)_2$ at pH 4, then Cr(III) coprecipitated from same solution at pH 9.	NAA	not mentioned	30
Flow injection extraction of Cr(VI) with NaDDC*. Total Cr after oxidation of Cr(III) to Cr(VI) and Cr(III) by difference.	Flameless AAS	Cr(VI): 16 ng/L Cr(III): 18 ng/L	29
Cr(III) is extracted at pH 6 in toluene as the 1,1,1-Trifluoroacetylactone complex. Total Cr extracted as above after reduction of Cr(VI) to Cr(III). Cr(VI) by difference.	Gas chromatographic, with ECD	Cr(VI): 13.3 ng/L Cr(III): 3.2 ng/L	42
Cr(III) coprecipitated with $Ga(OH)_3$ at pH 9-10. Total Cr after reduction of Cr(VI) to Cr(III) and Cr(VI) by difference.	Flameless AAS	20 ng/L	36
Flow injection extraction of Cr(III) with immobilized quinolin-8-ol. Total Cr after reduction of Cr(VI) to Cr(III) and Cr(VI) by difference.	Flameless AAS	not mentioned	43

*PDC is pyrrolidinedithiocarbamate, DDC is diethyldithiocarbamate

As an illustration of the amount of labour typically involved in the above methods, the sample pretreatment in the gas chromatographic method of Mugo and Orians [42] is outlined.

- Transfer sample to reaction vessel, adjust pH to 6.6 ± 0.2 with CH_3COOH, and add ligand (trifluoroacetylacetone) and extracting solvent (toluene).
- Shake for 5 s, then heat in microwave oven for 3 min.
- Remove from microwave oven, shake for 5 s, return to microwave oven and heat for a further 3 min.
- Cool completely to room temperature, with shaking for the first 10 min.
- Transfer to separatory funnel, separate and discard aqueous layer.
- Shake organic layer from above with deionized water, allow to separate, add NaOH and shake for 20 s. (This step is said to be critical).
- Separate organic layer and rinse twice with deionized water.
- Transfer extract to clean glass vial for subsequent injection into GC column and quantification.

The above sample pretreatment is for the determination of Cr(III) only; total Cr is determined after reducing Cr(VI) to Cr(III) with Na_2SO_3, then following the above procedure. Cr(VI) is then obtained by difference. The various steps involved in the above procedure make the analysis time very long; in addition to the time, it should be realized that contamination risks are being magnified at each stage and with every chemical being used in the analytical procedure.

The methods described by Sperling et al. [29] and Pasullean et al. [43] are arguably the best among the existing non-electrochemical methods but they do require some specialized and expensive equipment in contrast to the very simple equipment required in the electrochemical methods, as will be discussed in

Section 1.6. From the point of view of convenience, the appeal of both of these methods is greatly reduced by the need for an off-line oxidation [29] and reduction [43]. Sperling et al. oxidized Cr(III) to Cr(VI) by boiling samples at pH 9 with $K_2S_2O_8$ for 25 minutes at 105 °C, whereas Pasullean et al. reduced Cr(VI) to Cr(III) by a 20-min treatment with hydroxylamine hydrochloride at room temperature. Pasullean et al. [43] employed a cation exchange resin for the preconcentration of Cr(III). In the light of an investigation by Rai et al. [77] which shows that $Cr(OH)_3^0$ is the dominant Cr(III) species in solution, the reliability of this method could be compromised because the resin will be unable to bind Cr(III) species like $Cr(OH)_4^-$ and $Cr(OH)_3^0$.

1.5 VOLTAMMETRIC METHODS FOR TRACE ANALYSIS

Voltammetric methods of analysis, which have been used since the invention of polarography in 1922, witnessed a serious decline in use and was even threatened with extinction [78] with the development of Atomic Absorption Spectrometry (AAS) in the mid-1960's. The remarkable detection limits of AAS, coupled with its ability to determine almost all the metallic elements, was beyond the reach of classical polarography, which had come to be regarded as a very unattractive technique due to its clumsy instrumentation. However, there has been a resurgence of interest in the electroanalytical techniques during the past 25 years, mainly as a result of the appearance of vastly improved, commercially available instrumentation which has taken full advantage of the electronic revolution. In parallel with the instrumental developments, there have also been accompanying advances in the theoretical aspects of electroanalytical techniques with the development of, for example, a.c, pulse and stripping techniques. As a consequence, voltammetry is now established as an extremely versatile, sensitive, rapid and inexpensive analytical technique which has found applications in most areas of analytical chemistry. The fundamental principles of polarography are described in reference [79] while reference [80] recounts developments in polarographic techniques that have led to the renaissance and widespread adoption of voltammetry.

AAS (especially Electrothermal AAS) and more recently, ICP-MS and ICP-AES techniques are generally regarded as the ultimate methods of detection for ultra-trace analysis because of the detection limits attainable by these techniques. However, in the form of Anodic Stripping Voltammetry (ASV), voltammetry offers a technique that, in specific cases, can rival these techniques with respect to detection limits, reproducibility and ease of operation. The extreme sensitivity of ASV is due to the analyte preconcentration step inherent to the technique, whereas the spectrometric techniques rely on a prior analyte preconcentration step. Another advantage that ASV offers is that it can speciate the analyte species on the basis of their lability in the natural medium [13]. The principles and applications of ASV are described in standard analytical chemistry textbooks (e.g., [81]) and will not be covered here.

The applicability of ASV is contingent on the metal to be determined being soluble in mercury to form an amalgam. This requirement severely limits its widespread application in environmental analysis and ASV has remained more or less confined to the determination of Cu, Pb, Cd and Zn. In this respect, the applicability of ASV is very restrictive, in contrast to the capability of AAS or ICP techniques, which are readily applicable for the determination of most of the elements in the Periodic Table.

In parallel with ASV, Cathodic Stripping Voltammetry (CSV) techniques have also been used for trace element analysis. Until relatively recently, this technique was viewed as the 'mirror image' of ASV. In classical CSV, the analyte species is electrolytically preconcentrated as an insoluble Hg species on the electrode by the imposition of a relatively positive, constant potential during the deposition stage. The applied potential results in the formation of Hg_2^{2+} ions on the electrode surface. Analyte species capable of forming insoluble Hg compounds react with the Hg_2^{2+} to form an insoluble film on the surface of the electrode. During the stripping stage, a negative potential scan is applied on the electrode, resulting in the reduction of this insoluble compound to Hg^0 and the original analyte ion. The faradaic current resulting from this reduction forms the analytical signal. In this preconcentration mode, CSV is applicable to the analysis of mainly anionic species and has been used for the analysis of halides, cyanide, sulphide and a variety of organic compounds.

The applicability of CSV has now been extended to the determination of metallic species following considerable research into a new, non-electrolytic method of preconcentration during the last decade. This preconcentration method is based on the observation that many organic compounds exhibit surface active properties that are manifested by their adsorption from solution onto the surface of a solid phase. Adsorption has been regarded as an undesirable adverse effect in polarography for a long time but enhancements in polarographic waves

had been observed and attributed to adsorption since the early days of polarography [79, 82-84]. Pihlar et al. [85] were the first to exploit adsorption of the dimethylglyoxime complex of Ni on the Hg electrode for the preconcentration of Ni before its stripping. Since then, procedures for the determination of a large number of trace elements have been developed and applied to environmental samples. A recent paper by Fogg [86] includes a review of the historical development of the technique.

An extremely useful article which contains a detailed treatment of the fundamental principles of CSV, the mechanisms of complex adsorption and of the stripping step has been published by Wang [87]; other very informative papers [86, 88-91] provide excellent reviews on the development, potentials and applications of CSV.

The principle behind the new method is very simple: under optimized solution conditions, the analyte (generally metal ions) reacts with an added ligand to form a complex which is adsorbed on the surface electrode during the preconcentration stage. This complex is then reduced during the stripping stage, which consists of the application of a negative potential scan on the electrode. During the stripping stage, the reduction process producing the peak current may be due to the reduction of the metal ion, the reduction of the ligand or the simultaneous reduction of both the ligand and the metal ion. The

selectivity of the method is determined by the judicious choice of the complex-forming ligand and, since the reaction between the ligand and the analyte is usually dependent on the oxidation state of the analyte species, speciation analysis is generally achieved.

From the simple picture presented above, it can be conceived that with the choice of a proper ligand, any metallic species should be amenable to CSV determination, opening up the whole Periodic Table to this extremely sensitive, selective and inexpensive analytical technique. The reduction of the ligand can be used for the determination of metals which are reduced at very negative potentials. It is no wonder therefore that so much activity has been channelled towards the search for new ligands for CSV of trace metals in environmental samples. A comprehensive review of ligands used in, and metals determinable by CSV is given in reference [92].

Almost two decades after the technique was first used for the determination of nickel, there is some continuing debate as to the name of the technique. Since the adsorption phenomenon is utilized for preconcentration of the analyte species, the technique has also been referred to as Adsorptive Stripping Voltammetry, (AdSV), as well as Adsorptive Cathodic Stripping Voltammetry (AdCSV), whereas many workers simply refer to it as CSV based on the direction of the current flow during the reduction. Following a discussion on the

pros and cons of the different names used for the technique, Fogg [86] reached the conclusion that the term *cathodic stripping voltammetry with adsorptive accumulation* would be more informative. However, he acknowledged that the term cathodic stripping will continue to be used. In the present work, the term CSV is used throughout, with the understanding that the accumulation is adsorptive.

In contrast to the methods listed in Table 1.1, electrochemical methods for trace metal analysis are very fast and require relatively simple and inexpensive instrumentation. If the complexing ligand is chosen such that the reaction occurs selectively between the ligand and the analyte in a given oxidation state, speciation is achievable without lengthy separation steps and the preconcentration inherent to the technique precludes the need for a potentially contaminating preconcentration step. The whole analytical procedure can generally be carried out within the confines of a clean bench, which is a major asset in trace analysis. The fact that the material adsorbed on the mercury electrode is readily accessible for instantaneous reduction during the stripping stage leads to the flow of a large current, which is the analytical signal. Hence high sensitivities, i.e., extremely low detection limits, can be achieved. In CSV, detection limits in the sub-µg/L level are routinely achieved using preconcentration times of 1-3 min. All these assets make CSV potentially the most appropriate technique for environmental analysis.

1.6 VOLTAMMETRIC ANALYTICAL METHODS FOR CHROMIUM

Polarographic methods for the analysis of chromium have long been established but the detection limits do not permit their application to natural waters. The polarographic determination of Cr(VI) and Cr(III) is described, for example, in reference [93]. However, it was during the polarographic study of Cr in supporting medium containing EDTA and nitrate ions that an important observation was made by Tanaka and Ito [94]. These authors found that the Cr polarographic waves were unusually high in this medium and attributed it to the catalytic re-oxidation of an intermediate Cr(II)-EDTA complex by nitrate ions. More details and the full implications of this effect are discussed in Section 4.3. Zarebski [95] studied this effect further, with three different, related ligands, EDTA, cyclohexanediamminetetraacetic acid (CDTA), and diethylenetriamminepentaacetic acid (DTPA), as supporting electrolytes (in the presence of nitrate ions) and found that DTPA was more suitable than EDTA as supporting electrolyte for the polarographic determination of Cr. He also found that in the presence of DTPA, the sensitivities of Cr(III) and Cr(VI) were different and described a method incorporating the coprecipitation of Cr(III) as $Cr(OH)_3$ and of Cr(VI) as $BaCrO_4$ for the speciation of chromium. Reported detection limits were 5 µg/L for both species..

In 1985, Golimowski et al. [96] were the first to recognize the role of adsorption in the polarographic determination of Cr in the presence of DTPA as supporting electrolyte. They showed that the Cr-DTPA is adsorbed on Hg whereas Cr-EDTA is not, hence the observation by Zarebski [95] that DTPA is more suitable than EDTA for the polarographic determination of Cr. Golimowski et al. [96] exploited the adsorption of the Cr-DTPA complex for the preconcentration of the analyte at a Hanging Mercury Drop Electrode and thus published the first CSV method for chromium. DTPA was used as the complexing ligand and the catalytic effect of nitrate ions was used for enhancement of the reduction currents. In what would be the first application of a voltammetric technique for the determination of chromium at levels prevalent in natural waters, they reported a detection limit of 20 ng/L for a 2-min deposition time. The superiority of this analytical method vis-a-vis the non-electrochemical methods discussed in Section 1.4 was unquestionable. The CSV method provided not only the required detection limit, but it did so without the need for any separate sample pretreatment steps.

However, Golimowski et al. [96] failed to consider that the sensitivity of Cr(III) was less than that of Cr(VI), although this observation had already been made by Zarebski in 1977. These authors also failed to observe that the response of Cr(III) was transient (see below). According to Golimowski et al. therefore, the method was applicable for the determination of total chromium and they claimed

success in its application for the determination of chromium in river, lake, sea and rain water.

Given the differing views of Zarebski [95] and of Golimowski et al. [96] regarding the applicability of the DTPA method for the determination to Cr(III), Torrance and Gatford [97] made a very thorough study of the CSV of the Cr-DTPA complex and confirmed that the responses of Cr(III) and Cr(VI) were indeed different. They found that the Cr(VI):Cr(III) response ratio was 1.4:1 at 0.1 µg/L and 1.2:1 at 1 µg/L of Cr respectively. These authors also found that with both Cr(III) and Cr(VI) there was a kinetic effect that produced a decrease in peak current with time; this decrease was more severe for Cr(III), with a decrease of 15% in the first 5 min after the addition of DTPA. Therefore it was concluded that Cr(III) and Cr(VI) cannot be determined in a solution unless all Cr(III) is oxidized to Cr(VI). They achieved this by heating the sample solutions with bromine water and attained detection limits of 0.023 µg/L Cr as Cr(VI).

Scholz et al. [98] also confirmed that the DTPA method works reliably only for Cr(VI) and proposed that, for the speciation of chromium, total chromium be determined as Cr(VI) after prior conversion of Cr(III) to Cr(VI) by uv-irradiation. Cr(VI) only was determined after a prior step in which the Cr(III) was removed from solution by coprecipitation with $Al(OH)_3$. Cr(III) could then be obtained by difference.

In analogous methods, triethylenetetraaminehexaacetic acid (TTHA) [99, 100] has been used as the complexing ligand in the CSV determination of chromium as Cr(VI). Cr(III) was not determined.

The use of DTPA as the complexing ligand in the determination of chromium was further studied by Boussemart et al. [101], who devised and optimized a method for the speciation of chromium in seawater. These authors observed that the sensitivity for Cr(III) was about 70% of the Cr(VI) sensitivity. They also found that the response for Cr(III) was transient, disappearing completely in about 30 min. They therefore devised a method whereby the CSV peak current was recorded under optimized conditions immediately after the addition of DTPA to the voltammetric cell. The peak current at this time would be equivalent to the response due to Cr(III) and Cr(VI). Then, after 30 min (when the Cr(III) was believed not to be responding), they carried out a determination of Cr(VI) by a Cr(VI) standards addition. The concentration of Cr(III) was estimated from the initial response of Cr(III) plus Cr(VI). Thus, they reported a detection limit of 0.1 nM (ca. 5 ng/L) for a 2-min deposition time. Although they used this method for the speciation of Cr in seawater from the N.W. Mediterranean [101, 102], it is deficient in that the Cr(III) can only be estimated. Apparently, these authors failed to consider the findings of Torrance and Gatford [97] regarding the differing ratios of Cr(VI):Cr(III) responses at different concentrations as well as the rapidly decreasing response of Cr(III). The rate of decrease of the Cr(III)

response is such that by the time the solution is purged and the first voltammetric run completed, there already is a substantial loss in signal. If, as is normal practice, voltammetric runs are carried out in triplicate and, as proposed, a deposition time of 2 min is chosen, it would be impossible to quantify the initial response due to the Cr(III). However, this method is very useful because it enables total Cr(VI) to be determined without any sample pretreatment step.

Probably having realized the deficiencies of the above method, Boussemart and van den Berg later published another method [103] for the determination of Cr(III) in seawater. In this case, the Cr(III) was preconcentrated by adsorption on silica. The adsorbed Cr(III) was later released by converting it to Cr(VI) by uv-irradiation and this Cr(VI) was determined by CSV, with DTPA as the complexing ligand.

Besides the polyaminodiacetic acids (DTPA and TTHA), cupferron [104], diphenylcarbazide (DPCA) [105] and very recently, 2,2-bipyridine [106] have been used as complexing ligands for the CSV determination of chromium. The detection limits attained by these methods are respectively 1, 20 and 1 ng/L. With cupferron and 2,2-bipyridine, identical responses are obtained for Cr(III) and Cr(VI) whereas in the method with DPCA, only Cr(VI) can be determined. Further, the DPCA method cannot be applied to seawater because chloride ions interfere.

1.7 NEED FOR A NEW METHOD

From the discussion in Sections 1.4 and 1.5, it can be seen that analytical methods with the required sensitivity for the speciation determination of chromium in seawater can be based on both non-electrochemical and electrochemical techniques. However, better detection limits are attainable with electrochemical techniques. Additionally, the electrochemical techniques generally involve less sample pretreatment and are faster and cheaper to perform. For these reasons, electroanalytical methods are preferable for the determination of chromium.

Of the stripping techniques discussed in Section 1.5, the method based on DTPA seems best suited to the determination of Cr(VI) in seawater, because Cr(III) does not respond. However, the difficulty faced in determining Cr(III) is a major drawback. Considering the methods described above, the complete speciation of chromium would need the complete oxidation of Cr(III) to Cr(VI) or the physical separation of the Cr(III) species as done in the methods by Boussemart and van den Berg [103] or Scholz et al. [98]. These pretreatment steps are lengthy and are potentially likely to introduce analyte losses as well as contamination in the analytical method. The incorporation of sample pretreatment steps seems to be contrary to the spirit of electroanalytical

techniques where excellent sensitivity coupled with simplicity and minimal sample handling is lauded as the great asset of the technique.

The complete speciation of chromium could in principle be achieved without any need for sample pretreatment by the use of two different complexing ligands, for example, DTPA for Cr(VI) only and then cupferron or 2,2-bipyridine for total chromium (Cr(III) plus Cr(VI)). The difference between total chromium and Cr(VI) would then be equivalent to Cr(III). However, adoption of such a speciation scheme has apparently not yet been investigated, probably because it would entail undesirable additional time and costs (costs and purification of additional chemicals etc.) in the overall methodology.

In view of the lack of a simple CSV method for the speciation of chromium in seawater, it was believed worthwhile to develop a new method. The main objective of this research was therefore to develop a new CSV method for the determination of chromium at ultra-trace levels. A major goal of this new method was to be able to determine chromium species without the incorporation of pretreatment steps that would make it unattractive from the perspective of convenience and contamination. Hence, from the very onset, all steps that were likely to introduce contamination, analyte losses or speciation changes during the determination or which would make the total analysis time too long were precluded. Thus techniques incorporating the physical separation of the analyte

species (e.g., coprecipitation, centrifugation and filtration) or oxidation/reduction steps that were long (e.g., uv-irradiation, heating, boiling, etc.) were precluded.

CHAPTER 2

EXPERIMENTAL

2.1 REAGENTS

Concentrated hydrochloric acid, nitric acid and ammonia used throughout the analytical process was of the highest purity available. These reagents, obtained from Seastar Chemicals Inc., are purified by double sub-boiling distillation in quartz and will be referred to as Q-HCl, Q-HNO_3 and Q-NH_3 respectively. Dilutions of these reagents are then referred to so as to reflect the dilution factor obtained, e.g., Q/2-HCl means conc. Q-grade HCl diluted 1:1 with Nanopure water.

Water used throughout (for dilution, rinsing or as the sample) was distilled and then deionised with a NANOpure II system (Barnstead). This distilled, deionised water will henceforth be referred to as Nanopure water.

Seawater used as the sample during most of the optimization experiments was obtained from the Ocean Sciences Centre, Logy Bay, Newfoundland. Upon collection in precleaned polyethylene bottles, the seawater was wrapped in double polyethylene bags and kept refrigerated at 4 °C at all times. The trace metal content of this seawater (referred to as Logy Bay seawater) is routinely

monitored by ASV (10 min deposition) in our laboratory: no cadmium, copper or lead has been detected in this seawater and the zinc concentration varies in the range 0.1-0.2 µg/L. The chromium content of this seawater was found to be 0.101 µg/L and it was used without any purification for most of the method development work.

When required, (for example, in calculating detection limits), this seawater was purified by a method of coprecipitation with $Fe(OH)_3$ as follows:
0.1 mM of $FeCl_2$ was added to the Logy Bay seawater in a wide-mouthed plastic bottle, and the pH adjusted to ~7. The solution was stirred for 30 min and then left standing overnight on the clean bench. At this pH, Cr(VI) is reduced to Cr(III) and coprecipitated with $Fe(OH)_3$ as the latter is precipitated out as a result of the aerial oxidation of Fe(II) and hydrolysis. After the oxidation of Fe(II) is complete, the precipitate is filtered out through 0.45 µm Millipore membrane filters. The filtrate, referred to as purified seawater, is collected and used as required. The above procedure is slightly modified from one used by Cranston and Murray [33] for the speciation and determination of Cr by an atomic absorption spectrometry method.

'Suprapur' potassium chloride, used as the supporting electrolyte, was obtained from BDH Inc. and was used without purification.

Xylenol Orange (XO) ('Baker Analysed'), was obtained as the sodium salt and used without purification. An attempt was in fact made to purify this compound by a chromatographic method, described by Sato et al. [107] but it was found to be impractical in view of the fact that this compound had to be made up weekly (see below) and also because of the extremely dilute solutions involved. It is believed that XO does not introduce any contaminant Cr in the analysis because no Cr peaks were detected in blank solutions. Working solutions of 2.5 mM XO were made up by dissolving the appropriate amount of the salt in Nanopure water. It was observed that aqueous solutions of XO visibly darkened on keeping for about 2 weeks. No deterioration in the efficacy of these solutions in the CSV of chromium was observed, however, even after keeping for months. Nonetheless, XO solutions were made up weekly.

PIPES (piperazine N,N'-bis[2-ethanesulphonic acid]) (SigmaUltra, Sigma Chemical Co.) was used as the buffer reagent. This compound is insoluble in water but soluble in aqueous ammonia. An aqueous solution of mixed buffer (PIPES/HCl/NH_3) was made up such that final concentrations were as follows: PIPES, 0.1 M; NH_3, 2.5 M and HCl, 0.1 M. 100 µL of this solution added to 10 mL of Nanopure water gave a pH of 8.4; further addition of 50 µL, 0.2 M HCl to this solution gave a pH of 7.1. In seawater, the pH on addition of 100 µL buffer was 8.2; a final pH of 6.7 could be obtained upon the addition of 100 µL of HCl (0.2 M) to this solution.

A 5 M solution of sodium nitrate, $NaNO_3$, was made up by dissolving the appropriate amount of the salt in Nanopure water; $NaNO_3$ was either Suprapur grade (Merck) or AnalaR reagent (BDH) which was purified in the lab by a coprecipitation method as described in the purification of seawater. When purified by this method, $NaNO_3$ was found to contain less than 0.03 nM Cr [101]. Since it was found that Fe is a potential interferent in the CSV of Cr, the purified $NaNO_3$ was further purified by ion-exchange with Chelex-100. 0.1 g of Chelex-100, H^+ form, (Bio-Rad Laboratories) was added per 100 mL of $NaNO_3$ at pH 7 and the mixture stirred for at least 24 hours before filtering through 0.45 µm Millipore membrane filters. However, in view of the poor solubility of $Fe(OH)_3$ in neutral, aqueous solutions (K_{sp}= 2.64×10^{-39}) [108], this ion-exchange step was subsequently found to be unnecessary and later batches of $NaNO_3$ were spared this treatment. No quantifiable amount of Cr could be detected in the purified $NaNO_3$ or the Suprapur grade $NaNO_3$.

A 1.5 M solution of sodium sulphite, Na_2SO_3, was made up by dissolving the appropriate amount of the salt (AnalaR reagent, BDH) in Nanopure water and purified by a 12-h treatment with Chelex-100 and filtration.

Stock solutions of Cr(VI), 100 mg/L, were made by dilution of a 1000 mg/L Cr (as $K_2Cr_2O_7$) AAS standard (Fischer Scientific) and also by dissolving the appropriate amount of the K_2CrO_4 (BDH) in Nanopure water. The responses of

both these standards were similar. A stock solution of Cr(III), 1000 mg/L, was made by dissolving the appropriate amount of the $CrCl_3.6H_2O$ ('Baker Analysed') in Nanopure water. Working standard solutions of Cr(VI) and Cr(III) were made up from the stock solutions by appropriate dilutions on a daily (25 µg/L, 100 µg/L), or weekly (1 mg/L) basis.

A 0.01 M solution of $FeCl_2$, used in the purification of seawater and $NaNO_3$, was made by dissolving the appropriate amount of $FeCl_2.4H_2O$ (BDH) in 0.1 M Trace Metal grade HCl.

2.2 MATERIALS

Only plasticware made of polyethylene, polypropylene or Teflon was used for the storage of reagents and samples. Calibrated automatic pipettes, fitted with plastic pipette tips, were used for solution transfer.

Test solutions were contained in either Teflon (Fischer Scientific) or glass (EG&G, PAR) voltammetric cells.

Filtration of samples and reagents, whenever required, was carried through 25 mm (diameter), 0.45 μm Millipore membrane filters (HA type, Millipore Corporation), used in conjunction with a filter holder and 10 or 30 mL syringes.

2.2.1 Cleaning of Materials

Prior to use, all plasticware was subjected to a thorough cleaning procedure as described below. The cleaning procedures described have been adapted from Bruland et al. [109].

Bottles for sample and reagent storage were cleaned in the following way. After rinsing with acetone to remove organic impurities, they were immersed in a hot (~60 °C) solution of 5% microdetergent (Cole-Parmer) bath for 24 hours, rinsed with copious amounts of Nanopure water, filled with 6 M HCl (reagent grade) and soaked in a 2 M HCl (reagent grade) bath for at least two weeks. After this

period of time, they were again rinsed well and filled with 0.1 M HNO_3 (Trace Metal grade) (or 0.1 M Q-HCl for 30-mL bottles which were used to contain standards of very low concentrations), wrapped in double polyethylene bags and stored for at least 2 weeks. Before use, these bottles were thoroughly rinsed with Nanopure water.

Small items, such as disposable tips, filter holders, syringes and voltammetric cells, were cleaned in a similar manner. After the detergent wash, items were placed in an acid bath (3 M reagent grade HCl at ~60 °C) for 48 hours, followed by another 7.5 M Trace Metal grade HNO_3 bath at ~60 °C for 24 hours. Disposable tips were then rinsed with and kept immersed in Nanopure water until use.

Filter holders, syringes and voltammetric cells were further cleaned in a 1 M Q-HCl bath, rinsed well with Nanopure water and allowed to air dry on the clean bench. Filter holders and syringes were used for specific reagents so there was no danger of cross contamination.

The Millipore membrane filters were soaked in a 2 M Q-HCl bath for at least three weeks. Before use, they were rinsed well with Nanopure water and placed in filter holders and then further rinsed by passing large amounts of Nanopure water through them.

2.3 THE CLEAN BENCH

In keeping with trace metal analysis protocols, all sample handling, reagent storage and the experimental analyses were carried out on a clean bench which conformed to Class-100 specifications. The clean bench is a metal free enclosure (24"(L) x 48"(W) and 30"(H)) which is continuously purged by a laminar flow of filtered air. The unidirectional air flow is maintained by a fan which operates by drawing air through a pre-filter and then pushing it through a high efficiency particle air (HEPA) filter (EAC1, mode MAC 10) and throughout the enclosure. The positive pressure thus created ensures that no airborne contaminants enter the working area. The filtering unit was kept on all the time; when not being used, a plastic curtain was hung on the open side of the clean bench. The clean bench is itself located in a room with restricted access and the air supply to this room is scrubbed by coarse filters.

The working area of the clean bench is made of high density polyethylene and was regularly rinsed with distilled, deionised water and wiped dry with lint-free wipers (Kimwipes). All operations inside the clean bench were carried out wearing disposable polyethylene gloves (Fischer Scientific).

2.4 INSTRUMENTS

Voltammetry experiments were carried out mostly with a EG&G Princeton Applied Research Model 384B Polarographic Analyzer (henceforth referred to as Model 384B Polarographic Analyzer) interfaced to a personal computer through the PAR Model 394 Analytical Voltammetry Software. Every step of the analysis (e.g., purging, drop dispensing, stirring, scanning, data acquisition, etc.) is automated; the interfacing to the computer provides more flexible control of data acquisition and analysis by allowing storage and manipulation of data.

Some experiments during the early periods of the project were carried out without the software, in which case the results were displayed as current/potential plots on a Houston Instrument DMP-40 plotter.

The electrode used was a PAR Model 303A SMDE operating in the Hanging Mercury Drop Electrode (HMDE) mode. The reference electrode was a saturated KCl Ag/AgCl electrode and the counter electrode was a platinum wire. All solutions could be stirred by a Teflon-coated star shaped magnetic bar (Fischer Scientific) which was driven by a PAR Model 305 Stirrer. This stirrer was normally operated in the 'auto' mode and at the 'high' setting. A mechanism for de-aeration of the sample solution is incorporated in the electrode system.

The electrode was always kept on the clean bench. Between samples, the electrode was thoroughly cleaned by first rinsing with Nanopure water, then immersing in 1 M Trace Metal grade HNO_3 for at least 30 min, then rinsing with Nanopure water, 0.1 M Q-HCl and again with Nanopure water. When not in use, the electrode was kept immersed in 0.1 M Q-HCl.

Some cyclic voltammetric experiments were carried out with a Model CS 1087 Computer Controlled Electroanalytical System (Cypress Systems Inc., Kansas, USA). This instrument was used in conjunction with the PAR Model 303A SMDE, in which case a PAR Model 174 or Model 384B Polarographic Analyzer was used to power the electrode for the purpose of dispensing the mercury drops. This instrument will henceforth be referred to as the Cypress System.

In all the voltammograms displayed in the course of this thesis, the polarographic convention is used. In this convention, cathodic current is considered positive and potentials are plotted so that the potentials increase in a negative manner to the right-hand side of the i-E curves.

All pH measurements were made with a Chemtrix Type 60A pH meter, in conjunction with a combined glass pH electrode (Broadley James). The pH meter was calibrated at least once a week with pH buffers 4.01, 6.86 and 7.41. The glass electrode was kept permanently on the clean bench and its use restricted to measuring pH of test solutions; therefore the test solution could be

moved back and forth from the HMDE to the pH electrode without contamination. This was required because accurate pH adjustments sometimes had to be made during the course of the experimental procedure (e.g., in speciation determinations, Na_2SO_3 is added at pH 2, then the solution pH brought back to pH 7.1 for the actual determination). After use with any particular sample, the pH electrode was thoroughly cleaned first by rinsing with Nanopure water, then immersing it in 0.1 M Trace Metal grade HCl for 5 min and finally rinsing again with Nanopure water. When not in use the electrode was kept immersed in Nanopure water or 0.1 M KCl (for longer periods of time).

2.5 SAMPLE COLLECTION

For determination of chromium in the North West Atlantic Ocean, samples were collected during a cruise on board the CSS Hudson on 10 August 1993 during the 1993 IOC (Intergovernmental Oceanic Commission) cruise and supplied by Dr William M. Landing of Florida State University. Samples for chromium determination were collected at Station 2: 54°50' N, 48°46' W. The seawater samples were collected in pre-cleaned 500 mL polyethylene bottles and immediately frozen, without any acidification or filtration. Sample bottles were kept wrapped in double polyethylene bags and frozen at -14 °C until used.

2.6 TYPICAL EXPERIMENTAL PROCEDURE

To illustrate the normal sequence of events in the course of a typical experiment, the determination of Cr in seawater is described.

A 9.85 mL aliquot of seawater is pipetted into a voltammetric cell (using an Eppendorf Maxipettor pipette 4720 and Maxitip) and 50 µL, 0.2 M Q-HCl is added. The solution is mixed by stirring with a magnetic bar for about 1 min (Section 3.4). Then 100 µL of 0.1 M PIPES buffer solution and 750 µL 5 M $NaNO_3$ is added. The pH of the solution is adjusted to the desired value (~6.7 in the case of seawater) by the addition of 0.2 M Q-HCl and/or Q/10 NH_3 solution. 50 µL of 2.5 mM XO is pipetted into the solution and the voltammetric cell placed in the thoroughly rinsed electrode. This solution is purged with UHP nitrogen, with stirring, for 6 min and a voltammetric programme initiated.

The following is now performed under voltammetric control: the mixture is purged for a further 10 s (stirring on); 2 mercury drops are dispensed and dislodged and then another drop dispensed. The analyte is collected (preconcentrated), with stirring, on the Hg drop at the appropriate potential (generally -1.2 V) for a suitable length of time (normally 60 s). Stirring is stopped and after a quiescence time of 10 s, the potential is scanned at 200 mV/s from -1.2 to -1.6 V, using a Square Wave modulation. The i/E plot is displayed on the computer

screen and the i/E data can be stored for further analysis. This voltammetric programme is repeated to obtain duplicate or triplicate data, as desired.

Calibration is done by the method of standard additions: following the addition of a spike, the solution is purged for 2 min and the voltammetric programme initiated again. Usually, peak currents for 3 standard spikes were obtained for calculating the analyte concentration in the sample.

CHAPTER 3

METHOD DEVELOPMENT

3.1 CHOICE OF LIGAND

The first task in the development of the new CSV method was to select a ligand which would permit the sensitive and selective determination of the two chromium species. For ease of use and for its universal applicability, the following characteristics of the potential ligand were set as pre-requisites:

1. commercial availability in an acceptable degree of purity
2. solubility in water and stability of aqueous solutions
3. non-toxicity
4. adsorbability of its Cr complex on mercury.

The search for a ligand started with an examination of the structures of some ligands already being used for the CSV of Cr and other metals. Ligands that have been successfully employed in the CSV of Cr include DTPA [96, 98, 101] and TTHA [100] which are members of the polyaminodiacetic acid family of compounds, the best known example of which is EDTA. The excellent chelating properties of this class of compounds is due to the iminodiacetic acid group.

Cupferron [104] and diphenylcarbazide [105] have also been employed in the CSV determination of Cr. Another organic compound which is extensively used in trace metal analysis, including CSV of trace metals, but not in the CSV of Cr, is 8-hydroxyquinoline. The structures of DTPA, diphenylcarbazide, cupferron, and 8-hydroxyquinoline are shown in Fig. 3.1. The excellent complexing ability of all these molecules is attributed to the electron donating nitrogen and oxygen atoms in close proximity of each other.

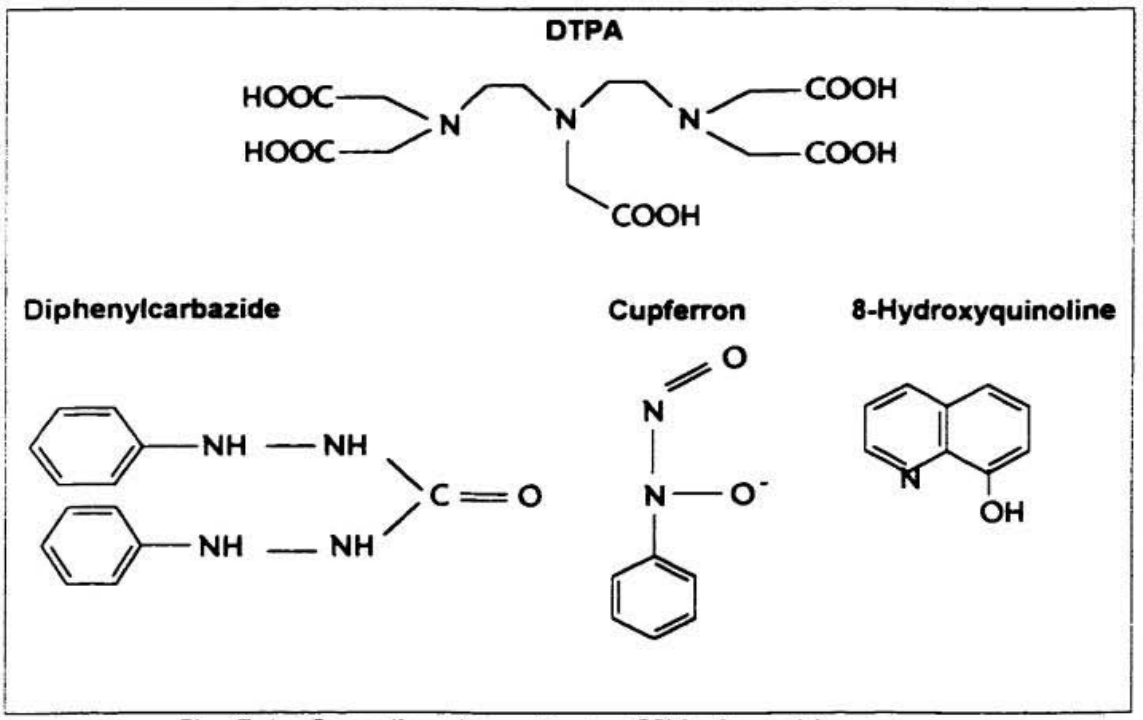

Fig. 3.1: Some ligands used in the CSV of metal ions

Based on these structures and complexing abilities of the iminodiacetic acid group of, for example, DTPA and that of the oxine group in 8-hydroxyquinoline, it was predicted that a compound having a hydroxyl group in the proximity of the

nitrogen of an iminodiacetic acid group would be an excellent ligand for the CSV of metals and therefore a molecule with the following moiety was sought

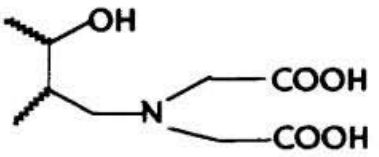

One class of compounds with the above moieties is the complexones. Of the various compounds from this class of compounds routinely used as indicators in analytical chemistry, Xylenol Orange (Fig. 3.2) was found to be best suited with respect to its availability, solubility and stability.

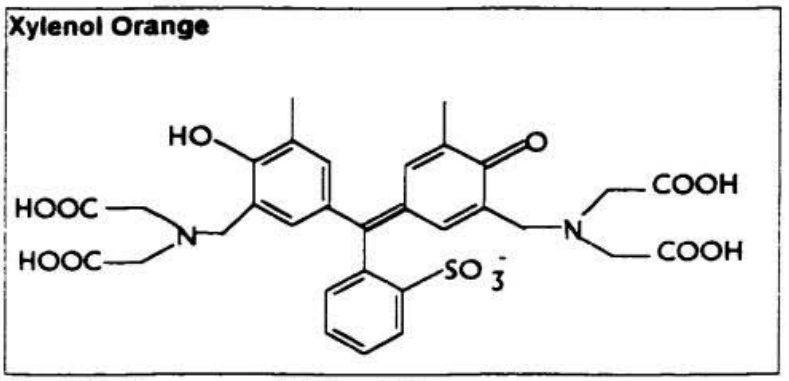

Fig. 3.2: Structure of Xylenol Orange

As can seen from the structural formula, this compound would be expected to form stable complexes with metal ions and the occurrence of three benzene rings in the molecule would lead to efficient adsorption on the mercury surface. There have been two very recent reports on the utilization of XO as the ligand in

the determination of Pb [110] and La [111]. The applicability of this compound in the CSV of Cr was evaluated through a set of preliminary experiments.

3.1.1 Xylenol Orange

Xylenol Orange (o-cresolsulphonphthalein-3',3"-bis(methyliminodiacetic acid), henceforth referred to as XO, was first synthesized by the Mannich condensation of formaldehyde, iminodiacetic acid and o-cresolsulphonphthalein by Korbl, Pribil and Emr [112] for use as a metallochromic indicator. This compound is now considered to be the most useful of the metallochromic indicators [113, 114] and is commercially available as the sodium salt. The colour reactions of XO with diverse cations are very sensitive and it is an outstanding indicator in complexometric titrations because it gives very sharp colour changes over the whole range from pH 0 to 11 [115]. The analytical applications of XO as an indicator have been compiled by Bishop [116].

Following the report of the synthesis of XO, there was some brisk interest in the application of the compound to spectrophotometry in the 1960's. XO readily forms coloured complexes with many metal ions and was therefore successfully used in spectrophotometric determination of many metals, including Cr. The applications of XO in spectrophotometry have been reviewed [114, 115, 117].

During the same period, studies on the complexation reactions of XO and on the properties of metal-XO complexes were undertaken. However, the equilibria existing in aqueous solutions of XO are very complicated because of the existence of protonated species [113]. XO is a H_6XO type polybasic acid. The

study of the complexation reactions of XO are further complicated by the fact that it has two complexation sites and it has been reported that each of these can react independently with metal ions [118]. Due to this, few data are available on the stability constants of metal-XO complexes. References [114, 119] have a compilation of available data on the complexes of XO with metals ions. After the considerable initial interest in XO, the application of this compound has been more or less restricted to its role as an indicator in complexometric titrations.

For the spectrophotometric determination of Cr with XO [120], the coloured complex was formed by boiling Cr(III) with excess XO at pH 1.9-2.2. The complex has a 1:1 Cr(III)-XO ratio and an apparent formation constant of 3.7×10^3.

3.2 PRELIMINARY EXPERIMENTS

A rapid appraisal of XO was made as follows:

1. The chromium complex was expected to be reduced at ~ -1.1 to -1.6 V during the stripping stage of the CSV determination. This assumption was based on the reduction potentials of $Cr(III)_{aq}$ and other Cr complexes. For example, some $E_{1/2}$ values for the reduction of some Cr(III) species are given in Table 3.1 [121].

Table 3.1: Reduction potentials of some Cr complexes

Cr species	Product	$E_{1/2}$ (vs SCE)
$Cr(H_2O)_6^{3+}$	Cr(II)	-0.91 V
$Cr(H_2O)_6^{3+}$	Cr(0)	-1.47 V
$[Cr(H_2O)EDTA]^-$	$[Cr(H_2O)EDTA]^{2-}$	-1.250 V
$[Cr(H_20)EDTA]^-$	Cr(0)	-1.60 V
Cr(III)-TTHA	Cr(II)-TTHA	-1.202 V
Cr(III)-DTPA	Cr(II)-DTPA	-1.16 V

The selected ligand would therefore have to provide an 'analytically clean' region at potentials more negative than ~ -1.1 V; specifically, no ligand reduction peaks should be observed.

The voltammogram of XO (at pH 6.2) for a cathodic Square Wave scan from -0.15 V to -1.7 V is shown in Fig. 3.3. pH 6.2 was chosen because, from the distribution diagram of XO (Fig. 3.4), it can be seen that at this

pH, equimolar amounts of H_3XO^{3-} and H_2XO^{4-} will be present in solution and since these species were believed to be the complex forming species, a preliminary evaluation at pH 6.2 seemed reasonable.

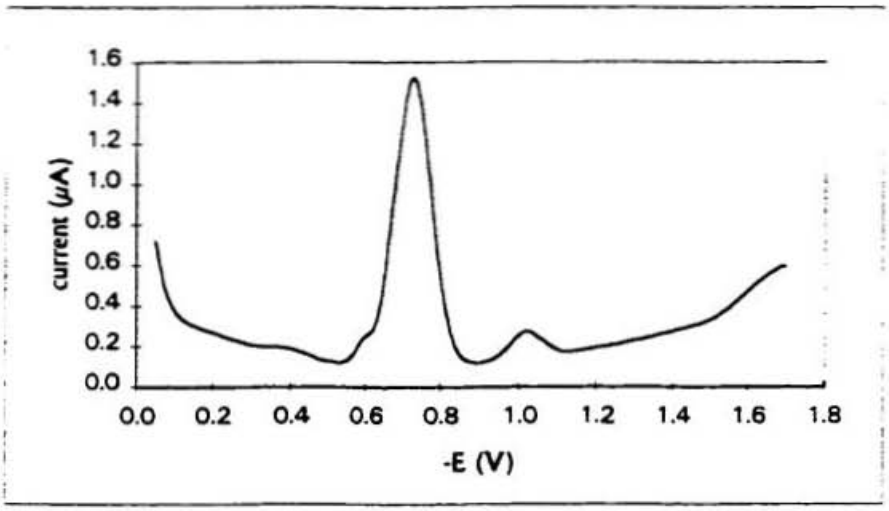

Fig. 3.3: CSV of XO at pH 6.2. Nanopure water and KCl supporting electrolyte, [XO] = 25 μM. Square wave scan rate = 200 mV/s

Fig. 3.3 shows that an analytically clean region is indeed obtained in the -1.1 to -1.7 V region. The peak at ~ -0.75 V in the voltammogram of XO results from an electrochemical reduction of the XO. The shape of the peak (the smaller peaks immediately preceding and following the main peak) suggests that this reduction occurs from an adsorbed state and the product remains adsorbed on the electrode [79]. However, given the complexity of the XO molecule, these peaks may also be resulting from more than one simultaneously occurring reduction processes.

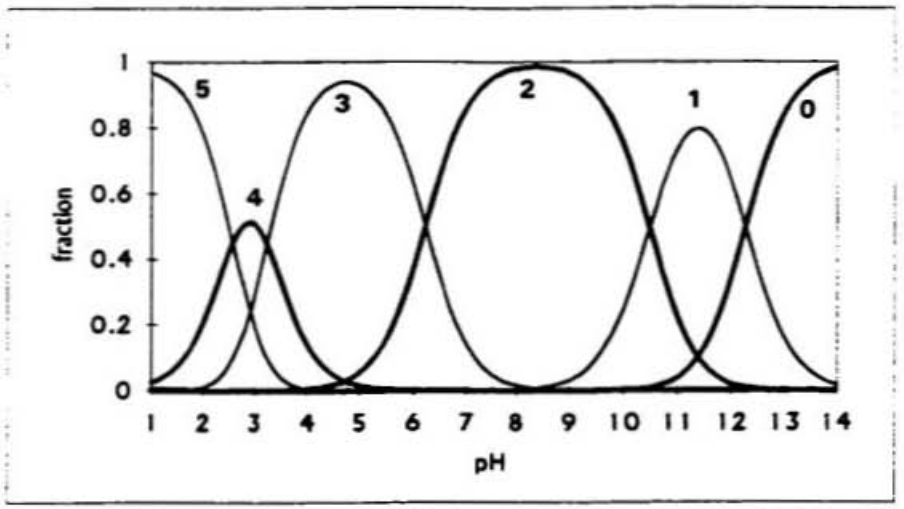

Fig. 3.4: Distribution of XO species in aqueous solution. 0-5 represent species XO^{6-}, HXO^{5-}, H_2XO^{4-}, H_3XO^{3-}, H_4XO^{2-} and H_5XO^{-} respectively. Data from ref. [119]

2. When 5 µg/L of Cr(VI) was added to an aqueous solution of XO and a voltammogram (cathodic scan, from -0.15 v to -1.65 V) obtained after a prior 60-s deposition at -0.15 V, a new peak appeared at ~-1.43 V. The height of this peak increased when the scanning was initiated from -1.15 V, after an accumulation at -1.15 V.

   This peak was found to be enhanced by increasing the deposition time and also by increasing Cr concentrations. No such peak was observed in the absence of Cr. It was therefore concluded that the peak was the consequence of the reduction of a Cr-XO species. Fig. 3.5 shows the voltammograms for the -1.15 to -1.6 V region before and after the addition of Cr(VI).

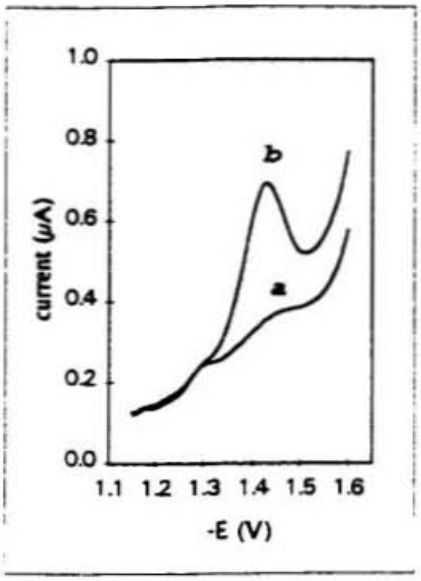

Fig. 3.5: Voltammograms showing the emergence of the Cr peak. (a) no added Cr, (b) 5 μg/L Cr(VI)

3. Both Cr(III) and Cr(VI) species generated the new peak, so the CSV method would be amenable to the determination of Cr(III) as well as Cr(VI). The Cr(III) peak was stable with time, in contrast with the observation that the Cr(III)-DTPA peak is transient [97, 101].

4. The Cr-XO reduction peaks seen above are not sensitive enough for the determination of Cr at the levels expected in natural waters (< 0.5 μg/L) and, in common with some existing CSV methods, a catalytic regeneration step would have to be incorporated with the reduction current measurement step so as to enhance the sensitivity of the method. Nitrate ions are known to oxidize Cr(II) species to Cr(III) [94, 122] and have been utilized for sensitivity enhancement in CSV methods for Cr determination

[96-101]. The role of NO_3^- in the catalytic mechanism is fully discussed in Section 4.3.

Addition of increasing amounts (100 µL aliquots) of 5 M $NaNO_3$ (AnalaR) to the Cr-XO solutions was shown to greatly enhance the Cr peaks seen above. In fact, the peak enhancement was so great that some source of contamination was immediately suspected. It was subsequently found that the AnalaR $NaNO_3$ contained high concentrations of Cr. Thereafter, only Suprapur grade or purified, Cr-free $NaNO_3$ was used. Addition of Suprapur $NaNO_3$ enhanced the Cr peaks in the expected manner. Voltammograms for the addition of NO_3^- to a XO/Cr solution, Cr to a XO/NO_3^- solution, and XO to a Cr/NO_3^- solution are shown in Fig. 3.6. These voltammograms clearly demonstrate that the peaks are due to Cr/XO and that NO_3^- enhances the peaks.

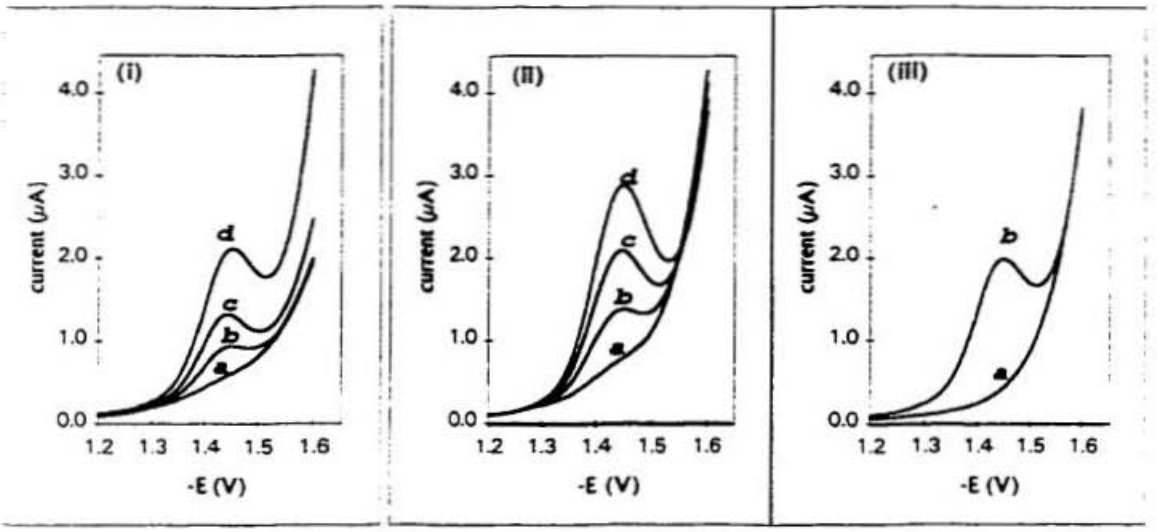

Fig. 3.6 (i): Addition of NO_3^- to a XO/Cr solution. [Cr] = 1 μg/L
μL NO_3^- added: (a) 0, (b) 100, (c) 300, (d) 800
(ii): Addition of Cr (100 μg/L) to a XO/NO_3^- solution.
μL Cr added: (a) 0, (b) 50, (c) 100, (d) 150
(iii): Addition of XO to a NO_3^-/Cr solution. [Cr] = 1 μg/L
μL XO added: (a) 0, (b) 50

5. The Cr-XO reduction peaks were found to be remarkably stable when Cr-XO solutions were left standing in the presence of mercury dispensed during the CSV experiments. There was hardly any loss in signal after 1 hour and even after being kept in the voltammetric cell for 3 days, the observed peak heights were about 40-50% of the original peak heights. This loss is due to the adsorption of species on the container walls and is normal, given the low amounts under consideration. The stability of the response is in sharp contrast to the observation that elemental mercury interferes in the CSV of Cr with DTPA as the complexing ligand [101].

Having demonstrated that the adsorptive deposition of the Cr-XO complex followed by its catalytic reduction at the Hg electrode in the presence of NO_3^- could form the basis of a new CSV method for Cr, conditions with respect to chemical and instrumental parameters were optimized for the determination of Cr in freshwaters and seawater.

3.3 CHOICE OF POTENTIAL MODULATION MODE

Square Wave (SW) voltammetry is now considered to be the most sensitive voltammetric technique available for ultra-trace analysis [123-125]. The superiority of this technique lies in the scheme of current measurement and the high scan rates attainable. The working of SW voltammetry is explained in most standard analytical chemistry textbooks, e.g., [126, 127] and in reference [124] and will not be repeated here. Reference [125] is an excellent source of information on the theory and application of SW voltammetry.

However, in this particular case, given the catalytic effect of NO_3^- in the stripping stage, a potential scan in the SW modulation may not necessarily be the best. This is because during the reverse pulse of the SW, the potential may remain negative enough to maintain the reduction of the Cr which is being chemically oxidized by the NO_3^-. In such a case, a cathodic current will occur even during the reverse pulse. This would then lead to a smaller resultant analytical current. This effect is demonstrated in Section 4.3. Better peaks may therefore be obtained by using a Differential Pulse (DP) modulation for the stripping step. A quick comparison between SW and DP modes of modulation showed that the SW mode was far better than DP. Fig. 3.7 compares voltammograms for 0.5 µg/L Cr in SW, DP and Linear Sweep (LS) modes.

At this concentration level, the DP peak is ill-defined and not amenable to quantitative analysis whereas excellent peaks are obtained for the SW modulation. A SW modulation was therefore selected for the stripping step in all CSV experiments. No peak was obtained if a linear sweep scan was utilized. The linear sweep voltammogram is included in the comparison because it has some implications in the cyclic voltammetry of the complex, discussed in Section 4.4. Linear Sweep Voltammetry (LSV) is very insensitive as compared to pulse (DP and SW) voltammetric techniques and is usually not used for trace analysis.

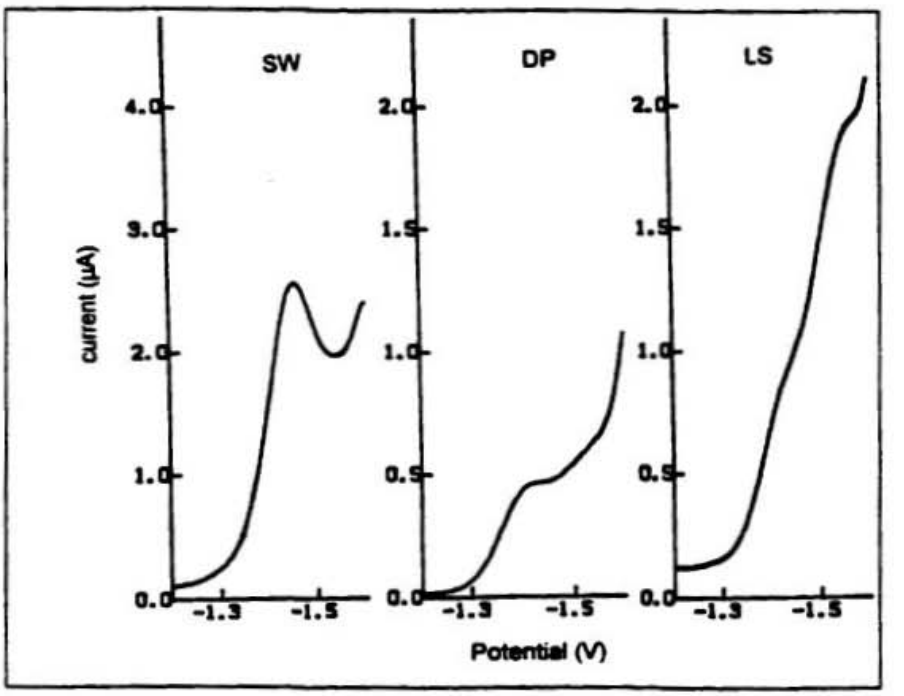

Fig. 3.7: Comparison of Square Wave (SW), Differential Pulse (DP) and Linear Sweep (LS) scanning modes.

3.4 CHOICE OF BUFFER

The optimum pH for Cr determination was found to be 7.10±0.05 in Nanopure water and 6.7±0.1 in seawater (Section 3.5.1). Preliminary work was carried out in Nanopure water buffered with $HOAc/OAc^-/NH_3$. Although the buffer capacity of the acetate system at this pH is very low, it worked well for buffering Nanopure but it was impossible to buffer seawater to a pH greater than about 6.2 with $HOAc/OAc^-/NH_3$; a new buffer system then had to be found. Three different buffers were tried:

HEPES (*N*-2-Hydroxyethylpiperazine-*N*'-2-ethanesulphonic acid), $pK_a = 7.56$

Bis-Tris (bis[2-Hydroxyethyl]iminotris[hydroxymethyl]methane), $pK_a = 6.5$ and

PIPES (piperazine N,N'-bis[2-ethanesulphonic acid]), $pK_a = 6.8$

The buffering capacity of HEPES in Nanopure water and seawater was good but a large peak extending from -1.35 V to - 1.85 V and centred at -1.7 V was observed in Nanopure water buffered to pH 6.8 with HEPES. This peak is probably due to the reduction of H^+ and since this peak is in the region of the analytical peak, no further use was made of HEPES.

Bis-Tris/HCl was found to be very effective at buffering Nanopure water but not very good for seawater at pH 6.7; the pH of Bis-Tris buffered seawater kept decreasing with time. However, excellent buffering (in both Nanopure water and

seawater) could be obtained when a mixture of Bis-Tris, HOAc, OAc^- and NH_3 was used. However, the presence of $OAc^-_{(aq.)}$ led to very high background currents at potentials more negative than -1.4 V, especially in seawater at pH 6.7, so it was decided not to use this combination of buffers.

PIPES, used in conjunction with NH_3 and HCl, was very efficient in buffering Nanopure water to pH 7.1 and seawater to pH 6.7 and it did not have any adverse effect on the background current. Further, its use as the buffer resulted in higher peak currents than the Bis-Tris. Hence, it was adopted for all further work.

Two observations made during experiments for the choice of a buffer system are worth mentioning:

1. it was found that under similar conditions, using a combination of Bis-Tris, HOAc, OAc^- and NH_3 as the buffer gave rise to CSV responses that were almost twice as high as the responses obtained when HOAc/OAc^-/NH_3 or Bis-Tris/HCl was used separately. This behaviour was not further investigated.
2. The buffering of seawater posed an unexpected and unexplained complication. It was found that when the buffering of seawater was attempted by adding the required amount of buffer, either Bis-Tris or PIPES (and HCl/NH_3, for final adjustment to the desired pH), the pH of

the solution gradually rose to a value about 1-1.5 pH units above the required pH and then slowly to decrease back to the originally adjusted value. The pH of seawater therefore kept changing for about 30 minutes under these circumstances. However, if the seawater is first acidified with of 0.2 M HCl (to pH ~ 3.5), stirred for a few seconds and then buffered to the desired pH with Bis-Tris or PIPES, the solution achieved a stable pH. Therefore, in all experiments, seawater as well as Nanopure water samples were briefly acidified with 50 µL of 0.2 M HCl and then buffered to the desired pH by the addition of PIPES and NH_3/HCl under pH meter control.

3.5 OPTIMIZATION OF CHEMICAL PARAMETERS

For obtaining the best analytical conditions, the following parameters were optimized: pH, deposition potential, ligand concentration, concentration of NO_3^-, buffer concentration and deposition time. Optimization experiments were carried out by studying the effect of variation of the parameters on the height of the reduction current, i_p. Results of the optimization exercise are presented in Sections 3.5.1-3.5.6.

With the notable exception of pH, all optimized instrumental and chemical parameters were found to be similar for Cr(III) and Cr(VI) in both seawater and Nanopure. The sensitivity of the method was found to about ~30% lower in seawater as compared to Nanopure water and additionally, the sensitivity for Cr(III) was ~30-35% lower than Cr(VI) sensitivity in both media. Unless otherwise specified, all the results shown pertain to seawater solutions containing 1 µg/L added Cr(VI).

A typical voltammogram, obtained under optimized conditions, is shown in Fig. 3.8, by way of illustrating the method of calculating the peak height and some other parameters used in the course of this thesis.

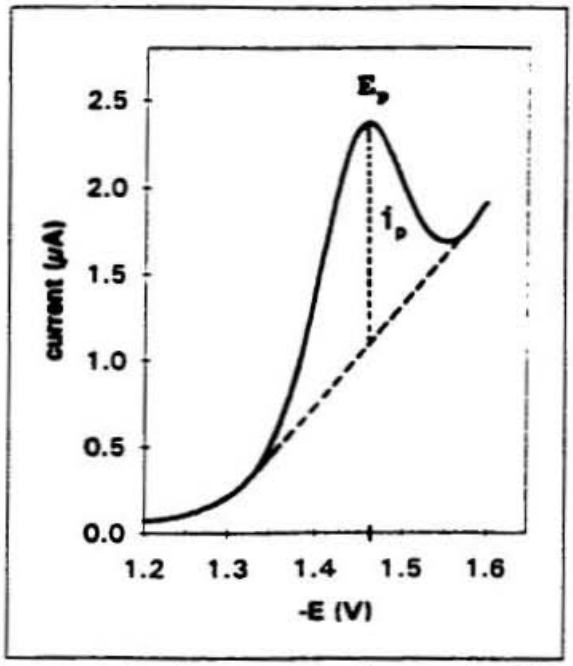

Fig. 3.8: A typical voltammogram showing the Cr peak

3.5.1 pH

Fig. 3.9 shows the dependence of i_p on the pH of the sample in seawater and in Nanopure water.

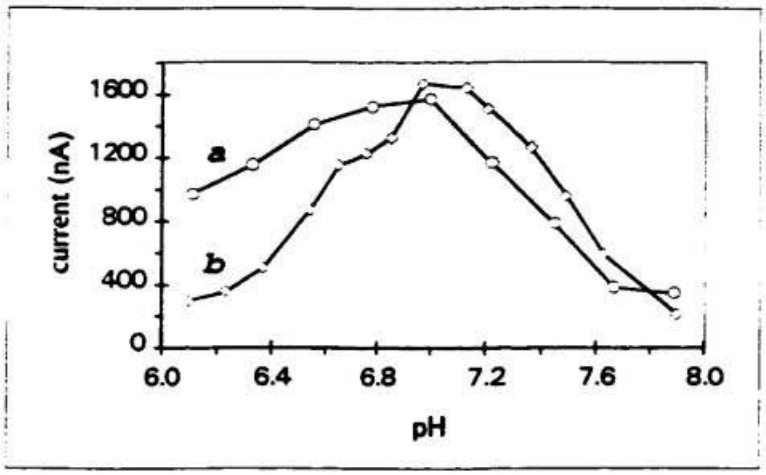

Fig. 3.9: Dependence of reduction peak current on pH. (a): seawater, 0.15 μg/L Cr and (b): Nanopure water, 0.1 μg/L Cr.

The i_p-pH plots show that the i_p is highly pH-dependent and maximum sensitivity occurs within a very narrow pH range. Hence for accurate calibration, it is very important to maintain the pH to within ±0.05 units, especially in Nanopure water. This can be achieved by using the PIPES/NH_3/HCl combination as described in Section 3.4.

For Cr determination, the optimum pH was chosen to be 7.1 in Nanopure water and 6.7 for seawater because the rate of change of the response with pH is least at these pH.

3.5.2 Deposition Potential

The dependence of i_p on the deposition potential in the proximity of the half-wave potential is shown in Fig. 3.10. The response to E_{dep} at deposition potentials less negative than -0.9 V is different for Cr(VI) and Cr(III) and forms the basis for the speciation Cr. This is discussed further in Section 3.7.

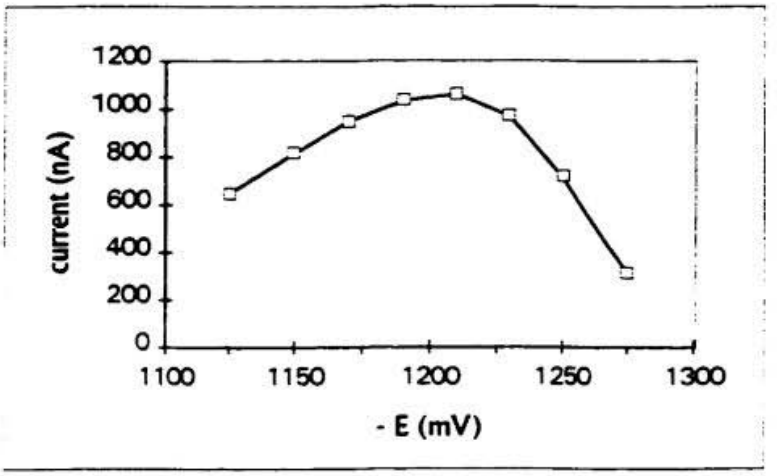

Fig. 3.10: Dependence of peak current on deposition potential

From the i_p/E graph, a deposition potential of -1.2 V was found best for optimal Cr determination.

3.5.3 Concentration of XO, [XO]

Fig. 3.11 depicts the variation of i_p with [XO].

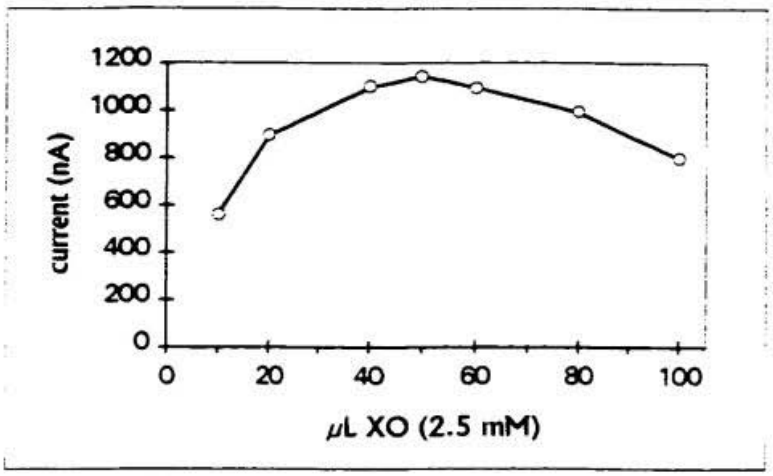

Fig. 3.11: Dependence of peak current on [XO]

The best sensitivity was attained with an addition of 40-60 μL of 2.5 mM XO. For all further work, 50 μL of 2.5 mM XO was used. This is equivalent to a final concentration of ~12.5 μM XO which, at a Cr level of 0.5 μg/L (~0.01 μM), is more than 1000 times greater than [Cr]. Optimal [XO] was found to be independent of [Cr] in solution for an added Cr of up to 10 μg/L.

3.5.4 Concentration of Nitrate Ions, [NO_3^-]

The effect of [NO_3^-] on i_p is shown in Fig. 3.12; i_p values have been corrected for the effect of dilution on [Cr] but not on [XO].

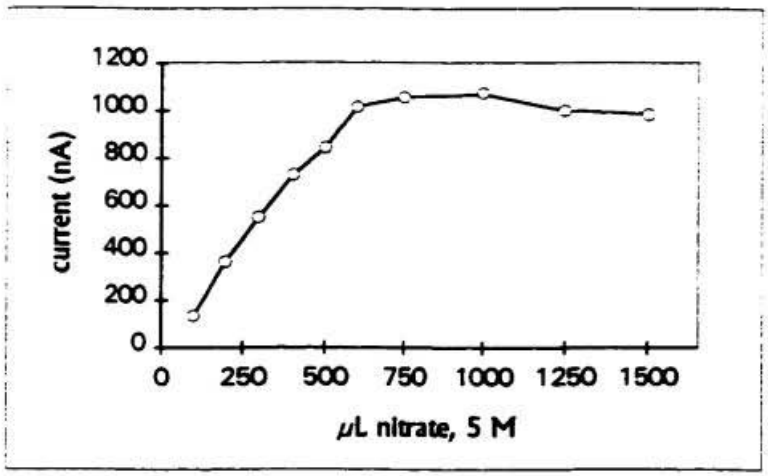

Fig. 3.12: Dependence of peak current on nitrate concentration

i_p increases almost linearly with [NO_3^-] until about 600 µL of 5 M NO_3^- has been added. Thereafter, i_p increases non-linearly until 1 mL NO_3^- has been added. Beyond this [NO_3^-], a slight decrease is noticed with increasing NO_3^-. This decrease is probably due to a decrease in [XO] as more and more NO_3^- is added.

For all further work, 750 µL of 5 M $NaNO_3$ was used in both Nanopure and seawater. This gives an effective concentration of ca. 0.35 M NO_3^- in solution.

3.5.5 Concentration of Buffer

The stock buffer solution was 0.1 M PIPES in NH_3. Variation of the buffer concentration did not affect i_p over a range of 20-250 µL added buffer solution (~0.2-2.5 mM final PIPES concentration). The concentration of buffer to be used was therefore contingent on the buffer capacity of the solution rather than its effect on the voltammograms. At the lower concentration end (for a buffer addition of less than 50 µL) the solution pH, especially in seawater, was highly changeable whereas excellent buffer capacity was achieved upon an addition of 100 µL buffer, equivalent to a final PIPES concentration of ~1 mM. All solutions were therefore buffered with 100 µL of the buffer solution.

3.5.6 Deposition Time, t_{dep}

As expected for stripping analysis, i_p increased with increasing deposition time. Fig 3.13 depicts the voltammograms for increasing deposition times, from 30 s to 10 min.

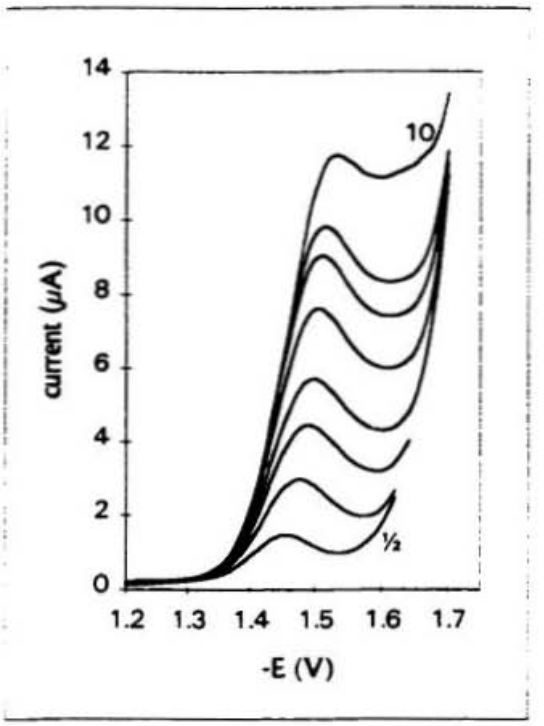

Fig. 3.13: Effect of deposition time on the peak current. Voltammograms obtained for t_{dep} ½, 1, 1½, 2, 3, 4, 5 and 10 min respectively.

The values of i_p are plotted against t_{dep} in Fig 3.14. Also shown in Fig. 3.14 is the variation the sensitivity with t_{dep} (sensitivity is the peak height per unit time).

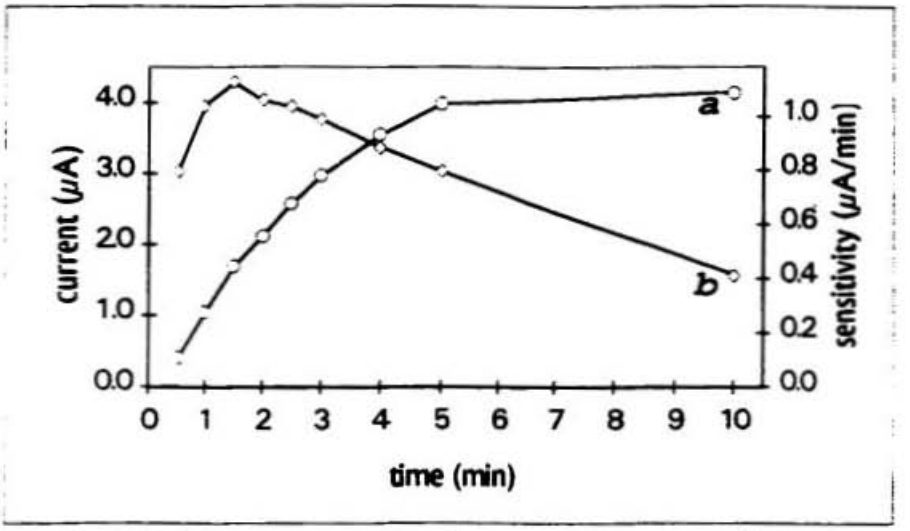

Fig. 3.14: Dependence of peak current, (a) and sensitivity, (b) on deposition time.

The shape of the peaks deteriorate as t_{dep} is increased, because of an increase in the background current.

I_p hardly increases for deposition times greater than 5 min: this is probably due to a complete coverage of the mercury surface by the adsorbate. Maximum sensitivity is obtained for a 90-s deposition but a deposition time of 60 s was found to be adequate for the determination of Cr at levels encountered in seawater and was adopted for all further work.

3.6 OPTIMIZATION OF INSTRUMENTAL PARAMETERS

3.6.1 Drop Size

The PAR Model 303A SMDE offers the choice of 3 fixed drop sizes - 'Small', 'Medium' and 'Large', with a volume ratio of 1:2:4, corresponding to an area ratio of 1:1.6:2.5 (EG&G PAR Model 303A SMDE manual). Assuming spherical drops, the actual calculated areas of the drops are: Small Drop = 0.0096 cm^2, Medium Drop = 0.0156 cm^2 and Large Drop = 0.0261 cm^2 (personal communication, EG&G Princeton Applied Research).

Since the analytical signal is dependent upon the amount of analyte deposited on the electrode prior to the scanning step, it is obvious that a higher value of i_p will be obtained with an increase in the electrode area. However, the increase in i_p will also be accompanied by an increase in the background current. Fig. 3.15 compares voltammograms for the 3 drop sizes. The calculated values of i_p are 578, 883 and 1304 nA for small, medium and large drops respectively. Since a background subtraction method has been employed for quantification (Section 3.9), large drops were used for analysis, resulting in higher i_p values; this meant that shorter deposition times could be used.

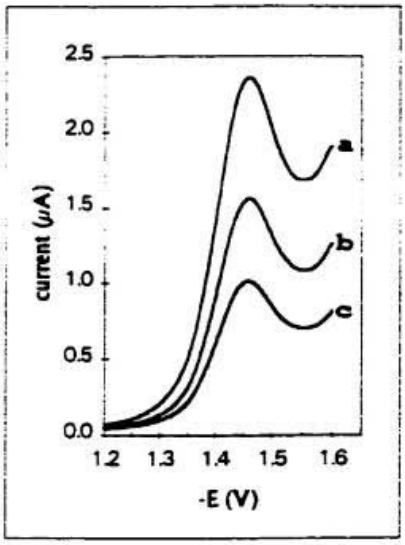

Fig. 3.15: Cr peaks using large (a), medium (b) and small (c) drops

3.6.2 Stirring Rate

Stirring during the accumulation step affects the mass-transport to the electrode and it is obvious that a higher stirring rate will lead to a faster rate of accumulation and, provided the surface saturation of the electrode is not reached, a greater amount of the analyte species will be deposited on the electrode. The stirrer used in the experiments (EG&G PAR Model 305 Stirrer) is specifically designed for use with the Model 303A SMDE. Two stirring rates are possible: 400 rpm and 700 rpm. Fig. 3.16 shows voltammograms resulting from the operation of the stirrer in the non-stirring, slow and fast modes. The calculated values of i_p are 222 nA (no stirring), 994 nA (slow) and 1249 nA (fast). The stirrer was used in the fast mode for all experiments.

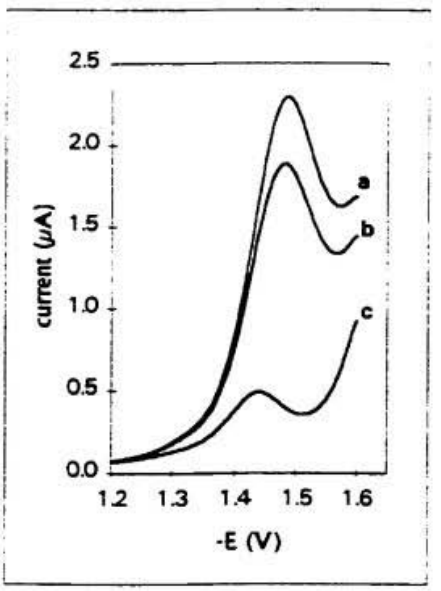

Fig. 3.16: Comparison of stirring rates. (a) fast stirring, (b) slow stirring and (c) no stirring

3.6.3 Square Wave Parameters

Although Square Wave voltammetry has now been employed for stripping analysis for more than a decade, there has still not been any systematic study of the effect of the various SW parameters (square wave amplitude, frequency and step increment) on the analytical response. Indeed, a survey of the literature on the application of SW voltammetry in the adsorptive CSV of electrochemical systems similar to the Cr-XO-NO_3^- system (i.e., when a reversible electrochemical reduction occurs from an adsorbed state and the resulting current is catalytically enhanced), shows that no attempt has been made to correlate i_p with SW parameters. Optimization of SW parameters has been achieved with the sole objective of obtaining the best i_p. The following work was also carried out strictly from a point of view of obtaining the best analytical signal from the system but where possible, an attempt has been made to rationalize the results of this study in terms of information available in the literature.

3.6.3.1 Square Wave Amplitude (E_{sw})

According to the theory of SW voltammetry [128], for a reversible system, the reduction current should increase with an increase in the amplitude because on the reverse pulse, the reducible species is regenerated by oxidation of the reduced species. This increase in the current is accompanied by an increase in $W_{1/2}$, the peak width at half height. For such systems, $W_{1/2}$ is 90.5/n mV (n is the number of electrons involved in the reduction) for small values of E_{sw} and approaches $2E_{sw}$ for very large values of E_{sw}. O'Dea et al. [129] however deemed it reasonable to maximize the value $i_p/nW_{1/2}$, which, in analytical terms, is related to the sensitivity times the resolution and their results show that the value $nE_{sw} = 50$ is optimal.

In the present study, $W_{1/2}$ remained almost constant at ~85 mV as E_{sw} was varied in the 10-90 mV range. Table 3.2 and Fig. 3.17 show the effect of E_{sw} on some analytical parameters. I_b is the baseline current at E_p; it is obtained by subtracting i_p from the total current at E_p.

Table 3.2: Effect of variation of E_{sw} on i_p and E_p (scan rate = 200 mV/s)

E_{sw} (mV)	i_p (nA)	i_b (nA)	i_p/i_b	$-E_p$ (mV)
10	235	268	0.877	1464
20	445	515	0.864	1462
25	517	606	0.853	1462
30	574	736	0.780	1458
40	703	964	0.729	1456
50	770	1187	0.649	1450
60	744	1363	0.546	1446
70	731	1492	0.490	1436
80	681	1646	0.414	1432
90	502	2019	0.249	1428

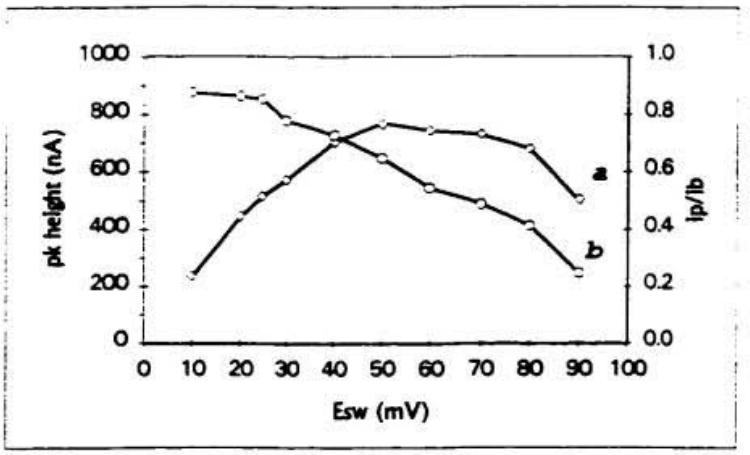

Fig. 3.17: Effect of E_{sw} on i_p (a), and i_p/i_b (b)

The peak current attains a maximum value at E_{sw} = 50 mV, and then decreases with a further increase in E_{sw}. The decrease in i_p beyond 50 mV can be explained by the fact that there is a consecutive irreversible process coupled to the reduction process (see Section 4.5). Very high values of E_{sw}, in the forward

pulse, make the potential negative enough for the second process to occur. Since this step is irreversible, there are less and less species for the catalytic regeneration and therefore a decrease in i_p is observed. A similar observation has recently been published [130] for the SW voltammetry of the Dimethyl Yellow. This example does not involve catalytic regeneration however.

In the choice of a value of E_{sw} to be adopted for the purpose of further analytical work, another parameter which had to be considered was the baseline current. As E_{sw} increases, so does the baseline current. The increase in the background current with increasing E_{sw} is depicted in Fig. 3.18 which compares voltammograms obtained for some values of E_{sw} from 10 mV to 50 mV.

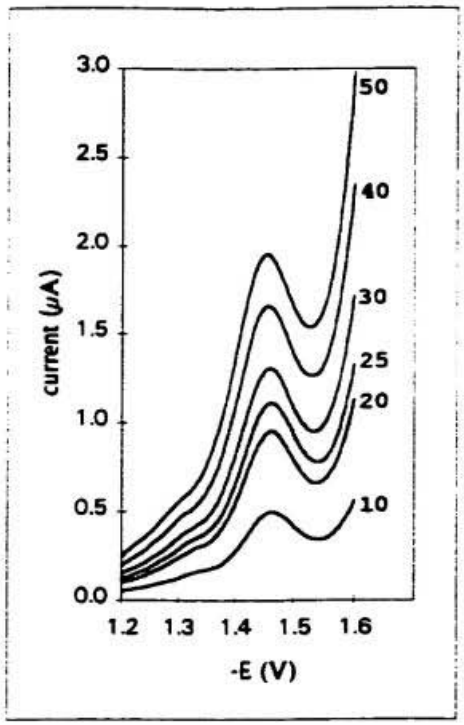

Fig. 3.18: Effect of E_{sw} on the Cr peaks. Voltammograms for E_{sw} = 10, 20, 25. 30, 40 and 50 mV.

Since the reduction current is seen on the rapidly increasing part of the voltammogram, the ratio of i_p/i_b can be critical in the proper quantification of the peak heights, especially at very low levels of the analyte. Fig. 3.17 shows that at E_{sw} = 25 mV, a good compromise is attained between a reasonable high value of i_p and the ratio i_p/i_b, so this value was adopted for all further work.

3.6.3.2 Step Increment, E_s and Frequency, f

Since the scan increment and the frequency of the scanning step are related (scan rate = E_s x f), these two parameters are discussed together. Tables 3.3-3.5 show the effects of E_s and f on i_p.

Table 3.3 Effect of variation of E_s at constant frequency (f= 100 Hz, E_{SW}=25 mV)

E_{step} (mV)	i_p (nA)
2	717
4	1009
6	1103
8	1202
10	1235

Table 3.4: Effect of variation of E_s at constant scan rate (E_{SW}=25 mV)

f (Hz)	E_{step} (mV)	i_p (nA)
100	2	706
50	4	638
33	6	609
25	8	612
20	10	586

At a constant frequency, i_p rises with increasing E_s in the range studied. However, the analytical signal is known to be only a weak function of E_s and the maximum E_s generally chosen is 10n mV [125]. The increase in i_p with E_s in this case is therefore attributed to the concomitant increase in the scan rate. This can be seen from Table 3.4 where E_s and f are varied in such a way as to keep

the scan rate constant at 200 mV/s. In this case, the highest i_p is obtained from the lowest E_s, which also means the highest frequency - see below.

In SW voltammetry, E_s, from an analytical point of view, can be related the resolution of the reduction peak: a small value of E_s will result in the data points being closer to each other and will give a visually pleasing voltammogram. Also, smaller values of E_s will lead to less error in peak height calculation; this can be critical at very low levels of analyte. For adequate peak definition and evaluation, the smallest value allowed by the instrument, i.e., E_s= 2 mV was therefore adopted for further work.

Table 3.5 and Fig. 3.19 show the effect of the frequency (at constant E_s) on i_p.

Table 3.5: Effect of variation of f at constant E_s (E_s=2 mV, E_{sw}=25 mV)

f (Hz)	i_p (nA)	i_b (nA)	i_p/i_b
40	332	509	0.652
50	394	575	0.685
60	470	670	0.701
70	561	702	0.799
80	389	1068	0.364
90	623	1000	0.623
100	656	1034	0.634
110	689	1031	0.668
120	720	1143	0.630

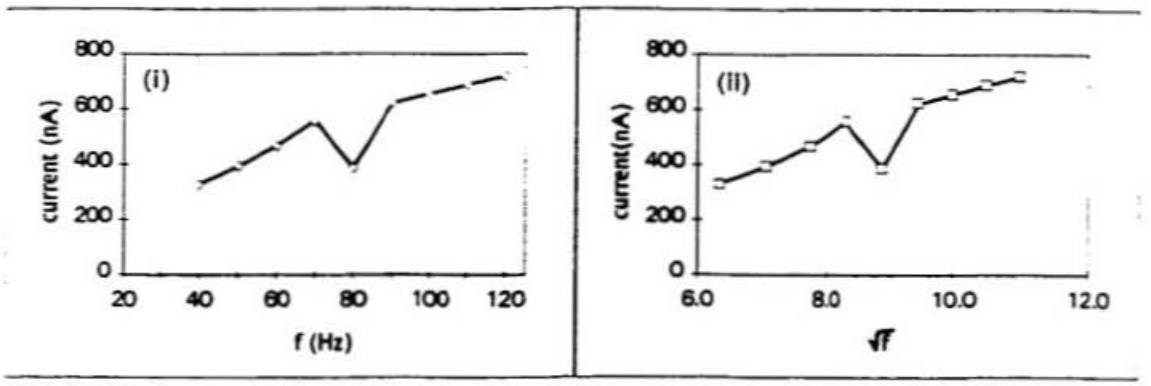

Fig. 3.19: Variation of i_p with f (i) and $f^{1/2}$ (ii).

As expected from theory, i_p increases with f; i_p is in fact proportional to $f^{1/2}$ for reversible processes [125]. A higher frequency leads to greater sensitivity because a given amount of analyte is reduced in a shorter time. It should be noted, however, that increasing the frequency also leads to an increase in the background current because a shorter time elapses between successive current measurements, with the result that the capacitance current is less fully decayed at the time of the measurement. This is shown by the increasing i_b in Table 3.5. The i_p/i_b values do not change significantly in the range of frequency studied, however, because of a proportional increase in i_p.

The value of i_p is abnormally low at 80 Hz; this f value also seems to be the demarcation line between two distinct linear portions in the i_p-$f^{1/2}$ plot; one in the 40-70 Hz region (r = 0.99, slope = 112 nA $s^{1/2}$) and the other in the 90-120 Hz region (r = 1, slope = 66 nA $s^{1/2}$). Illustrative voltammograms for f = 50, 70, 80 and 90, 110 Hz are shown in Fig. 3.20.

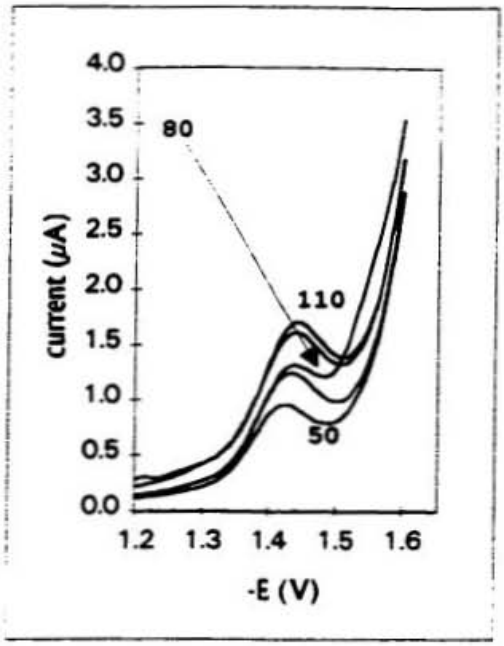

Fig. 3.20: Voltammograms at 50, 70, 80, 90 and 110 Hz

The abnormal behaviour at 80 Hz was not investigated any further but it is thought to be due to a resonance phenomenon between the applied frequency and the natural frequency of the mercury drop on the HMDE [131]. This may also be responsible for the different instrumental responses witnessed above in the two frequency regions.

On the basis of the i_p-f response, a frequency of 100 Hz was arbitrarily chosen for all further work. This, combined with a E_s value of 2 mV, gives an effective scan rate of 200 mV/s which translates into a scanning time of 2 s for a 400 mV range (the normal analytical peak is obtained on scanning the potential from -1.2 V to -1.6 V).

3.7 SPECIATION

The optimized conditions for the determination of Cr, worked out in Sections 3.5 and 3.6 are summarized below. These conditions will be used for all further work described in Chapter 3.

CHEMICAL PARAMETERS

- pH: 6.7 (Seawater), 7.1 (Nanopure water)
- E_{dep}: -1.2 V
- [XO]: 12.5 μM
- $[NO_3^-]$: 0.35 M
- [Buffer]: 1 mM PIPES

INSTRUMENTAL PARAMETERS

- Drop Size: Large
- E_{SW}: 25 mV
- E_s: 2 mV
- f: 100 Hz

After the optimization process, the next objective in the method development was to devise a means for the Cr speciation on the basis of its oxidation state, i.e., Cr(VI) and Cr(III). It has already been found that both Cr species can complex with XO to give CSV electroactive complexes. The sensitivity for Cr(III) is about 65-70% that of Cr(VI). This difference in sensitivity between Cr(III) and Cr(VI) at first seemed to severely limit the applicability of the method because it meant that it would be impossible to quantify even the total Cr in a sample unless a pretreatment step is carried out to convert total Cr to either one or the other form. Under these circumstances, speciation would be impossible to implement.

3.7.1 Selective Determination of Cr(VI)

Examination of i_p-E_{dep} plots revealed an avenue for the elaboration of a speciation method. In Section 3.5.2 it was seen that in the proximity of the reduction potential of the Cr-XO complex, both Cr species give the best response for E_{dep} = -1.2 V. The dependence of i_p on E_{dep} was further investigated by varying E_{dep} over the potential ranging from 0 to -1.3 V. During these experiments, the experimental procedure was slightly modified: following the analyte deposition at a given E_{dep} for 70 s, the potential was scanned from -1.2 to -1.6 V. Before the potential scan, the solution was allowed to reach quiescence by manually turning off the stirrer during the final 10 s of the deposition period and no instrumental equilibration step incorporated in the voltammetric set-up, as was done in previous experiments when the potential scan was initiated from the same potential as E_{dep}. This is because the working of the Polarographic Analyser is such that during an instrumentally initiated equilibration stage, the electrode assumes the potential at which the scan is to be started; in this particular case a 10-s equilibrium step would entail a deposition of Cr(VI) and Cr(III) from -1.2 V for 10 s, which is not desirable.

At the chosen scan rate of 200 mV/s, the scan will take only 2 s for completion and the electrode would experience a potential of -1.2 V to about -1.25 V (the potential at which both Cr(III) and Cr(VI) are liable to be deposited) for only

about 0.25 s. Any Cr deposited during the scanning period can therefore be neglected.

Fig. 3.21 shows that the dependence of i_p on E_{dep} for Cr(III) and Cr(VI).

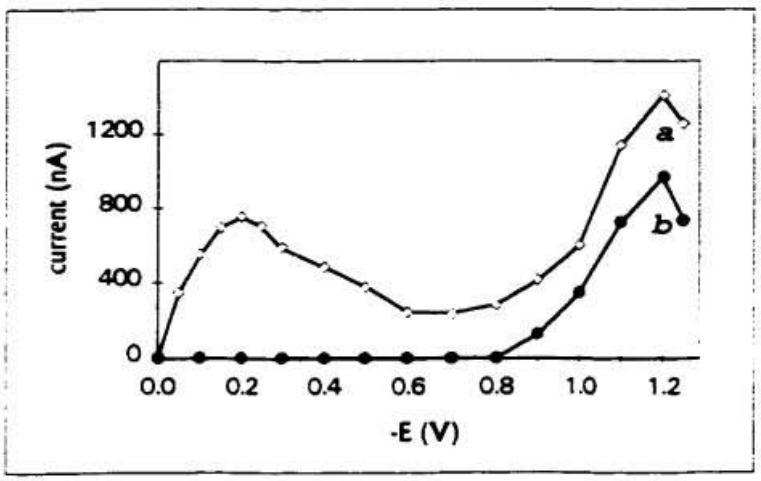

Fig. 3.21: Variation of i_p with E_{dep} (a): Cr(VI), (b): Cr(III)

The striking features of Fig. 3.21 are:

1. reduction peaks for Cr(III) and Cr(VI) show similar dependence on deposition potential at E_{dep} more negative than -0.9 V.
2. For E_{dep} less negative than -0.9 V, no Cr(III) peaks are obtained but Cr(VI) peaks can still be detected over the deposition potential range of -0.05 to -0.8 V.
3. In the potential region less negative than -0.9 V, the sensitivity for the determination of Cr(VI) is optimum at E_{dep}= -0.2 V. Under similar

conditions, the peak height resulting from a deposition at -0.2 V is about 50-60% of the peak height from a deposition at -1.2 V.

The i_p-E_{dep} plots in Fig. 3.21 will be discussed further in Chapter 4, with reference to the mechanism of the electrode processes.

The observation that Cr(III) could be detected only for deposition potentials more negative than -0.9 V immediately leads to the possibility of a speciation method based on the selective deposition/determination of the Cr(VI)-XO species. In a solution containing both Cr species, Cr(VI) can be selectively determined by deposition at -0.2 V followed by scanning from -1.2 V. Cr(III)-XO species will not be deposited at this potential.

To avoid possible confusion and for the sake of brevity, henceforth Cr peaks resulting from a deposition potential of -0.2 V and -1.2 V will be referred to as $^{-0.2V}$Cr and $^{-1.2V}$Cr respectively.

3.7.1.1 Optimization of Cr(VI) Response

The $^{-0.2V}$Cr(VI) response was optimized with respect to chemical parameters (pH, [XO] and [NO_3^-]) as in Section 3.5. All optimized parameters were found to be identical to $^{-1.2V}$Cr(VI) and $^{-1.2V}$Cr(III) and so the optimization results are not discussed here. As already mentioned, the sensitivity of the $^{-1.2V}$Cr(VI), $^{-0.2V}$Cr(VI) and $^{-1.2V}$Cr(III) peaks is different, approximately in the ratio 3:1.5:2.

The fact that, except for their relative sensitivities, peaks resulting from $^{-1.2V}$Cr(VI), $^{-0.2V}$Cr(VI) and $^{-1.2V}$Cr(III) optimize under similar chemical conditions implies that, irrespective of the deposition potential or of the initial oxidation state, the voltammetric peak is being produced by the reduction of the same Cr-XO species. This will be discussed further in Chapter 4.

3.7.2 Speciation Strategies

Following the selective determination of Cr(VI) as $^{-0.2V}$Cr(VI), for the complete speciation of Cr, a method now had to be devised for the determination Cr(III). Two different approaches were explored:

1. masking of Cr(VI) as either a precipitate or a soluble complex and determination of Cr(III) by the CSV of its XO complex, with a deposition at -1.2 V, or
2. determination of total Cr as either $^{-1.2V}$Cr(VI) or $^{-1.2V}$Cr(III) following an oxidation or a reduction step; the difference between total $^{-1.2V}$Cr and $^{-0.2V}$Cr(VI) would then be equivalent to Cr(III).

An important aim of the speciation method was to keep it as simple and as convenient as possible. The search was for a sample pre-treatment step which was rapid, involved minimal sample manipulation and required minimum use of additional reagents, hence minimizing contamination from reagents. Therefore, any step involving for example, filtration, heating, digestion, u.v irradiation etc. was precluded. Furthermore, for the sake of contamination control, all sample manipulation was to be performable on the clean bench and in the voltammetric cell.

3.7.3 Masking of Cr(VI)

The rationale behind masking Cr(VI) was to make all Cr(VI) in solution non-labile by preventing the formation and deposition of the Cr(VI) derived Cr-XO complex. Any reduction peak observed in the CSV of a Cr(VI)/Cr(III) could then be ascribed to Cr(III) only.

To this end, the precipitation of Cr(VI) as chromates ($BaCrO_4$, $PbCrO_4$) was attempted but proved unsuccessful, probably because of the minute amounts of Cr involved. At 18 °C the solubility products of $BaCrO_4$ and $PbCrO_4$ are $1.6x10^{-10}$ and $1.77x10^{-14}$ respectively [108]. For a solution containing 0.5 µg/L (~10 nM) Cr(VI) as CrO_4^{2-}, the quantitative (99%) precipitation of the CrO_4^{2-} as $BaCrO_4$ and $PbCrO_4$ will require a minimum solution concentration of 1.6 M Ba^{2+} and $1.77x10^{-4}$ M Pb^{2+}. It would be impractical to add such levels of metals ions in solution. However, coprecipitation of $BaCrO_4$ with $BaSO_4$ has been used as a basis for the speciation of Cr in water by Differential Pulse Polarography [95].

A second approach to masking Cr(VI) species was through the use of a complexing agent which would selectively bind Cr(VI) and keep it in solution. Such an approach is well known in titrimetric analysis and has also been employed in CSV; for example, Vukomanovic and vanLoon [132] used citrate for obviating the interference of Al(III) in the determination of V when using pyrocatechol violet (PCV) as the complexing ligand. Apparently, the citrate

complexation of Al(III) prevented the formation of the interfering Al-PCV complex.

For this method to work in the present case, the complexation reaction has to occur selectively between Cr(VI) and the complexing agent. Further, the resulting complex should not adsorb on the mercury drop or be electroactive (from the bulk solution). ADDC (ammonium diethyldithiocarbamate, $(C_2H_5)_2NCSSNH_4$) is a well known chelating agent in trace metal analysis. It is reported that ADDC (or NaDDC) can form complexes with at least 50 elements. Interestingly, it has been found that this compound complexes Cr(VI) but not Cr(III) [133]. A survey of the literature showed that it has not previously been used as a ligand in CSV, most probably because its complexes do not adsorb on mercury. Therefore, it seemed particularly well-suited as a masking agent for Cr(VI) and its potential was evaluated.

Some CSV experiments were therefore carried out by adding an excess of ADDC to the Cr-XO in the voltammetric cell. Results showed that although ADDC did not interfere with the determination of Cr, it was not effective as a masking agent for Cr(VI): $^{-0.2V}$Cr(VI)-XO reduction peaks could still be seen in the CSV experiments.

In the light of the processes thought to be occurring at the electrode surface, the failure to mask Cr(VI) is not surprising. In Chapter 4, it is postulated that the Cr

complex that is deposited and eventually reduced to produce the analytical peak is Cr^{III}-XO; this complex is formed on the electrode surface by the reaction between adsorbed XO and Cr(II) produced *in situ* by the reduction of Cr(III) or Cr(VI) species. Any Cr species in solution (including the Cr(VI)-DDC complex) reaching the electrode during the deposition stage is susceptible to get reduced, react with adsorbed XO and subsequently respond during the stripping stage.

Similarly, in the case of masking by precipitation of Cr(VI) as chromates, there is the possibility of the precipitate itself adsorbing on the mercury and interfering in the determination stage. Also, the loss of Cr(III) by coprecipitation was possible.

Hence an interference free determination of only Cr(III) does not seem possible as long as the Cr(VI) species are present in the voltammetric cell and it became apparent that speciation by masking Cr(VI) could not be achieved without the incorporation of a separation step. This approach to speciation was therefore abandoned and the focus shifted to determination of total Cr.

3.7.4 Determination of Total Chromium

Oxidation of Cr(III) to Cr(VI) (with, for example, $KMnO_4$ or $K_2S_2O_8$), or reduction of Cr(VI) to Cr(III) (with Fe^{2+}) is thermodynamically possible and is routinely used in titrimetric analysis. An attempt was therefore made at converting total Cr to either Cr(VI) or Cr(III) species by direct introduction of the oxidant or reductant to the voltammetric cell.

The oxidation of Cr(III) was attempted by separately adding a 50-fold excess (relative to Cr) of $KMnO_4$ and $K_2S_2O_8$ to solutions of Cr(III) in a voltammetric cell. CSV of these solutions under optimized conditions resulted in the emergence of $^{-0.2V}$Cr peaks, indicating that oxidation of Cr had indeed occurred with $KMnO_4$ and $K_2S_2O_8$. However, recovery of the resulting Cr was very low (< 40%) and further additions of Cr showed that the CSV sensitivity of Cr determination was greatly reduced in the presence of these oxidizing agents.

Similarly it was seen that reduction of Cr(VI) could be achieved by Fe^{2+}, as evidenced by the complete disappearance of $^{-0.2V}$Cr(VI) peaks from Cr(VI)/XO solutions to which a 50-fold excess of Fe^{2+} had been added. However, it was found that the resulting Cr(III) was no longer CSV labile, i.e., Cr peaks were not seen even from a deposition potential of -1.2 V. The excess Fe^{2+} in solution interfered with the determination of Cr. The interference due to Fe^{2+} is addressed more fully in Section 3.8.4.

The low recovery of Cr and the subsequent interference from the oxidizing/reducing agents in the above experiments pointed to the fact that for accurate and interference-free Cr determinations, it is imperative that any excess oxidant/reductant be removed from the solution before the CSV step. This was not possible without the incorporation of additional step(s) in the procedure; getting rid of MnO_4^- or $S_2O_8^{2-}$, for example, would involve heating/boiling the solution and this was not desirable.

3.7.5 Reduction of Cr(VI) at low pH

It is well known that Cr(VI) is reduced on keeping at low pH [39, 134, 135] and that this reduction is accelerated in the presence of organic matter [34, 134, 135]. Mugo and Orians [42] even claim that when stored at pH 2, Cr(VI) is reduced to Cr(III) within 24 hours. Experiments were therefore carried out to assess whether the reduction of Cr(VI) in a solution at high acidity would be quantitative and rapid enough to be applicable for the speciation of Cr by the CSV method.

However, it was found that on keeping a 0.5 µg/L Cr(VI) solution at pH 1.8 for three days, $^{-0.2V}$Cr(VI) could still be detected, i.e., reduction was either incomplete or had not occured. It could not be ascertained whether any Cr reduction had actually taken place because there was the possibility of Cr losses to the container walls.

In another series of experiments, solutions of Cr(VI) and XO were kept mixed at pH 2.1-2.5 for up to 3 days in Teflon containers. After suitable periods of time, these solutions were analyzed for $^{-0.2V}$Cr(VI) under CSV optimized conditions. It was anticipated that at this pH, the reduction of Cr(VI) would be driven by the formation of a complex between XO and the Cr(III) produced *in situ*. Accordingly, if the complete reduction of Cr(VI) occurred, no $^{-0.2V}$Cr peak should be detectable.

As expected, it was found that the $^{-0.2V}$Cr peak heights progressively decreased with time, disappearing completely in 36 hours. This meant that all the Cr(VI) had been reduced in 36 hours but surprisingly, after this period of time, no Cr was detected in solution, i.e., even for a deposition potential of -1.2 V, no Cr peak could be seen. In contrast, when solutions containing Cr(III) were taken through a similar procedure, reduction peaks were still visible after 3 days. This shows that the Cr species resulting from the reduction of Cr(VI) is not CSV-labile.

Such a result was also noted during the attempted reduction of Cr(VI) by Fe^{2+} (Section 3.7.4), where it was seen that the resulting Cr was not CSV-labile.

Reduction of Cr(VI) produces Cr(III) which, in the presence of XO, will react *status nascendi* to form a Cr^{III}-XO complex. The absence of $^{-1.2V}$Cr peaks from solutions in which the chemical reduction of Cr(VI) is carried out in the presence of XO shows that the Cr^{III}-XO complex formed in this manner is not CSV labile. This CSV inertness can be explained by the fact that the complex is not adsorbed on the Hg surface. This observation has major implications in the formulation of a scheme for the electrode processes leading to the production of the analytical peak. This will be addressed further in Chapter 4.

3.7.6 Reduction of Cr(VI) with SO_2

Solutions of sulphur dioxide (SO_2) and sulphites are often used as reducing agents; from the following values of standard reduction potentials [19],

$SO_4^{2-} + 4H^+ + (x-2)H_2O + 2e \rightarrow SO_2 .xH_2O$ $\quad E^0 = +0.17\ V$

$SO_4^{2-} + H_2O + 2e \rightarrow SO_3^{2-} + 2OH^-$ $\quad E^0 = -0.93\ V$

$Cr_2O_7^{2-} + 14H^+ + 6e \rightarrow 2Cr^{3+} + 7H_2O$ $\quad E^0 = +1.33\ V$

$CrO_4^{2-} + 4H_2O + 3e \rightarrow Cr(OH)_3(s) + 5OH^-$ $\quad E^0 = -0.13\ V,$

the reduction of Cr(VI) by SO_2 is thermodynamically feasible in an acidic as well as a basic medium:

Acidic: $Cr_2O_7^{2-} + 3SO_2 .xH_2O + 2H^+ \rightarrow 2Cr^{3+} + 3SO_4^{2-} + (3x+1)H_2O$

$E^0 = +1.16\ V$

Basic: $2CrO_4^{2-} + 3SO_3^{2-} + 5H_2O \rightarrow 2Cr(OH)_3(s) + 3SO_4^{2-} + 4OH^-$

$E^0 = +0.80\ V$

K_2SO_3 and Na_2SO_3 have in fact been employed as reducing agents for Cr(VI) in the speciation of Cr by an atomic absorption spectrometry [51] and a gas chromatographic [42] method. The action of acids on sulphites produces SO_2 which exists as $SO_2.xH_2O$ (x = ~7) in aqueous solutions [19]. In the search for a reducing agent that could be easily decomposed prior to the CSV experiments, SO_2 seemed particularly attractive because any excess SO_2 can readily be expelled from solutions by purging with nitrogen.

The applicability of Na_2SO_3 as a reducing agent in the speciation of Cr was evaluated and it was seen that under the right experimental conditions, Cr(VI) could be reduced almost instantaneously by SO_2, with a quantitative recovery of the resulting Cr(III). These experimental conditions and some characteristics of the reduction are discussed below.

3.7.6.1 Effect of SO_3^{2-} on the CSV peak of Cr-XO

Under conditions optimized for the determination of Cr by the CSV of the Cr-XO complex , the addition of 50 µL of 1.5 M Na_2SO_3 to the voltammetric cell resulted in a 50% decrease in the $^{-1.2V}$Cr reduction current. Much smaller $^{-0.2V}$Cr peaks were still visible. Addition of a further 50 µL of Na_2SO_3 caused all Cr peaks to be completely suppressed; fresh additions of Cr(VI), Cr(III) or XO to this solution failed to produce any Cr peaks. This shows that

1. at pH ~7, the reduction of Cr is either not occurring or incomplete.
2. SO_3^{2-} interferes with the CSV of Cr and therefore excess SO_3^{2-} has to be removed from the solution prior to the addition of XO.

Excess SO_3^{2-} can be totally decomposed and expelled from solution by purging the solution for about 6 minutes at pH < 3.

3.7.6.2 Optimization of Reduction Parameters

Effect of pH on completeness of reduction and on recovery

Experiments to study the effect of pH on the reduction of Cr(VI) by SO_3^{2-} were carried out at the 0.2, 0.5 and 1 µg/L Cr(VI) concentration levels in Nanopure water.

50 µL of purified 1.5 M Na_2SO_3 was added to aliquot solutions known concentrations of Cr(VI) at the desired pH. The solutions were stirred for 2-3 min and purged for 6 min at the same pH. After purging, the solution pH was adjusted to 7.1 by adding Q-NH_3, additional reagents (NO_3^-, XO) were added, and then CSV experiments were performed for the determination of Cr as $^{-0.2V}Cr$ and $^{-1.2V}Cr$. The absence of a $^{-0.2V}Cr$ peak was taken to mean that complete reduction of Cr(VI) had occurred. In solutions where reduction was complete, the resulting Cr was quantified by a Cr(III) standard additions method of calibration to determine the recovery of the Cr following the reduction.

Results showed that a complete reduction of Cr(VI) was possible only at pH values less than ~ 3.8; $^{-0.2V}Cr$ peaks could still be seen at pH greater than 4.

The pH at which the reduction was carried out had a further effect on the recovery of Cr(III). Recoveries at different Cr levels and for different reduction pHs are shown in Table 3.6.

Table 3.6: Effect of pH on recovery of Cr

Spike	Reduction pH	% recovery of total Cr as Cr(III)
0.5 µg/L Cr(VI)	3.8	not quantified
0.5 µg/L Cr(VI)	3.5	< 10
0.5 µg/L Cr(VI)	3.0	36
0.5 µg/L Cr(VI)	2.6	86
0.5 µg/L Cr(VI)	2.2	90
0.5 µg/L Cr(VI)	2.0	98
0.5 µg/L Cr(VI)	1.8	95
0.5 µg/L Cr(VI)	1.5	80
0.5 µg/L Cr(III)	2.0	95
0.5 µg/L Cr(VI) + 0.5 µg/L Cr(III)	2 ± 0.1	96
0.1 µg/L Cr(VI) + 0.1 µg/L Cr(III)	2 ± 0.1	98 ± 2
0.5 µg/L Cr(VI) *(in seawater)*	2.0	94
0.1 µg/L Cr(VI) *(in seawater)*	2 ± 0.1	93 ± 2
0.1 µg/L Cr(VI) + 0.1 µg/L Cr(III) *(in seawater)*	2 ± 0.1	93 ± 2

These data show that the pH at which reduction is carried out is critical for the proper working of the reduction method. The recovery is almost 100% at pH

values between 1.8-2.2 but rapidly deteriorates between pH 2.2 and 3.8. As mentioned earlier, above pH ~3.8, reduction of Cr(VI) is incomplete.

Recovery experiments with solutions initially spiked with Cr(III) and taken through the procedure (i.e., addition of 50 µL Na_2SO_3 at ~pH 2, purging at pH 2 for 6 min then carrying out CSV experiments under optimal chemical and instrumental conditions) showed that the reduction step had no effect on Cr(III) as recoveries ranged from 97-101%.

A complete study of the pH on the completeness of reduction or on the recovery of Cr in seawater samples was not undertaken but stemming from the Nanopure water results, it was confirmed that at pH 2±0.1, reduction of Cr(VI) is indeed complete in seawater. Recoveries of 91-95% were consistently obtained. These recovery experiments were carried out in purified seawater.

Concentration of Na_2SO_3

It was not felt necessary or beneficial to optimize the concentration of Na_2SO_3 to be employed in the reduction process for the following reasons.

1. Results obtained from using 50 µL of the 1.5 M Na_2SO_3 were excellent; experiments showed that even at a 10 µg/L level of Cr(VI), reduction was complete and instantaneous with this amount of Na_2SO_3. A chromium concentration of 10 µg/L is at least 20 times the concentration

to be expected in natural water samples so it is anticipated that Cr reduction will be complete in any type of natural water samples.

2. Upon reaction with acids, excess Na_2SO_3 is completely decomposed and remains in solution as dissolved SO_2. The concentration of SO_2 in solution will be determined by its solubility and anyway, before the addition of XO and other reagents excess SO_2 is purged off. Any extra amount of Na_2SO_3 would simply result in additional Na^+ ions which are inert in the system.
3. no quantifiable amount of Cr could be detected in Na_2SO_3 so there is no danger of introducing contamination from the reagent itself.

3.7.7 Chromium Speciation Scheme

The successful reduction of Cr(VI) by SO_3^{2-} as evidenced by the total removal of $^{-0.2V}$Cr peaks from samples initially spiked with Cr(VI) and by the quantitative recoveries permits the formulation of a scheme for the rapid and reliable speciation of Cr in aqueous samples. This can be achieved by performing CSV experiments on 2 separate sample aliquots: Cr(VI) can be determined in one sample aliquot and total Cr as Cr(III) in the other.

Cr(VI) can be determined by carrying out the CSV of the sample solution under optimized conditions by the deposition of the Cr-XO complex at -0.2 V followed by a voltammetric scan from -1.2 to -1.6 V. A peak at ~ -1.45 V will be indicative of Cr(VI). The amount of Cr(VI) can be quantified by a Cr(VI) standard addition method.

Total Cr can be determined by first reducing any Cr(VI) to Cr(III) as follows. The sample in a voltammetric cell is acidified with 1:1 Q-HCl and 50 µL 1.5 M Na_2SO_3 added to it. Care must be taken to ensure that the pH of this solution does not exceed 2.1; the addition of Na_2SO_3 causes an increase of ~0.2 units in the pH, so a pH of 1.8 before the addition of the Na_2SO_3 is recommended. After a brief period (~2 min) of stirring, the sample is purged for 6 min. The sample is then buffered to pH 6.7 (in seawater) or 7.1 (Nanopure) by the addition of Q-NH_3 and 100 µL PIPES, under pH meter control. Addition of $NaNO_3$ and XO followed

by normal CSV runs with a Cr(III) standard addition calibration will lead to the determination of total Cr as $^{-1.2V}$Cr(III).

The difference between the total Cr and Cr(VI) will then be equivalent to Cr(III) only.

3.8 INTERFERENCES

Three main types of interferences can occur in CSV. These are interference from naturally occurring surface active agents, from dissolved organic matter and from other metals. The extent of each of these types of interferences was investigated by a study of the effect of addition of the potential interferents on the CSV peak heights of 1 µg/L Cr solutions, under optimized conditions. These studies were done mostly in Nanopure water and the results were confirmed in seawater.

3.8.1 Surface Active Agents

Interference from surfactants would be due to competitive adsorption on the mercury electrode, resulting in a decrease in the amount of electroactive species adsorbed and consequently a decrease/elimination of the voltammetric peak. In some cases, surfactants have also been shown to have a positive interference in CSV [136, 137].

TX-100 (Triton X-100, polyethylene glycol tert-octylphenyl ether), a non-ionic detergent, has been used as a model in the study of the effect of surfactants on the CSV reduction peaks [138].

The effect of TX-100 on i_p for 1 µg/L Cr(VI) in seawater is shown in Fig. 3.22. TX-100 strongly affects the CSV response of $^{-1.2V}$Cr, completely suppressing the signal at a concentration of 0.3 mg/L. However, the response for $^{-0.2V}$Cr(VI) is slightly more tolerant to the presence of TX-100, a concentration of 0.4 mg/L of the latter causing a decrease of only 11% of the original signal. At higher surfactant concentrations, the Cr response rapidly deteriorates: at the 1 mg/L level, there is a 77% loss in the Cr reduction current.

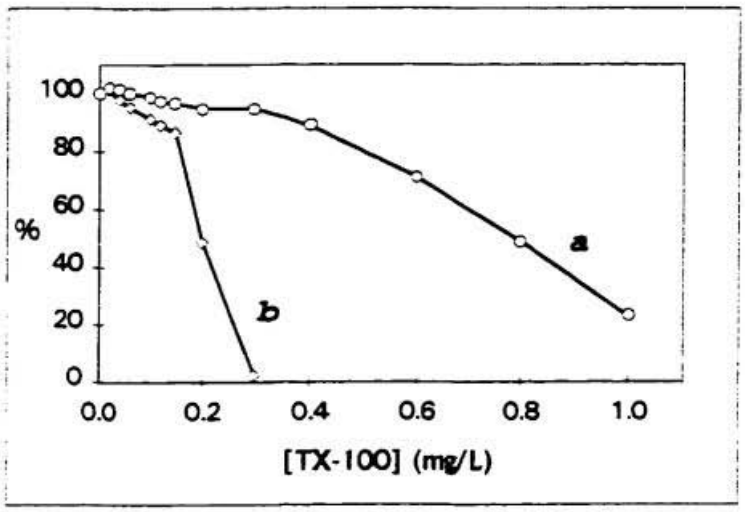

Fig. 3.22: Effect of TX-100 on the peak current. The response is expressed as a percentage of the current at zero addition of TX-100. (a): $^{-0.2V}$Cr(VI), (b): $^{-1.2V}$Cr(VI)

The effect of SDS (sodium dodecyl sulphate, an anionic surfactant) on the CSV of Cr was also studied. SDS did not affect the CSV response of either $^{-0.2V}$Cr(VI) or total $^{-1.2V}$Cr at concentrations of up to 1 mg/L. Even at a concentration of 10

mg/L SDS, the $^{-1.2V}$Cr response showed a decrease of only 2% but at this level, the $^{-0.2V}$Cr(VI) showed a greater decrease (22%).

The effect of these surfactants on the CSV response is somewhat surprising and revealing. The fact that SDS does not affect the total Cr response is understandable because at the deposition potential of -1.2 V, the tendency for the negatively charged surfactant to get adsorbed will be negligible. At -0.2 V however, the net charge on the electrode is positive and hence strong adsorption of SDS is expected, with a resulting decrease in the $^{-0.2V}$Cr(VI) reduction peak current. That such a depression of the peak is not seen shows that XO is itself very strongly adsorbed on the mercury surface. The same conclusion can be reached from the observation that there is a greater tolerance to TX-100 from a deposition potential of -0.2 V. XO, being negatively charged, can compete with TX-100 for adsorption on mercury at -0.2 V. At -1.2 V, the charge on the electrode becomes negative and adsorption of XO is greatly reduced and eventually totally inhibited by an increasing concentration of TX-100, resulting in a complete suppression of the Cr peak at relatively low concentrations of TX-100.

Natural waters contain surface active compounds which have an effect similar to 0.1-2 mg/L TX-100 [90, 138, 139]. Since the effect of the surfactants is simply to inhibit the adsorption of the Cr-XO complex on the electrode surface, the

determination of Cr in seawater can be carried out without interference, but at a reduced sensitivity, by the CSV method if a standard addition method is adopted for quantification. The sensitivity of the CSV method as applied to the determination of Cr in the Logy Bay seawater samples as well as in the open ocean water samples was found to be about 70% the sensitivity in Nanopure water. Using DTPA as the complexing ligand in the CSV of Cr, Boussemart et al. [101] found a similar relative sensitivity and showed that major cation competition was responsible for the lower sensitivity in seawater. This would mean that the concentration of surfactants encountered in all the seawater samples studied is too low and does not affect the sensitivity of Cr determination.

3.8.2 Dissolved Organic Matter (DOM)

Dissolved organic matter (DOM) can interfere in the CSV method by competitively complexing the metal species. To find the potential effect of DOM on the CSV peaks for Cr, citric acid, tartaric acid, humic acid (HA) and fulvic acid (FA) were added to the Cr-XO mixture in seawater.

Citric acid and tartaric acid did not affect the reduction peak heights of $^{-0.2V}$Cr(VI), $^{-1.2V}$Cr(VI) and $^{-1.2V}$Cr(III) at concentrations of upto to 0.12 mM citric acid or tartaric acid. However, in the presence of these organic acids, the reduction peaks for Cr(III) were found to slowly decrease in height and disappear completely in about 3 hours. The peaks corresponding to $^{-1.2V}$Cr(VI) and $^{-0.2V}$Cr(VI) were stable with respect to time. Complexation of Cr(III) is known to be very slow [19] so the gradual decrease of the Cr(III) peak can be explained by the slow complexation of the added metal by the organic ligand.

It is noteworthy that XO, which is itself a strong ligand does not preferentially complex Cr(III); this has some implications in the formulation of electrode processes to be discussed in Chapter 4.

Most of the dissolved organic matter in natural waters is in the form of humic substances (HS), which consist of humic acids (HA) and fulvic acids (FA). Interference from HA and FA can be as a result of their complexing action on the

metal ions and/or their strong adsorption tendencies. Humic substances are known to adsorb strongly on mercury [140].

In the present study, the interfering behaviour of HA and FA was found to be similar. The effect of HA on the analytical peak height is shown in Fig. 3.23.

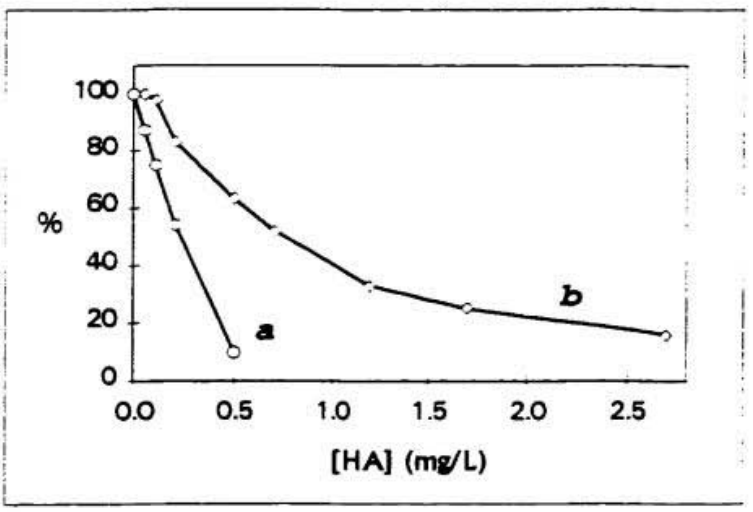

Fig. 3.23: Effect of humic acid on the peak current. The response is expressed as a percentage of the current at zero addition of HA. (a): $^{-0.2V}$Cr(VI), (b): $^{-1.2V}$Cr(VI)

The CSV sensitivity of Cr is greatly inhibited by the presence of humic substances. For Cr(VI), this inhibition is more severe from a deposition potential of -0.2 V. From a deposition potential of -1.2 V, both Cr(VI) and Cr(III) peaks are similarly affected. This suggests that the interfering action of humic substances is due more to their competitive adsorption on the mercury electrode than to their complexing the metals ions because Cr(VI) cannot be complexed by organic ligands without prior reduction to Cr(III).

The observed effect of dissolved organic matter (citric acid and tartaric acid) implies that the CSV method will fail to detect organically bound Cr in solution. This is not a serious limitation of the method when applied to seawater because the dissolved organic matter concentrations in seawater is very low. According to Sharp [141] and Carlson et al. [142], the best estimate of the concentration of Dissolved Organic Carbon, DOC, (which is related to DOM) in oceanic surface waters is 70 μM. In deeper waters, the DOC concentration will be lower.

DOC in inland surface waters is widely variable, depending on the type of water body (rivers, lakes), the climate and the nature of vegetation in the area. Serious interferences can occur in the application of the CSV method in the determination of Cr in such waters because in addition to being richer in organic matter, these waters tend to be more acidic. Cr(VI) reduction to Cr(III) and its subsequent non-lability through complexation will be favoured under these conditions.

Since DOM does not interfere with the CSV of Cr(VI), accurate determination of Cr(VI), if present, can be carried out in these waters. However, total Cr and Cr(III) results may be erroneous because as a result of its complexation with organic matter, Cr(III) will be non-labile. In circumstances where interference from DOM is encountered, complete destruction of the organic matter by u.v.

irradiation of the samples [143], with concomitant oxidation of Cr(III) to Cr(VI), will need to be carried out and then total Cr determined as Cr(VI).

3.8.3 Other Metals

The extensive use of XO in analytical chemistry, as an indicator in metallochromic titrations and as a complexing agent in spectrophotometric analysis, is an indication of the extreme versatility of the compound towards complexation with metal ions. It is therefore believed that under the right conditions, especially of pH, determination of a wide range of metals should be achievable by the CSV of the metal-XO complexes. In the present case, a full study was not carried out but at pH ~7 in Nanopure water, metal-XO reduction peaks were observed for Cu (-222 mV), Pb (-490 mV), Fe (-400 mV), Cd (-660 mV) and Zn (-1060 mV). The reduction peaks of Cu, Fe and Pb are potentially amenable to the development of extremely sensitive CSV methods for determination of these metals after an optimization procedure. The proximity of the peaks, especially, Fe and Pb, suggests that at high levels, interference by overlapping peaks might occur. A method for the determination of Pb with XO has recently been described in the literature [110], but surprisingly, the authors report that 400 nM Fe(II) or Fe(III) did have any significant interference in the determination of Pb. This is arguable because of the proximity of the Pb and Fe peaks. Cd cannot be determined by this method since the Cd-XO reduction peak is completely masked by the reduction peak of XO itself. The reduction peak for Zn is very insensitive and it is doubtful whether it can be made analytically useful. Some additional investigations were carried on the CSV of

Fe-XO and the results are discussed in relation to the interference of Fe on Cr (Section 3.8.4).

The capability of XO to complex a wide range of metal ions is not necessarily a boon because metal-XO complexes may lead to serious interferences.

In CSV, interference by other metals can be in the form of

1. competition for the available ligand for complex formation which may result in the analyte complexation being inhibited or even totally suppressed. Such interference can be remedied by the addition of extra amounts of the ligand in solution.
2. extraneous metal complexes formed may interfere by competing with the analyte complex for adsorption on the electrode; the analyte can still be quantified, albeit at reduced sensitivity, if a method of standard addition is used for calibration.
3. the interfering metal ion may be reducible on the mercury electrode at potentials in the vicinity of the analyte E_p and cause a direct or partial overlap with the analytical peak. Such reduction may occur from prior adsorption of the interfering species on the electrode or from the bulk of the solution.
4. the interfering metal (or other species) may interact with the analyte ion and prevent the formation of the analyte-ligand complex.

As mentioned, the first two types of interferences described above are not necessarily very serious and can be corrected for. However, interference resulting from the reduction of the interferent species in the vicinity of the analyte E_p and/or any interaction between the interferent and analyte species will have serious consequences on the validity and acceptability of the analytical method.

The effect of metal ions on the CSV peaks for $^{-0.2V}$Cr(VI) and $^{-1.2V}$Cr (as Cr(VI) and Cr(III)) was studied by metal additions to seawater and Nanopure water containing 1 µg/L of Cr, under optimized conditions. It was found that additions of up to 50 µg/L Al^{3+}, Bi^{3+}, Cd^{2+}, Co^{2+}, Cu^{2+}, Mn^{2+}, Mo^{3+}, Ni^{2+}, Pb^{2+}, UO_2^{2+} and Zn^{2+} caused little or no change in the height of the Cr reduction peak. The effect of Fe on the CSV of Cr is discussed separately in Section 3.8.4.

3.8.4 Iron

Interference due to Fe was predictable in view of the observation that during speciation studies, an attempt to reduce Cr(VI) by Fe^{2+} was partially successful. The effect of Fe on the Cr CSV peak was studied by following changes in i_p upon the addition of varying amounts of Fe in Cr(III) and Cr(VI) solutions in Nanopure water. Results showed that the effect of Fe was dependent on the oxidation states of both Fe and Cr. As mentioned earlier, the Fe-XO complex is CSV-electroactive. Some aspects of the CSV of the Fe-XO complex are included because they provide an important insight into the mechanism of the complexation reaction between XO and the metal ion and the adsorption of the analyte on the electrode.

3.8.4.1 CSV of Fe-XO

Several methods exist for the stripping voltammetry of Fe, using, for example, hydroxamic acids [144], catechol [143], Solochrome Violet RS [145] and 1-nitro-2-naphthol [146] as chelating agents. In parallel with the role of NO_3^- in the CSV of Cr, hydrogen peroxide has been employed for the sensitivity enhancement in the determination of Fe. The analytical peaks are observed at ~ -0.35 to -0.5 V and, in all cases, they have been ascribed to the Fe(III)/Fe(II) reduction.

In the CSV of Fe in the presence of XO, at pH ~ 6.8-7 (not optimized), Fe reduction peaks were seen at ~ -0.4 V. The best deposition potential for these peaks was found to be -0.15 V. As in previous methods for Fe, H_2O_2 led to an enhancement in peak heights. However, the peaks were only seen for Fe(II)-XO; extremely small peaks resulted from Fe(III)-XO. Fig. 3.24 compares the CSV peaks for Fe(II) and Fe(III).

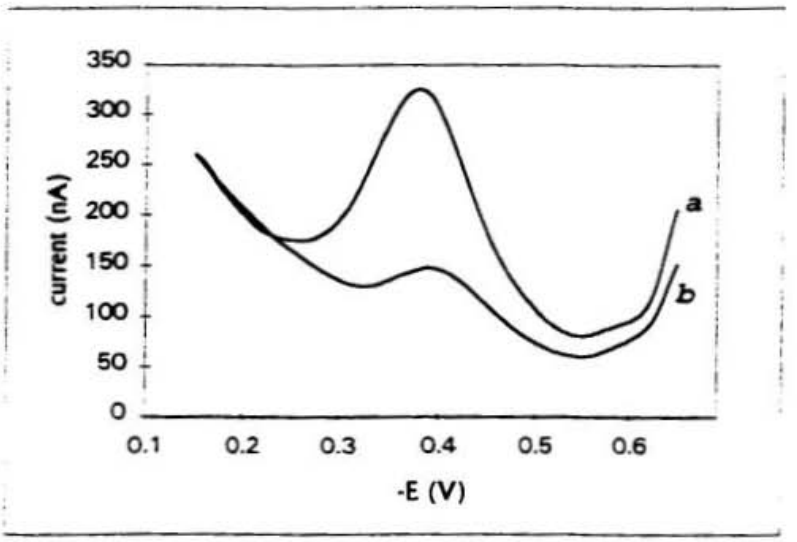

Fig. 3.24: CSV peaks for 2 μg/L Fe^{2+} (a) and Fe^{3+} (b), obtained under similar conditions in Nanopure water.

The observation that Fe(II) but not Fe(III) is CSV labile is very surprising. The observed peak potential (~ -0.4 V) and the peak enhancement by H_2O_2 suggest that the observed peak can only be due to a Fe(III)-Fe(II) reduction and therefore the adsorbed species has to be a Fe(III)-XO complex. A 1:1 complex is known to be formed between Fe(III) and XO in solution and has been utilized

as the absorbing species in a spectrophotometric method for the determination of Fe(III) [147].

The CSV-inertness of Fe(III) can only be explained by postulating that a strong Fe^{III}-XO complex is formed in solution but this complex is not adsorbed on the mercury. Free XO is very strongly adsorbed on the mercury (Section 4.2) and competes preferentially with Fe^{III}-XO for adsorption sites on the electrode. XO therefore interferes in the adsorption of the Fe^{III}-XO complex in a manner akin to the interference in CSV by surface-active compounds.

On the other hand, Fe(II) is CSV labile because Fe^{2+} reacts with the already adsorbed XO to form the Fe^{II}-XO complex, which remains adsorbed. Since at this potential (E_{dep} = -0.15 V), Fe(II) is unstable, the Fe^{II}-XO undergoes oxidation to Fe^{III}-XO. Such an oxidation step has been used to explain the CSV-lability of Fe(II) with catechol [143] and with 1-nitro-2-naphthol [146].

During the stripping stage, the Fe^{III}-XO complex is reduced with the production of the analytical peak. The scheme of events leading to the production of the analytical peak is summarized below.

Deposition stage:

$$XO \rightarrow XO_{ads}(Hg)$$

$$Fe(II) + XO_{ads}(Hg) \rightarrow Fe^{II}\text{-}XO_{ads}(Hg)$$

$$Fe^{II}\text{-}XO_{ads}(Hg) \rightarrow Fe^{III}\text{-}XO_{ads}(Hg) + e$$

Stripping stage:

$$Fe^{III}\text{-}XO_{ads}(Hg) + e \rightarrow Fe^{II}\text{-}XO_{ads}(Hg)$$

$$\uparrow \_\_\_\_\_ H_2O_2 \_\_\_\_\_ \downarrow$$

In Chapter 4, it is postulated that the electroactive Cr-XO species is similarly formed by the interaction between Cr(II) produced at the electrode and $XO_{ads}(Hg)$.

3.8.4.2 Interference by Fe

Fe^{3+} has no effect on the determination of either $^{-1.2V}$Cr(VI), $^{-0.2V}$Cr(VI) or Cr(III); Fe(III) additions of up to 100 µg/L did not affect the Cr reduction peak heights. Since it is assumed that the Fe^{III}-XO is not adsorbed on mercury, provided there is excess XO in solution, no interference will be seen.

The addition of 100 µg/L Fe^{2+} had no immediate effect on the Cr(III) peak but the Cr peak was seen to decrease with time. This decrease was slow, with a loss of only 5% in 15 minutes, 10% in 30 minutes and 25% in 1 hour. Thereafter, the Cr peak remained stable with time. During this time, the Fe(II) peak at -0.4 V remained constant. It was also noted that the decrease in the Cr peak with time was independent of the Fe^{2+} concentration, the same effect being observed at an Fe^{2+} concentration of 2 µg/L and 70 µg/L. It is important to note that the interference between Cr(III) and Fe^{2+} was effective only after the addition of XO to the Fe(II)/Cr(III) solution. This means that in a sample containing Cr(III) in the presence of Fe^{2+}, Cr(III) can be determined with a good degree of accuracy if the total time elapsed between the addition of the ligand to the sample and the determination of the peak height corresponding to the final standard addition is kept short. Complete analysis of a sample involving 3 standard additions, with triplicate peak height determination for each addition, can usually be completed within 8-10 minutes after the addition of XO to the sample.

Addition of Fe^{2+} to Cr(VI) led to an immediate decrease on the peak heights of $^{-1.2V}$Cr(VI) and $^{-0.2V}$Cr(VI), but the peaks did not show any further decrease with time. The effect of Fe^{2+} on the reduction peaks of Cr(VI) is shown in Fig. 3.25.

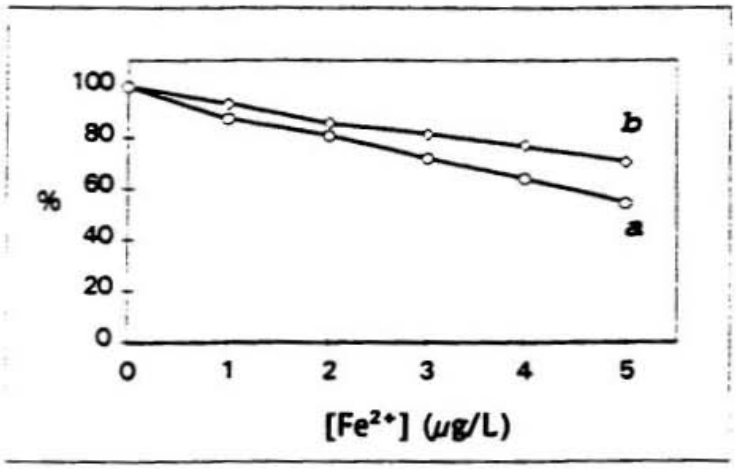

Fig. 3.25: Effect of Fe^{2+} on the peak current. The response is expressed as a percentage of the current at zero addition of Fe. (a): $^{-0.2V}$Cr(VI), (b): $^{-1.2V}$Cr(VI)

For a given addition of Fe^{2+}, the decrease in peak height is less for $^{-1.2V}$Cr(VI) than for $^{-0.2V}$Cr(VI). This is easily understood in the light of the fact that the interference seen is due to the decrease of Cr(VI) in solution as a result of chemical reduction by Fe^{2+}. The product of this reduction is Cr(III) which is still electroactive from a deposition potential of -1.2 V and contributes to the $^{-1.2V}$Cr peak. Surprisingly, the reduction in the Cr(VI) peak height is not accompanied by a reduction in the Fe(II) peak height, as would be expected from the fact that Fe(II) is electroactive but Fe(III) is not.

Whereas the interference of Fe^{2+} on Cr(VI) is explained by redox properties of the Fe(II)/Cr(VI) couple in solution, no simple explanation can be put forward for the interference of Fe^{2+} on Cr(III).

The concentration of dissolved Fe in seawater is extremely low, between 0.1 to 0.7 nM [137, 148] equivalent to about 0.005-0.04 µg/L. Fe concentrations as low as 0.02 nM have been reported in surface waters of the Pacific Ocean [149, 150]. At these concentration levels, no interference due to Fe will be observed in the determination of Cr in seawater by the CSV method but in inland surface waters, where the Fe content can reach mg/L levels, serious interferences should be expected. However conditions prevalent in such waters (e.g., high acidity, high DOC, high Fe) all point to the occurrence of negligible amounts of Cr(VI). As explained above, if the analysis is done rapidly, determination of total Cr as Cr(III) should not pose any difficulty even at high Fe levels. Such an analysis was carried in a riverine water reference material for trace metals (SLRS-3, obtained from the National Research Council of Canada) which has a certified Fe content of 100 µg/L. Application of this CSV method showed a Cr concentration of 0.32±0.04 µg/L, which is in good agreement with the certified value of 0.30±0.04 µg/L.

3.9 BACKGROUND SUBTRACTION

3.9.1 Need for Background Subtraction

At the optimum pH for the determination of Cr the reduction of H^+ on mercury becomes significant at E values more negative than -1.4 V. This results in a sharp increase in the background current. The background current is considerably higher in seawater than in Nanopure water, Fig. 3.26(i). This is due to the extra ions in seawater as a result of its salinity. Addition of inert electrolytes like KCl to either seawater or Nanopure water result in an increase in the background current, especially in the region of potential more negative than ~-1.45 V. $NaNO_3$, which is utilized for its role in the catalytic enhancement of the analytical CSV current, has a similar effect on the background current. The background currents in Nanopure water and in seawater after the addition of 750 µL of 5M $NaNO_3$ is shown in Fig. 3.26(ii) and the equivalent effect of only the addition of 750 µL 5 M $NaNO_3$ on the background current in Nanopure water and seawater is shown in Fig 3.26(iii). NO_3^- brings about a smooth increase in the background current. This increase was found to be proportional to the amount of NO_3^- added. Successive additions of 100 µL NO_3^- resulted in the same increase in the background current. The background current increased similarly with additions of NO_3^- even in the presence of XO.

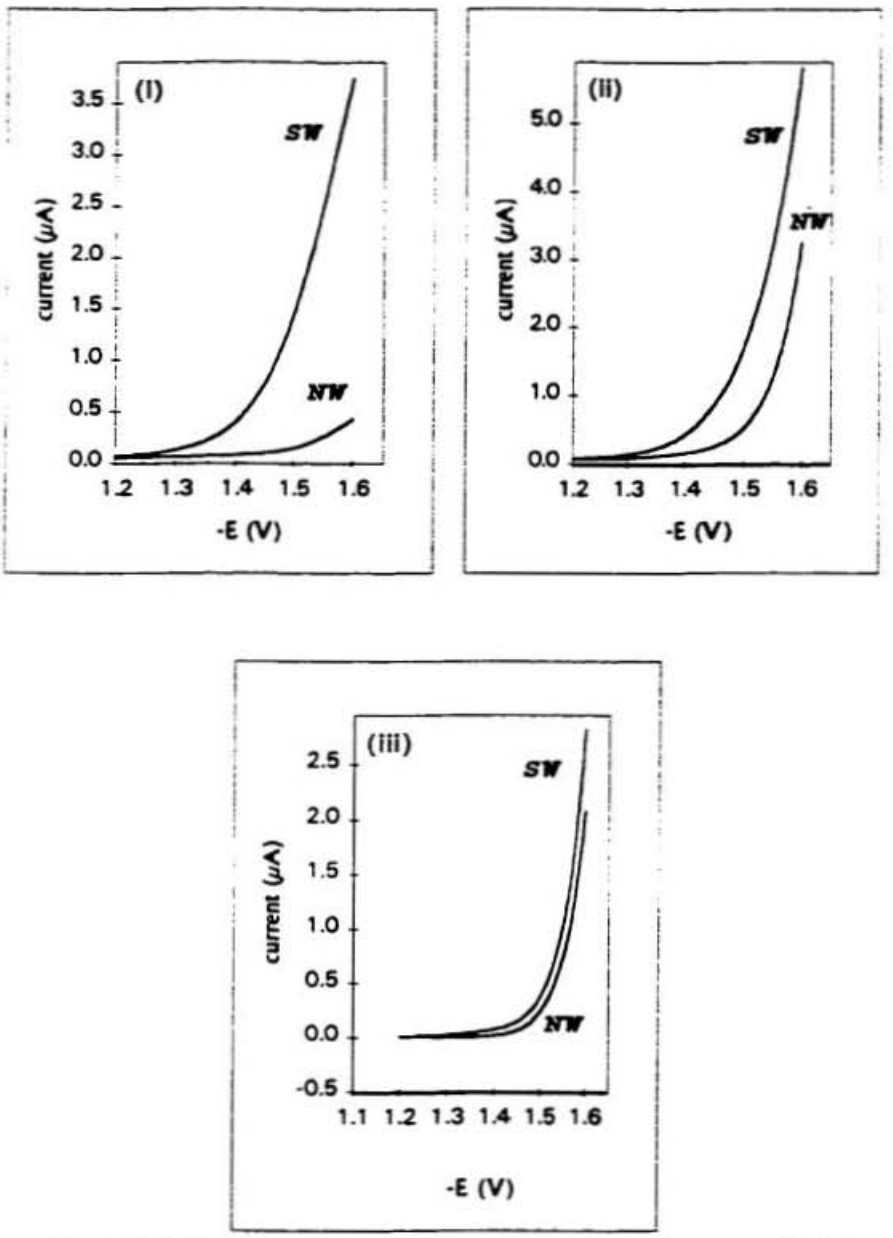

Fig. 3.26(i): Background currents in seawater (SW) at pH 6.5 and in Nanopure water (NW), with supporting electrolyte at pH 7.
(ii): Background currents in SW and NW after addition of NO_3^-.
(iii): Resultant effect of NO_3^- only.

The high background current, especially in seawater, has a deleterious effect on the Cr analytical peak as the latter occurs at ~ -1.45 V, which falls just within the sharply increasing region of the voltammogram. Despite the high sensitivity of this Cr-XO method, Cr peaks resulting from very low Cr (e.g., at the 0.1-0.2 µg/L levels encountered in seawater) cannot be adequately resolved from the background. The minimum [Cr] giving rise to a distinct, quantifiable peak was found to be ~0.2 µg/L in Nanopure water and ~0.3 µg/L in seawater (Cr(VI), 1-min deposition at -1.2 V). Higher [Cr] will be required for $^{-0.2V}$Cr(VI) and Cr(III) because these species respond typically 50-70% less sensitively than $^{-1.2V}$Cr(VI). Quantification of Cr in natural water samples would therefore be impossible unless the current resulting from the Cr reduction can be resolved from the background current. For achieving such resolution, a background subtraction method can be used. Background subtraction in this case would be analogous to the use of blanks in most of the spectrometric techniques.

3.9.2 Background Subtraction Method

The utilization of background subtraction techniques as a means of improving detection limits has a long history in electroanalytical techniques. In fact, the increased sensitivities seen in the pulse voltammetric techniques is attributed to the elimination of the capacitance current. Even better detectability can be achieved if most of the background faradaic current can also be subtracted from the analytical signal and to this effect several approaches have been used. In earlier methods, background subtraction was accomplished by recording the difference between two stripping currents with different deposition times at two matched electrodes immersed in the same sample [151-154] or between two matched electrodes in two different cells, one containing the sample and the other containing the electrolyte [155].

In an evaluation of background subtraction in polarographic methods, Bond [80] in 1980 pointed out that "the only really practical approach to subtractive polarography is to undertake two separate experiments with the same instrumentation and record the solvent and sample solutions separately from two different runs. The data from the solvent can be stored electronically and subtracted from subsequent scans on solutions containing the electroactive species of interest." He also stressed that the full advantages of background

subtraction could be exploited only with the availability of computerized instrumentation.

With the availability of computerized instrumentation background subtraction has indeed been implemented by using a single electrode [156-158]. The background is obtained by using different deposition times or different convection (stirring) rates and electronically stored. This background can then be subtracted from the normal voltammogram to yield the analytical current. Wang and Dewald [159] have also used a subtraction method where the background obtained from the electrolyte is subtracted from the sample voltammogram to yield the purely analytical current. Numerical methods have also been used to generate background currents [160-163].

With the increasing commercial availability of software designed specifically for voltammetric data retrieval and data manipulation, it is anticipated that background subtraction in voltammetric analysis will become more and more widespread. The PAR Model 394 Analytical Voltammetry Software offers extremely versatile and reliable data manipulation capabilities and background subtraction methods can easily be incorporated in the development of new methods.

The use of background subtraction methods in voltammetric methods of trace analysis will lead to reaching hitherto unattained limits of detection because it

has been noted by many authors that the limit of detection is determined not by the analytical current but by the background current [101, 164]. There cannot be any universal recipe for background subtraction in voltammetric methods because the nature of the background current is very specific to individual systems and very small changes in the morphology of the electrode may lead to imperfect background subtraction. Such changes in the electrode morphology can be brought about by the formation of hydrogen bubbles at the surface, plating of mercury, potential- or time-dependent adsorption or the precipitation of hydroxides [165]. All these will lead to different surface areas of the electrode and correspondingly, different values of the background current. Hence, any potential method must be carefully evaluated before being applied to a particular system. The effectiveness of some methods of background subtraction has been evaluated by Wang and Greene [165].

In the present case, several background subtraction techniques were considered. In the design of these methods, a primary objective was to keep the method as simple as possible, i.e., to avoid any additional data acquisition or data treatment step that would have a bearing on the total analysis time. Hence the method used by Wang [156], which utilizes the difference in the signal for two different deposition times, i.e., the response is equivalent to the voltammogram obtained from a 60-s deposition time minus the voltammogram resulting from a 15-s deposition, was written off as a potential method of

background subtraction. Implementation of such a method would increase the total analysis time.

The method of background subtraction which seemed most obvious and simple to use was one where the voltammogram of the buffered seawater or Nanopure water sample, with all necessary reagents added except the XO and obtained under similar instrumental conditions, as the 'blank' voltammogram. Addition of XO, and subsequently standard additions, to the sample would then yield the 'sample' voltammograms. Subtraction of the 'blank' voltammogram from the 'sample' voltammograms would be equivalent to a peak corresponding to Cr reduction only. This assumes that in the absence of the complexing ligand no Cr is reduced at the electrode, which is a fair assumption, especially considering the Cr concentration levels and the extremely short scan time.

The above method is equivalent to the method used by Wang and Dewald [159] and seems valid because

1. during interference studies, it was seen that no other metal ions give reduction peaks in the potential region of interest. Hence any peak in the subtracted voltammogram can be assigned as a Cr reduction peak.
2. at any pH, the effect of only XO on the voltammogram in the -1.2 to -1.6 V was an overall increase in the current over the potential range. For

illustration, the effect the addition of 50 µL XO (2.5 mM) in purified seawater at pH 6.7 is shown in Fig. 3.27.

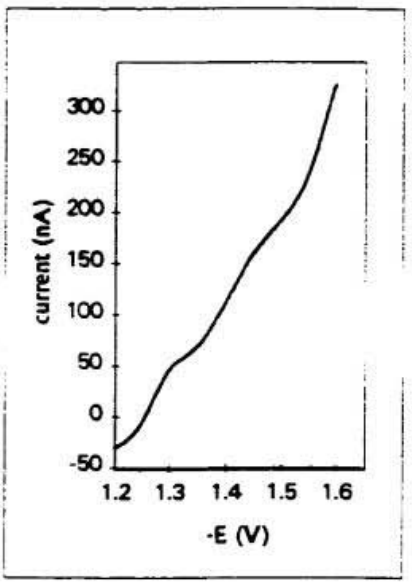

Fig. 3.27: Effect of XO on the background current in seawater at pH 6.7.

Unfortunately, this method of background subtraction did not give the expected results; Fig 3.28 shows a typical subtracted voltammogram obtained by the application of the method described.

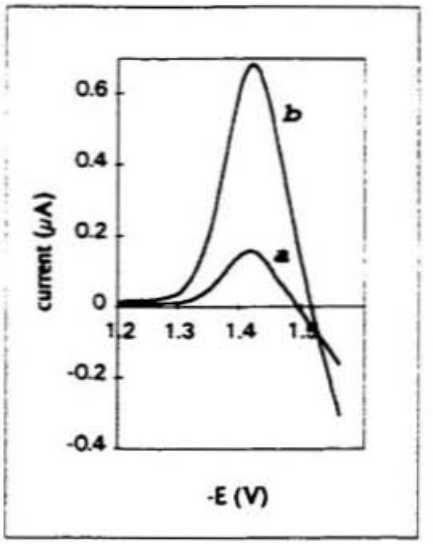

Fig. 3.28: Voltammograms equivalent to Cr only. These were obtained by subtracting the voltammograms of seawater containing NO_3^- from voltammograms of seawater containing NO_3^-, 50 μL XO and Cr(VI): (a) 0.113 and (b) 0.446 μg/L Cr.

The initial, increasing part of the voltammogram is as expected but in the potential region after the peak current has been reached, the current keeps decreasing. This means that, in these regions, the background current in the presence of the analytical electrode process is lower than in the absence of the process. From the processes thought to be occurring at the electrode during the stripping step (Section 4.2), this may be due to the deposition of metallic chromium or an inert Cr(II)-XO polymeric species on the Hg surface which hinders the reduction of H^+ and brings about a small decrease in the background current. This illustrates how small morphological changes in the electrode can lead to imperfect background subtraction. From the reason proposed to explain the shape of the resultant voltammogram in Fig. 3.28, it can be extrapolated that

background subtraction methods based on different deposition times or different convection rates will not be effective in the present case.

Interestingly, it was found that very good calibrations curves can be obtained even from the above-shaped voltammograms if peak heights are calculated by an extrapolation of the pre-peak baseline. However, this would involve manual peak height calculations, which would make it prone to error and lead to an increase in the total analysis time.

Stemming from the partial success of the above method, a slightly modified method of background subtraction was evaluated and found to be effective. This was based on the observation that in the absence of the ligand, the only effect of NO_3^- was a smooth increase in the background current. Also, the background current in buffered seawater is constant, i.e., it does not depend on the deposition time or the deposition potential. Therefore, voltammograms of buffered seawater (or Nanopure water with the appropriate amount of inert electrolyte) obtained before the addition of $NaNO_3$ and XO can equally be considered as the 'blank'. Voltammograms obtained after the addition of $NaNO_3$ and XO and subsequent standard additions would then be the 'sample' voltammograms. Subtraction as before would produce voltammograms which would constitute the total current resulting from the addition of $NaNO_3$ and XO, with a superimposed analytical peak, the height of which could be calculated

and used for calibration purposes. This method is attractive because for a given sample, the same background is constantly subtracted from all samples and spikes, so any systematic error introduced in the method will affect all the peak height measurements equally and be cancelled out.

The application of this method is demonstrated in Fig. 3.29.

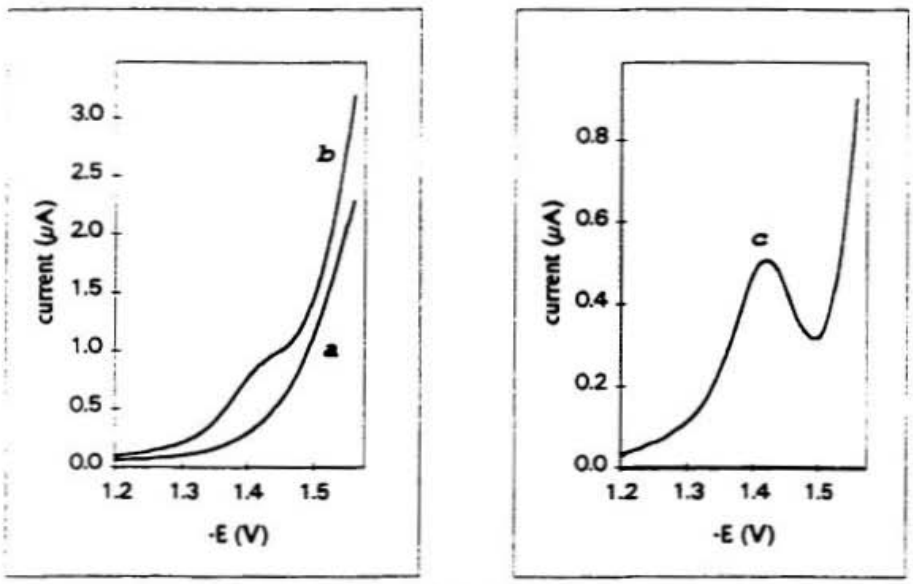

Fig. 3.29: illustration of the background subtraction method (a): voltammogram for buffered seawater only; (b): voltammogram obtained after the addition of XO, NO_3^- and 0.113 μg/L Cr and (c): b minus a, is equivalent to the resultant effect of XO, NO_3^- and Cr.

The application of this method for the determination of Cr in a Logy Bay seawater sample yielded the following results. Fig. 3.30 show the actual voltammograms. In the absence of a background subtraction, Fig. 3.30(i), the

peak currents cannot be measured accurately but after the background subtraction Fig. 3.30(ii), distinct peaks are visible and can be measured.

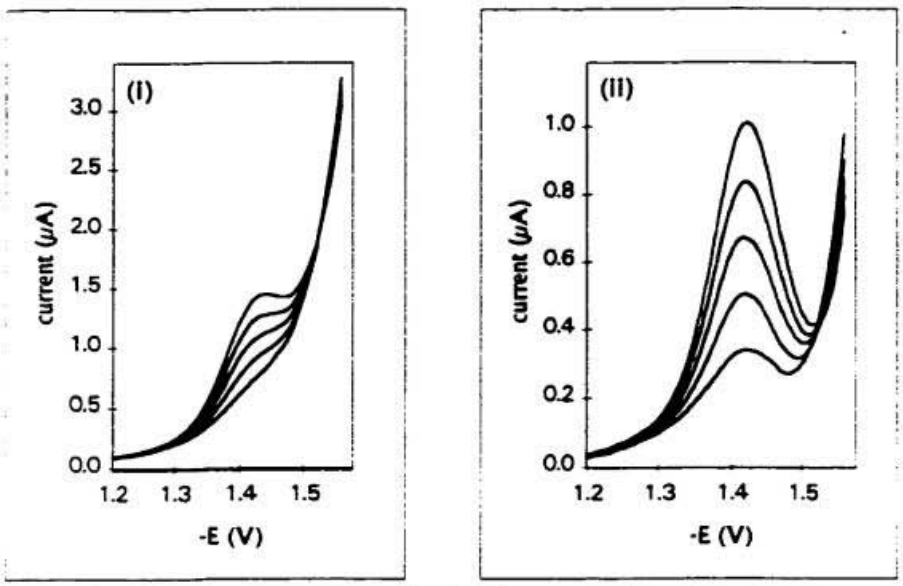

Fig. 3.30: calibration using background subtraction.
(i), unsubtracted and (ii), subtracted voltammograms for Cr additions of 0, 0.113, 0.225, 0.336 and 0.446 μg/L Cr .

From Fig. 3.30(ii), the following peaks heights were calculated.

Added Cr (μg/L)	peak height (nA)
0	125.8
0.113	271.5
0.225	417.8
0.336	565.7
0.446	724.7

The above values give a straight line (r^2 = 0.9995) with a slope of 1338 nA.(μg/L)$^{-1}$ and intercept 121.4, from which the Cr concentration can be

calculated as 0.101 µg/L. This value has been adjusted for the effect of the dilution of the seawater sample by the addition of required reagents.

Given the excellent calibration characteristics obtained, this method of background subtraction was adopted. The method is applicable for both $^{-0.2V}Cr$ and $^{-1.2V}Cr$ determinations and has been employed throughout this work for determination of Cr at low levels. The consistently reproducible and accurate results obtained when applied to riverine and seawater Reference Materials as well as during recovery experiments in purified seawater and Nanopure water is testimony to the accuracy of this method. Cr determination in all the seawater samples (Section 3.11) was carried out using this method of background subtraction.

3.10 ANALYTICAL PERFORMANCE

3.10.1 Accuracy and Precision

The accuracy of the technique was assessed by the analysis of Cr in trace metal reference standards from the National Research Council of Canada. Two reference waters, the Nearshore Seawater Reference Material (CASS-3) and the Riverine Water Reference Material (SLRS-3) were analyzed for Cr(III) and Cr(VI) by the method developed in this study. The results of the analyses are shown in Table 3.7.

Table 3.7: Analysis of Reference Materials

Sample	Certified Cr (µg/L)	Cr found (µg/L)		
	total Cr	$^{-1.2V}$Cr(III)*1	$^{-1.2V}$Cr(III)*2	$^{-0.2V}$Cr(VI)
CASS-3	0.092±0.006	0.088±0.008 (3.5%)*3	0.092±0.005 (2.3%)*3	n.q*4
SLRS-3	0.30±0.04	n.a*5	0.32±0.04 (5.4%)*3	n.a*5

*1. after reduction step
*2. no prior reduction step
*3. mean ± 95% confidence interval (RSD)
*4. not quantified; below detection limit
*5. not applicable; Fe interference (see Section 3.8.4.1)

The excellent agreement between the certified values and the values obtained by this method confirms the accuracy of the method. As expected, no Cr(VI) was found in these waters as a result of its storage at pH 1.6, but the agreement between the Cr values obtained as Cr(III) with and without the reduction step is

proof of the accuracy of the overall procedure, which includes the CSV step as well as the reduction step and the background subtraction method.

The very good precision of the method is reflected in the values of the relative standard deviations obtained in the above determinations. Similar RSD values were seen in the recovery experiments during the speciation exercise.

Repeated voltammograms in CASS-3 (which contains 0.092 µg/L Cr), without any Cr addition, produced average peak heights of 143.0±1.9 nA (mean±SD, n=5) with a RSD of 1.3%. This demonstrates the highly reproducible nature of the electrode processes leading to the peak formation.

3.10.2. Sensitivity and Detection Limits

For calibration purposes, all voltammograms were obtained after a 60-s deposition followed by a 10-s equilibration but it should be noted that during the equilibration time, the deposition of the analyte complex still occurs, albeit at a much reduced rate. The amount of analyte deposited during the equilibration stage has been neglected in the calculation of the sensitivity values reported below. The sensitivity is taken as being equal to the slope of the calibration graph per unit time and is reported as nA $(\mu g/L)^{-1}$ min^{-1}. From calibrations of Logy Bay seawater, average sensitivities for $^{-0.2V}$Cr(VI), $^{-1.2V}$Cr(VI) and Cr(III) were found to be respectively 1250, 865 and 675 nA $(\mu g/L)^{-1}$ min^{-1} (ca. 65, 45, and 35 nA nM^{-1} min^{-1}). Sensitivities in Nanopure water were about 30-35% higher.

Nanopure water and purified MSRL seawater were used for calculating 3σ detection limits and since the blank solutions failed to give peaks, σ values were calculated for 7 repeat voltammograms at a Cr level of ~0.1 µg/L (after the addition of 50 µL, 25 µg/L Cr). The calculated detection limits are shown in Table 3.8.

Table 3.8: Detection limits in ng/L

	$^{-0.2V}$Cr(VI)	$^{-1.2V}$Cr(VI)	Cr(III)
Nanopure water	2.2	1.2	1.8
Purified seawater	14	5.2	7.8

3.10.3 Linear Dynamic Range

In calibration curves in Nanopure water and Logy Bay seawater as well during the analysis of the seawater samples from the N.W. Atlantic Ocean (Section 3.11), where the method of background subtraction was employed, r^2 values of 0.999 were routinely obtained, attesting to the very good linearity of calibrations at low levels.

This method of background subtraction is not recommended for use at high concentrations because the resulting currents are so large that incomplete peaks result, i.e., the peaks become broad and the baseline beyond the peak is not reached.

Calibration curves for Cr(VI) additions to Nanopure water at 4 different deposition times are shown in Fig. 3.31. Unsubtracted peak height values have been used in these plots. The plots show that long deposition times will lead to considerable error in the calculations as the curves for 120- and 180-s deposition times are non-linear over almost the whole concentration range. This is because the mercury surface is saturated with the complex and added Cr does not bring about the expected increase in the peak height.

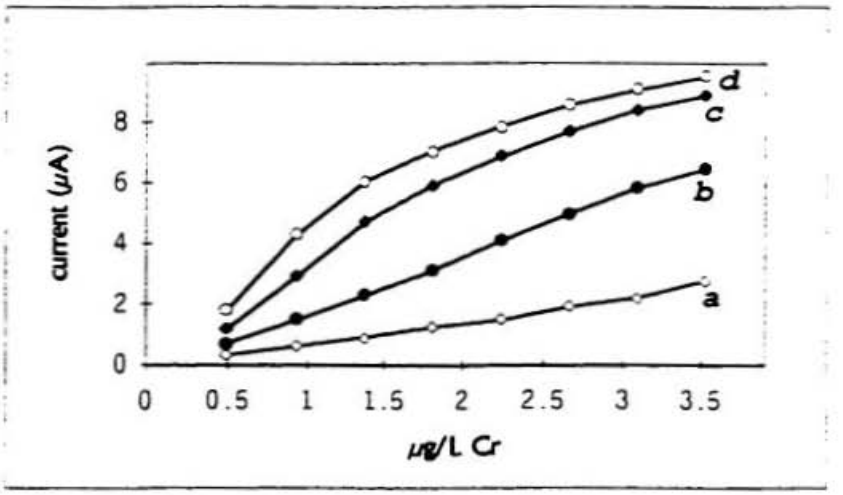

Fig. 3.31: Linearity of response for different deposition times. (a) 30 s, (b) 60 s, (c) 120 s and (d) 180 s.

Interestingly, careful examination of the curves for 30- and 60-s depositions show that after respectively 4 and 3 standard additions (each ~0.5 μg/L Cr), the calibration lines show a very slight outward curvature, i.e., fresh additions of chromium bring about a greater increase in peak height than expected. This is explainable in the light of the argument in Chapter 4 where it is shown that the species deposited is Cr^{II}-XO, which is formed by the reaction between Cr(II) species produced *status nascendi* and XO which is already adsorbed on the mercury. The deposition time also controls the amount of XO adsorbed; for a given, short, deposition time if high levels of Cr are present in solution, competition for XO may result in the formation and deposition of an interfering dinuclear Cr-XO-Cr complex. Simultaneous reduction of this complex and of the analytical Cr-XO complex would explain the curvature in the calibration plots.

The linearity of response for a 60-s deposition is very good for the 0-2 µg/L Cr range. It is recommended that application of this method with a 60-s deposition time be restricted to the analysis of samples with a Cr content not exceeding ~0.5 µg/L Cr. After three standard additions, the total Cr concentration in solution would be about 2 µg/L which is within the linear range. For analysis of solutions with high Cr content (unlikely in natural waters), the original samples can be diluted to the applicable concentration range or shorter deposition times can be used.

3.11 SPECIATION OF CHROMIUM IN THE N.W. ATLANTIC OCEAN

The CSV method developed in this work was applied to the determination of Cr species in the water column at a station located between Labrador and Greenland in the N.W. Atlantic Ocean. The seawater samples were collected in low density polyethylene bottles on 10 August 1993 (Section 2.5) and kept double-bagged and frozen at -14 °C until the analyses were performed. The seawater analyses were carried out during a one-month period in 1997. For the analysis, each frozen seawater sample was thawed at room temperature (it took about 5 hours for this to occur) and the analysis was usually completed within 3 hours of thawing. This was thought necessary for minimizing speciation changes and Cr losses through adsorption on the container surfaces. Each sample was analyzed separately for total Cr as Cr(III) (E_{dep}= -1.2 V, calibration by 3 standard additions of Cr(III)) and for Cr(VI) only (E_{dep} = -0.2 V, calibration by 3 standard additions of Cr(VI)). Moreover, simultaneously with the determination of $^{-0.2V}$Cr(VI), $^{-1.2V}$Cr(VI) was also determined. The value of $^{-1.2V}$Cr(VI) thus obtained should always be such that $^{-0.2V}$Cr(VI) $\leq$ $^{-1.2V}$Cr(VI) $\leq$ Cr(III) and this criterion provided an empirical check on the accuracy of the results. Two samples (samples 7 and 25) were analyzed in triplicate whereas all other samples were analyzed only once. However, all voltammetric runs were carried out in triplicate and electronically averaged to obtain the mean voltammogram;

this was then used for obtaining the values of i_p after a baseline subtraction as explained in Section 3.9. The experimental procedure is briefly summarized below.

Determination of total Cr as Cr(III)

(All voltammograms obtained by deposition at -1.2 V and scanning from -1.2 to -1.6 V)

- Transfer sample to voltammetric cell
- Adjust pH to ~ 1.8 with Q/2-HCl
- Add 50 μL of 1.5 M Na_2SO_3
- Stir for 30 s, place voltammetric cell in electrode and purge for 6 min.
- Buffer to pH ~6.6-6.7, replace in electrode and obtain blank voltammogram
- Add NO_3^-, XO and complete calibration by standard additions of Cr(III)

Determination of $^{-0.2V}$Cr(VI) and $^{-1.2V}$Cr(VI)

(Voltammograms for $^{-0.2V}$Cr(VI) obtained by deposition at -0.2 V and scanning from -1.2 to -1.6 V; voltammograms for $^{-1.2V}$Cr(VI) obtained by deposition at -1.2 V and scanning from -1.2 to -1.6 V).

- Transfer sample to voltammetric cell
- Buffer to pH ~6.6-6.7, place in electrode and obtain blank voltammograms
- Add NO_3^-, XO and complete calibration by standard additions of Cr(VI)

Results of the analyses are shown in Table 3.9 and have been plotted as a vertical profile in Fig. 3.32.

Table 3.9: [Cr] at 54.50°N, 48.46°W in the N.W. Atlantic Ocean

S. #	Depth (m)	pH	total Cr µg/L	Cr(VI) µg/L	Cr(III) µg/L	Cr(III)/ Cr(VI)
7	15	8.12	0.144	0.104	0.040	0.385
18	30	8.15	0.147	0.121	0.026	0.215
8	45	8.25	0.138	0.115	0.023	0.200
17	75	8.17	0.102	0.059	0.043	0.729
14	150	8.56	0.110	0.103	0.007	0.068
13	350	8.30	0.137	0.088	0.049	0.557
36	500	8.33	0.141	0.099	0.042	0.424
35	950	8.48	0.142	0.105	0.037	0.352
27	1407	8.46	0.165	0.164	0.001	0.006
21	1698	8.16	0.169	0.154	0.015	0.097
28	1990	8.42	0.162	0.160	0.002	0.013
22	2281	8.11	0.170	0.167	0.003	0.018
23	2573	8.25	0.179	0.179	0.000	0
24	2961	8.19	0.190	0.190	0.000	0
26	3398	8.30	0.119	0.119	0.000	0
34	3593	8.44	0.198	0.198	0.000	0
25*	3682	8.50	0.135	0.104	0.031	0.298

* - is 30 m above bottom

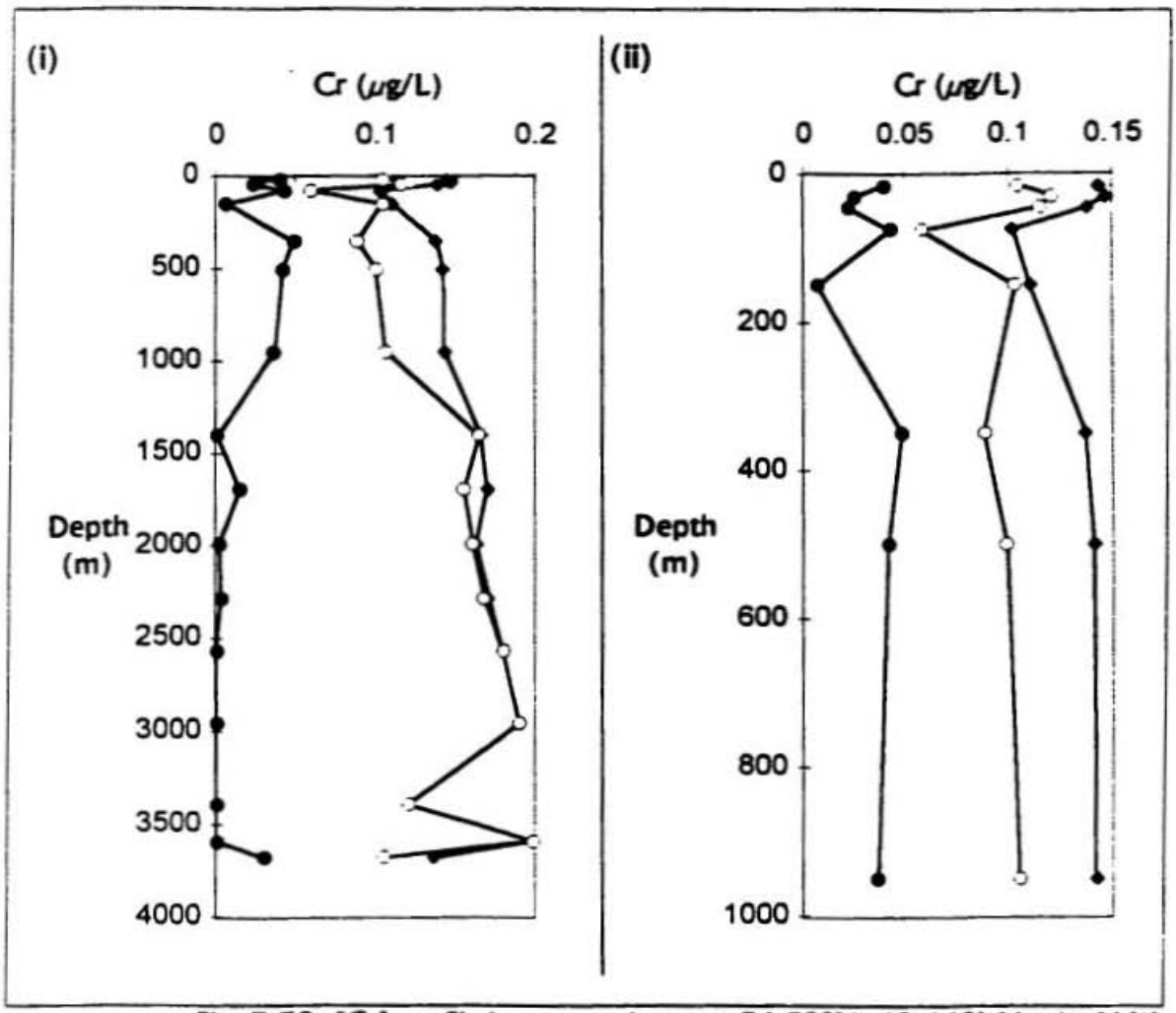

Fig. 3.32: [Cr] profile in water column at 54.50°N, 48.46°W in the N.W. Atlantic Ocean: •, total Cr; ○, Cr(VI) and •, Cr(III).
(i) shows the complete depth profile and (ii) is the profile for the top 1000 m

It should be mentioned at this point that the aim of this exercise was mainly to demonstrate that the newly developed method could be applied to the determination of Cr speciation in environmental samples. Therefore, no attempt

is made here to correlate [Cr] with other existing oceanic data for the water column. The [Cr] data obtained here will be integrated into an extensive study that has been undertaken by an interdisciplinary research group under the aegis of the Intergovernmental Oceanographic Commission. However, some general comments about the results can be made by comparing these results with available oceanic data on Cr. Cr profiles have been published for the Pacific Ocean [33, 42, 166, 169-171], the Mediterranean Sea [102, 171, 172], the North Atlantic Ocean [103, 171] and the North West Atlantic Ocean [167].

Campbell and Yeats [167] have determined total Cr at 2 stations in the N.W. Atlantic Ocean (50°47.9' N, 44°01.7' W and 53°00.0' N, 40°59.7' W), one station in the Labrador Sea (60°51.0' N, 56°14.6' W) and one station in the Baffin Bay (72°14.1' N, 65°56.9' W). These stations are in the same geographical region as the station from which the samples for this study were collected. The total Cr concentrations reported by these authors vary between 0.172 and 0.270 µg/L. The total Cr concentrations found in this study (0.102 to 0.198 µg/L) are about 25-40% lower than the values reported by Campbell and Yeats. Some factors that could explain the difference in the observed [Cr] in this study and the previous study are:

1. the seasonal variation of Cr; Campbell and Yeats do not mention the season during which the sampling was carried out.

2. the storage of samples after sampling. Campbell and Yeats acidified the water samples immediately upon collection. The storage at high acidity could be responsible for remobilizing organically bound and colloidal Cr. These processes would lead to higher [Cr] values. In contrast, for this study, the samples were refrigerated at natural pH upon collection and then stored for about 4 years. Adsorptive losses during the storage period as well as the fact that the CSV method used can detect only dissolved Cr would lead to lower [Cr].
3. shortcomings in the analytical technique used. Campbell and Yeats utilized a method based on the solvent extraction of Cr(III) with Alamine 336 for the preconcentration of Cr and subsequently quantified Cr by Flameless-AAS. Since such an analytical procedure is prone to introduced contamination, incorrect [Cr] values may result. For example analyte carry-over during the analysis could lead to higher values of Cr.

The total Cr profiles in Fig. 3.32 show that below the surface, there is depletion down to about 100 m followed by a gradual increase with depth. Cr(VI) and total Cr follow a similar vertical distribution. Such profiles have also been observed in the Pacific Ocean [33, 42, 166] and the Atlantic Ocean [167] and are indicative of a biointermediate behaviour, with a moderate degree of biogeochemical recycling. In contrast, in the Mediterranean Sea, Cr apparently has a conservative behaviour [102]. According to van den Berg et al. [102], a surface

depletion is not observed in the Mediterranean because of atmospheric inputs or low primary productivity in those oligotrophic waters.

The apparent Cr minimum observed at 3400 m has also been observed at approximately the same depth by Campbell and Yeats [167]. These authors have rationalized the Cr profiles with other hydrographic data and movement of water masses. It is anticipated that such correlation will also be made for the data shown in Table 3.9.

The Cr(III)/Cr(VI) ratios in Table 3.9 show that the predominant species in the water column is Cr(VI), which is thermodynamically the most stable form in oxygenated waters. Unfortunately no data are available for the speciation of Cr in these waters, but the speciation data is in agreement with recent data for Cr in oceanic waters [33, 42, 102].

The Cr(III) profile in Fig. 3.32 shows that Cr(III) is present especially within the region where total Cr depletion occurs. Cr(III) also shows an inverse correlation with Cr(VI) in this region. Both these factors could be explained by taking into consideration biological activity involving uptake/release of Cr that result in the transformation of Cr species by micro-organisms. Surface enrichment in Cr(III) can also occur through atmospheric deposition as well as by the photoreduction of Cr(VI) [168].

Absence of Cr(III) at greater depths is indicative of its being scavenged by sinking detritus which results in its removal from the water column. It is interesting to note that at the deepest point sampled, Cr(III) is detected again. This could be attributed to the remobilization of Cr(III) from the bottom sediments.

CHAPTER 4

ELECTRODE PROCESSES

In this chapter, the nature of the electrode process is investigated. Given the complexity of the equilibria in solution, however, the extreme difficulty faced in the complete identification of the ligand species actually involved in the complexation with Cr is acknowledged. The presence of two complexing sites on the ligand further complicates the study of the species in solution. XO can form ML, M_2L, ML_2 and M_2L_2 types of complexes [114]. The difficulties involved in a study of the complexes of XO has been recognized by several authors [114, 173].

With the above in mind, the study of the electrode processes is restricted to identifying the Cr species involved in the reduction rather than the complex itself. Also, no attempt is made to identify the XO species that are involved in the complexation process, although they are believed to be H_3XO^{3-} and H_2XO^{4-}. Therefore, in the following discussion, the charges on the complexes are omitted.

4.1 NATURE OF THE ADSORBED SPECIES

The following conclusions can be made from some observations noted during the course of Chapter 3.

1. The optimal conditions for the determination of $^{-0.2V}$Cr(VI), $^{-1.2V}$Cr(VI) and $^{-1.2V}$Cr(III) are exactly the same, which means that the analytical peak is likely to be due to the electrodic reduction of the same species in each case. Since the analytical peak is seen only in the presence of Cr and no other metal ion, it is unlikely that the peak is due to a reduction of the ligand. Also, since no peak is seen in the absence of the ligand, the species responsible for the analytical peak has to be a Cr-XO complex. Cr reduction is expected in the -1 to -1.7 V potential range [79].
2. The Cr(III)-XO complex formed in solution by the reaction between XO and nascent Cr(III) (from the chemical reduction of Cr(VI)) is not adsorbed onto the mercury (Section 3.7.5, pages 93-94).
3. Failure of Cr(III) to give reduction peaks at deposition potentials less negative than -0.8 V shows that either a Cr(III)-XO complex is not formed under the solution conditions or else a complex is formed but not adsorbed on the mercury electrode. Since it has been shown above that the Cr(III)-XO complex is not adsorbed on mercury, it can be confirmed that a Cr(III)-XO complex is not formed in solution; if it did, the response from a Cr(III) solution would show a gradual decrease with time, as was

the case with the gradual removal of Cr(III) from solution as a result of complexation with citric acid and tartaric acid (Section 3.8.2). However, very stable peaks are obtainable with Cr(III).

Another observation pertinent to this discussion is that under open circuit conditions, with either Cr(III) or Cr(VI) in solution, no analytical peak is observed. This observation was made by carrying out the experiment in the normal manner except that the electrode was switched off immediately after dispensing a new mercury drop and switched on just before the stripping stage. The solution was stirred as usual. This again shows that a Cr(III)-XO complex does not exist in solution. Nor does a Cr(VI)-XO exist because otherwise peaks would be observed during open circuit deposition of Cr(VI) solutions. That a Cr(VI)-XO complex does not exist in solution is trivial because Cr(VI) occurs as an anion and cannot be complexed.

All of the above observations lead to the conclusion that the analyte Cr-XO complex does not exist in solution but is formed *in situ* by the reaction between XO_{ads}(Hg) and a Cr species generated by the electrodic reduction of the Cr(III) and Cr(VI). The adsorption of XO is demonstrated in Section 4.2.

Given the electroactivity of Cr(III), the complex formed cannot be other than Cr^{III}-XO_{ads}(Hg). At the potential of its generation from Cr(III), the Cr^{III}-XO complex would be unstable because the complex is reduced at -1.45 V. This complex will

therefore immediately get oxidized to the Cr^{III}-XO complex and remain adsorbed. Hence, the species accumulated on the electrode during the deposition step is Cr^{III}-XO. This mechanism for the formation of Cr^{III}-XO is along the same lines as the reduction of Cr(III) in the presence of EDTA [174] and other N-substituted ethylenediaminetriacetic acids [175]. A similar mechanism was proposed for the adsorption of the electroactive species in the CSV of Fe (Section 3.8.4.1).

From Cr(III), the adsorbed complex is then formed as follows:

$$Cr(III)_{aq} + XO_{ads}(Hg) + e \rightarrow Cr^{II}\text{-}XO_{ads}(Hg)$$

$$Cr^{II}\text{-}XO_{ads}(Hg) \rightarrow \mathbf{Cr^{III}\text{-}XO_{ads}(Hg)} + e$$

The formation of the electroactive complex from Cr(VI) is straightforward. The reduction of Cr(VI) to Cr(III) is possible at potentials less than -0.05 V [96, 176]. However, depending on the deposition potential being used, the complex formation may proceed through the involvement of intermediates like Cr(V) and Cr(IV) which provide many pathways to the formation of Cr(III) species [177]. It is expected that the intermediates would be involved at less negative potentials (e.g., at -0.2 V) whereas, as the deposition potential is made more negative, the reduction of Cr(VI) could involve a one step, 3-electron reduction to Cr(III). $E_{1/2}$ for the 3-electron reduction of $Cr_2O_7^{2-}$ is -0.96 V (v SCE) [79]. Some possible pathways for the formation of Cr^{III}-XO on the electrode are shown below.

Formation of intermediates,

$$Cr(VI)_{aq} + e \rightarrow Cr(V)_{aq}$$

$$Cr(VI)_{aq} + 2e \rightarrow Cr(IV)_{aq},$$

followed by the formation of the adsorbed complex,

$$Cr(V)_{aq} + Cr(IV)_{aq} + XO_{ads}(Hg) \rightarrow Cr(VI)_{aq} + \mathbf{Cr^{III}\text{-}XO_{ads}(Hg)},$$

or

$$Cr(IV)_{aq} + Cr(IV)_{aq} + XO_{ads}(Hg) \rightarrow Cr(VI)_{aq} + Cr^{II}\text{-}XO_{ads}(Hg)$$

$$Cr^{II}\text{-}XO_{ads}(Hg) \rightarrow \mathbf{Cr^{III}\text{-}XO_{ads}(Hg)} + e$$

or [178],

$$3Cr(IV)_{aq} + 2XO_{ads}(Hg) \rightarrow Cr(VI)_{aq} + 2\mathbf{Cr^{III}\text{-}XO_{ads}(Hg)},$$

or, through a 3-electron reduction of Cr(VI),

$$Cr(VI)_{aq} + XO_{ads}(Hg) + 3e \rightarrow \mathbf{Cr^{III}\text{-}XO_{ads}(Hg)}$$

The different mechanisms leading to the formation and adsorption of the electroactive species would explain the different sensitivities for $^{-0.2V}$Cr(VI), Cr(III) and $^{-1.2V}$Cr(VI).

4.2 ADSORPTION ON MERCURY

In the formulation of a mechanism for the adsorption of the electroactive species during the deposition stage, it is claimed that during the reaction between Cr(II) and XO (as also between Fe(II) and XO: Section 3.8.4.1), the metal ion reacts with the ligand which is already adsorbed on the electrode. This was demonstrated by a series of experiments in which the solution in the electrode was changed by substituting the voltammetric cell. All these experiments were done in Nanopure water. Typically, these experiments were done as follows: a voltammetric cell (Cell 1) containing a test solution under given conditions (constituents, pH) was placed in the electrode and a voltammetric programme initiated. After a suitable deposition time t(1), at E_{dep} = E(1), while the voltammetric programme was still on, the voltammetric cell was substituted with a fresh cell (Cell 2) containing a deaerated solution under a different set of conditions. A further deposition was then effected under the previously initiated voltammetric programme (at E_{dep} = E(1) or a different potential E(2)) for a time t(2), following which a normal stripping voltammogram was obtained. Hence by varying the contents and pH of cells, E(1) & E(2) and the deposition times t(1) & t(2), a study could be made of the adsorption of the complex on the electrode.

Some observations and ensuing conclusions from these experiments follow. The observations below are valid for $^{-0.2V}$Cr(VI), $^{-1.2V}$Cr(VI) and Cr(III) and no

further distinction between these species will be made during the course of this discussion.

1. Normal analytical peaks result if the deposition of the complex is effected from a solution containing Cr and XO with or without NO_3^- but the stripping is carried in a solution containing only NO_3^- at pH 7. The peaks persist whether the stripping is carried out immediately or up to 2 min after changing the solution. This shows that the Cr-XO complex is very strongly adsorbed on the electrode and does not desorb back into solution in the absence of the XO/Cr in Cell 2.

   A similar conclusion can be reached from an observation that following a deposition at the optimum E_{dep} (-1.2 V), if the scanning during the stripping step is done from 0 V after an equilibrium time at this potential, peaks obtained are comparable to those obtained when scanning from -1.2 V.

2. If XO and Cr are deposited sequentially (XO from cell 1 and Cr from cell 2), Cr peaks are obtained as usual. The peak heights then depend on the deposition times t(1) as well as t(2). While it is normal that i_p should increase with increasing t(2), it was found that at constant t(2), i_p increased with increasing t(1). For example, for t(2) = 130 s, i_p values of 399, 1507 and 1857 nA were obtained for t(1) = 5, 50 and 100 s

respectively. This shows that the free XO is first deposited on the electrode and then Cr(II) complexes the adsorbed XO.

3. Voltammograms obtained by the deposition of XO at

    a) varying E(1) (in the range from 0 to -2 V) and

    b) varying pH (pH 3.5, 5.3, 7 and 10),

    followed by deposition of Cr (at E(2) = -1.2 V) and stripping led to comparable analytical peak heights for Cr. Similar peak heights were also obtained when XO was deposited under open circuit conditions. This shows that XO is strongly adsorbed on mercury, independently of pH and at all potentials.

All the above points establish that XO adsorption is achieved prior to the formation of the complex on the electrode. It can also be stated that after the stripping step, the XO remains adsorbed on the electrode as the free XO. This attests to the strength of the adsorption of XO on Hg.

It was stated in Section 3.2 that the Cr(VI) response is stable when solutions containing Cr(VI)-XO are left standing in the presence of mercury. This is remarkable because it is well known the reduction of Cr(VI) starts as soon as it comes into contact with mercury [79]; the stability in the presence of XO can be explained by the formation of an adsorbed film of XO on the mercury surface.

This film inhibits the reduction of Cr(VI) by preventing the direct contact between Cr(VI) and mercury.

4.3 ROLE OF NITRATE IONS

In the Square Wave experiments, addition of NO_3^- was shown to lead to enhanced peak heights. This enhancement has been attributed to the regeneration of the oxidized species by a catalytic reduction of NO_3^-. The occurrence of enhanced polarographic waves in the reduction of Cr complexes in the presence of NO_3^- was first observed and fully investigated by Tanaka and Ito [94] in a polarographic study of Cr(III)-EDTA. Subsequent work by the same authors [122] on Cr complexes with some other polyaminodiacetic acids (Cyclohexanediaminetetraacetic acid (CDTA), Trimethylenediaminetetraacetic acid (TRDTA) and N-(2-Hydroxyethyl)ethylenediaminetriacetic acid (HEDTA)) yielded similar conclusions on the nature of the effect of NO_3^- on the reduction current. These authors showed conclusively that Cr(II)-EDTA, the product of the electroreduction of Cr(III)-EDTA, chemically reduces NO_3^- in the vicinity of the electrode. In the process, Cr(III)-EDTA is regenerated and then electrochemically reduced again, with a concomitant enhancement of the reduction current.

The catalytic process can be summarized as:

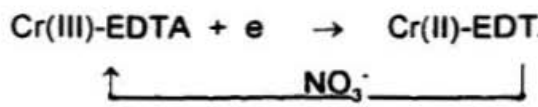

The products of the NO_3^- reduction in the above reaction have not been completely elucidated. Based on the observation that one mole of NO_3^- reacted with 8 moles of Cr(II)-EDTA, Tanaka and Ito [94] have proposed the following

$$8Cr^{II}\text{-EDTA} + NO_3^- + 10H^+ + 5H_2O \rightarrow 8[Cr^{III}(H_2O)EDTA]^+ + NH_4^+,$$

but invoke the possibility that the reduction to NH_4^+ need not go to completion; an intermediate product like NH_2OH may also result. It is noteworthy that according to these authors [94], aqueous Cr(II) ions do not participate in the catalytic process.

Later, Zarebski [95] and Lanza and Tadia [179] utilized the catalytic effect in the polarographic determination of Cr in the presence of polyaminocarboxylic acids. With the advent of adsorptive CSV as an analytical technique, the catalytic step was included in methods for the sensitive determination of Cr with DTPA [96,98, 101] and TTHA [99, 100] as the complexing ligands.

In all the methods utilizing the catalytic effect of NO_3^- for sensitivity enhancement in the determination of Cr, the catalytic mechanism proposed by Tanaka and Ito [94] has been assumed and none of the authors has ventured into any further investigation of this mechanism, nor of the product of the NO_3^- reduction. In fact,

NO_3^- has also been utilized for sensitivity enhancement in the voltammetric determination of uranium [180, 181] and molybdenum [182-185], but again, no mention is made of the possible fate of the NO_3^- in any of these cases.

Taking into account the very convincing work of Tanaka and Ito [94] and the universal acceptability of the mechanism whereby the Cr(II) complex is reoxidized by NO_3^- at the electrode, it was decided that it would not be worthwhile investigating the catalytic behaviour any further. So, it was accepted that in the CSV determination of Cr as the Cr-XO complex, the catalytic enhancement was brought about by the chemical oxidation of Cr^{II}-XO to Cr^{III}-XO by NO_3^-. This implies that the analytical current seen is originating from the following process:

$$Cr^{III}\text{-}XO_{ads}(Hg) + e \rightarrow Cr^{II}\text{-}XO_{ads}(Hg)$$

$$\uparrow \quad \_\_\_\_\_ NO_3^- \_\_\_\_\_ \quad \downarrow$$

The effect of NO_3^- can be demonstrated in several ways. The most obvious demonstration of the effect of NO_3^- on the reduction peaks is the great enhancement observed in the peak heights. As discussed earlier, in the absence of the catalytic effect brought about by NO_3^-, the method would be unsuitable for the determination of Cr at levels seen in environmental samples.

The effect of the NO_3^- can also be deduced from the cyclic voltammetry of the Cr-XO system in the presence and in the absence of NO_3^- (Section 4.5).

A more tangible demonstration of the effect of NO_3^- in the electrode process is provided by an examination of the forward pulse and the backward pulse components of SW voltammograms obtained in the presence and in the absence of NO_3^-. The resultant current in a SW voltammogram is the difference between the current recorded in the forward pulse and the current in the backward pulse of the Square Wave. In the SW cathodic scan of a simple, reversible electron transfer process, the forward pulse would result in a cathodic current whereas the backward pulse would result in an anodic current as the species reduced during the forward pulse are oxidized again during this pulse. Since the cathodic and anodic currents have opposite signs, the resultant current is larger than either the forward or the backward current. However, in the presence of a competing catalytic process for the reoxidation of the reduced species, depending on the kinetics of the chemical reoxidation reaction, the reverse pulse may result in a large decrease or even a complete elimination of the anodic current. In some cases, the reverse pulse may even lead to a cathodic current if, when the pulse is reversed, the applied potential remains negative enough for sustaining the reduction of the chemically oxidized species. In the latter case, the resultant SW current will be less than the forward pulse current. This is why

in certain applications, Differential Pulse voltammetry is preferred to Square Wave voltammetry.

For obtaining the components of the SW voltammogram, the experiments were carried out in Nanopure water at pH ~7.1 on the Cypress System. This instrument has the capability of resolving the SW voltammograms into its forward and backward components. Such resolution is not possible on the Model 384B Voltammetric Analyzer. The forward pulse and backward pulse current components as well as the resultant currents in the SW voltammetry of the Cr-XO system in the absence and in the presence of NO_3^- are shown in Fig. 4.1.

In the absence of NO_3^-, cathodic and anodic currents are seen respectively in the forward pulse and the backward pulse, whereas in the presence of NO_3^-, both the forward pulse and the backward pulse yield cathodic currents. The presence of cathodic currents in the backward pulse confirms that by the time the pulse is reversed, the electrochemically reduced Cr(II) species has already been chemically reoxidized to Cr(III) by the NO_3^- and during the backward pulse, this Cr(III) is again reduced electrochemically, hence the cathodic current.

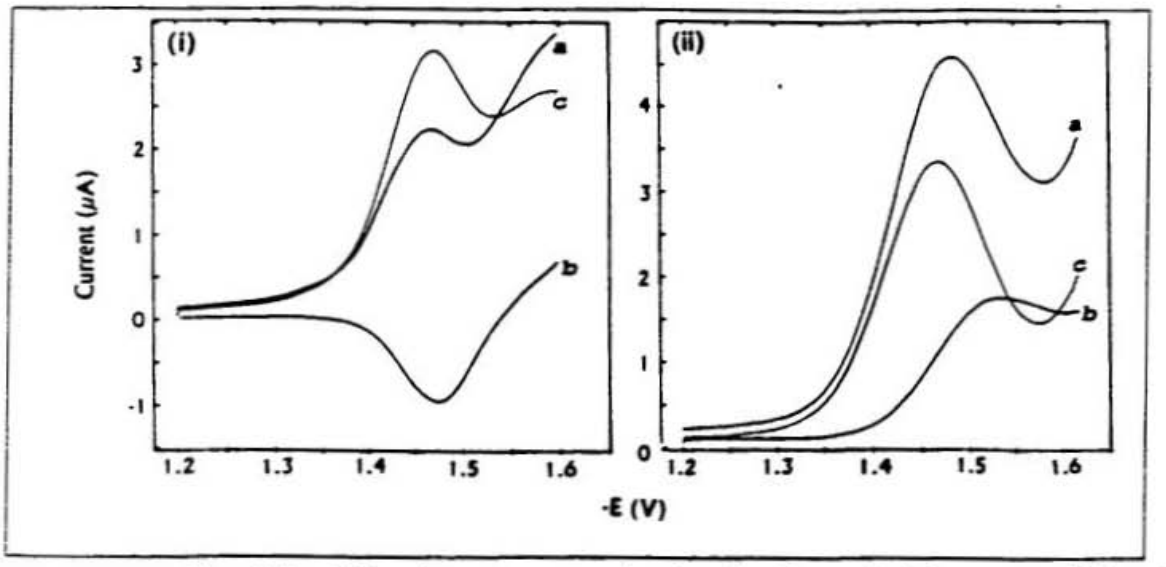

Fig. 4.1: SW voltammograms showing the forward *(a)*, reverse *(b)* and resultant *(c)* currents in the absence (I) and presence (II) of NO_3^-.

As demonstrated in Section 3.3, for the stripping process, the SW modulation is much more sensitive than the DP modulation, and this despite the cathodic current observed in the backward pulse of the SW modulation. This underlines the claim that the sensitivity achieved in SW voltammetry is unmatched by other voltammetric techniques.

The detection of an anodic current in the backward pulse of the SW voltammogram in Fig. 4.1. shows that the electron transfer step is reversible. This reversibility will be discussed further in Section 4.5.

4.4 VARIATION OF E_p WITH pH

Generally, the variation of E_p with pH can be used as a quick diagnosis for the number of electrons and (protons) involved is an electrochemical reaction. For a cathodic process involving *m* protons and *n* electrons as below,

$$Ox^{p+} + mH^{+} + ne \rightarrow Red^{(p+m-n)+},$$

E_p will shift cathodically by 59m/n mV per unit pH change.

A review of the literature on adsorptive stripping voltammetry showed that very few papers actually make any mention of the effect of pH on E_p. The few authors who do report such findings [110, 186-188] have not attempted to rationalize the experimental results in terms of the number of electrons involved in the process. This probably indicates that the above criterion may not be applicable to processes occurring from an adsorbed state. Vega & van den Berg [188] and Culjak et al. [187] have attributed the shift in E_p to the stabilization of the complex as a result of decreased proton competition at higher pH.

The variation of E_p with pH obtained in the present study, is shown in Fig. 4.2.

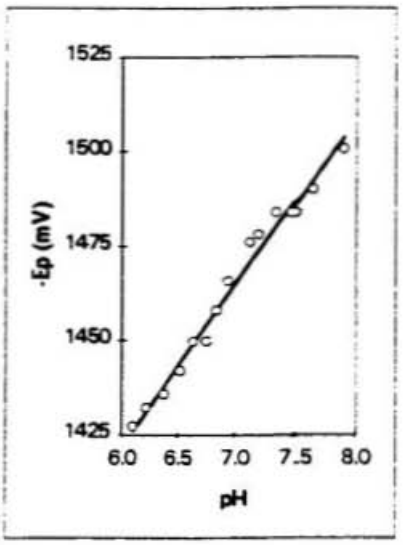

Fig. 4.2: Variation of E_p with pH.

A straight line fitted through the points in the graph has a slope of 43 mV/pH unit (r^2 = 0.98). Cathodic shifts in E_p of 30-45 mV/pH have been reported in several CSV methods [110, 186, 188]. It is difficult to interpret this value because it lies midway between 30 mV (two-electron process) and 59 mV (one-electron process). Strictly speaking, the value 43 mV/pH points to a process involving 3 protons and 4 electrons. It is highly unlikely for such a process to be occurring at the electrode.

4.5 CYCLIC VOLTAMMETRY

Cyclic voltammetry (CV) is a very powerful technique commonly used in the investigation of electrochemical reactions. Under favourable experimental conditions, CV can provide considerable information about mechanistic and kinetic parameters. CV can also be used for calculating the area occupied by the adsorbed molecule and predict its orientation on the surface.

Because of the particularities of the overall process leading to the analytical peak in the present study, some difficulties were anticipated in obtaining and interpreting the cyclic voltammograms. The main difficulty stemmed from the smaller currents witnessed in the cyclic voltammograms. Some factors responsible for this are:

1. the limited amount of the reducible complex available. This limitation is due to the fact that no complex is present in the bulk solution but is generated/deposited on the electrode.
2. NO_3^-, which in the normal stripping experiments enhance the reduction current by reoxidizing the reduced species, cannot be used in cyclic voltammetric investigations (see below).
3. the waveform used in cyclic voltammetry is a linear one. It was shown in Section 3.3 that the sensitivity of LSV is much lower than SW voltammetry.

Another factor which complicated the interpretation of cyclic voltammograms was that the peaks are seen on a rapidly increasing background current. This, in conjunction with the observation that the switching potential, E_{λ}, cannot be too negative with respect to the peak potential (see below) meant that the peaks were ill-defined and peak heights could only be roughly estimated.

In view of the above, the objective of CV was restricted to an investigation of the reversibility of the electrode process and attempting to find the number of electrons involved in the reduction of the adsorbed complex.

It was predictable that the analytical peak had to be the result of a reversible, one-electron charge transfer because of the subsequent participation of the reduced species in the catalytic reaction with NO_3^-. The product of an irreversible electron transfer would not participate in such a reaction. Furthermore, catalytic reactions tend to be centered on a one-electron reduction step, as the kinetics of a two-electron step would be too slow [188].

Preliminary cyclic voltammetric experiments were carried out on the Model 384B Polarographic Analyzer by generating and depositing the complex on the mercury electrode for 60 s. After a 10-s quiescence time, the electrode was subjected to a cyclic potential scan at 200 mV/s. The forward sweep was cathodic and the reverse sweep anodic. The switching potential was set at -1.6 V. Because of the expected low currents, relatively larger concentrations of Cr

were used for these experiments. All cyclic voltammetry experiments were done in Nanopure water at pH 7.1.

Cyclic voltammograms of 4 µg/L Cr, obtained in the presence of NO_3^- did not show any reverse peaks despite prominent forward peaks. This was expected because for a catalytic electrode process, the reduced species will be reoxidized faster chemically than electrochemically [189]. Thus an anodic peak will not be seen because by the time the reverse sweep is applied all the reduced species will have been reoxidized by the NO_3^-.

However, even in the absence of NO_3^-, anodic peaks consistently failed to materialize in the cyclic voltammograms of Cr-XO solutions (up to 50 µg/L Cr). As will be seen below, the anodic peaks were not seen in these voltammograms because of the scan rate and the switching potential employed.

As already mentioned above, the utilization of a linear potential scan in cyclic voltammetry results a dramatic loss in sensitivity and failure to see anodic peaks in cyclic voltammetry was initially ascribed to the extremely low values of the oxidation current. In fact, even the cathodic peaks were barely visible in the cyclic voltammograms (Fig. 4.3(i)). It was thought that if cyclic voltammograms could be obtained by applying a SW potential scan, the sensitivity of both the cathodic and anodic processes could be enhanced and the anodic peaks could then be seen.

Some SW stripping experiments were therefore carried out in which the complex was deposited at -1.2 V but the stripping scan was carried out from -1.6 V to -1.2 V. (In normal experiments, stripping is done by scanning from -1.2 V to -1.6 V). The sudden potential jump from -1.2 V to -1.6 V will generate a flux of reduced species at the electrode and, in the event of the reversibility of the process, a rapid anodic scan will produce an oxidation peak as the reduced species are reoxidized. This peak will be equivalent to the reverse peak of a normal cyclic voltammogram. However, since the Model 384B Voltammetric Analyzer does not discriminate between anodic and cathodic currents in the SW stripping mode, the shape of the voltammogram will still look like a cathodic peak.

Combination of a normal SW voltammogram (scan from -1.2 V to -1.6 V) and a 'reverse' SW voltammogram (scan from -1.6 V to -1.2 V) would then constitute a 'pseudo-cyclic' voltammogram. The advantage gained by this method is that a Square Wave modulation can be used for the potential sweep, resulting in larger currents. The usefulness of this method is evident on comparing the normal and the pseudo-cyclic voltammograms shown in Fig. 4.3.

Whereas no peak (cathodic or anodic) is found in the normal CV, a well defined cathodic peak and an anodic peak are seen in the 'forward' and 'reverse' sweeps of the pseudo-cyclic voltammogram. The peak on the reverse sweep is not well defined and looks like an inflexion rather than a peak but it indicates that the

reduction is reversible. It is noteworthy that the first hint on the reversibility of the electrochemical reduction was provided by pseudo-cyclic voltammetry.

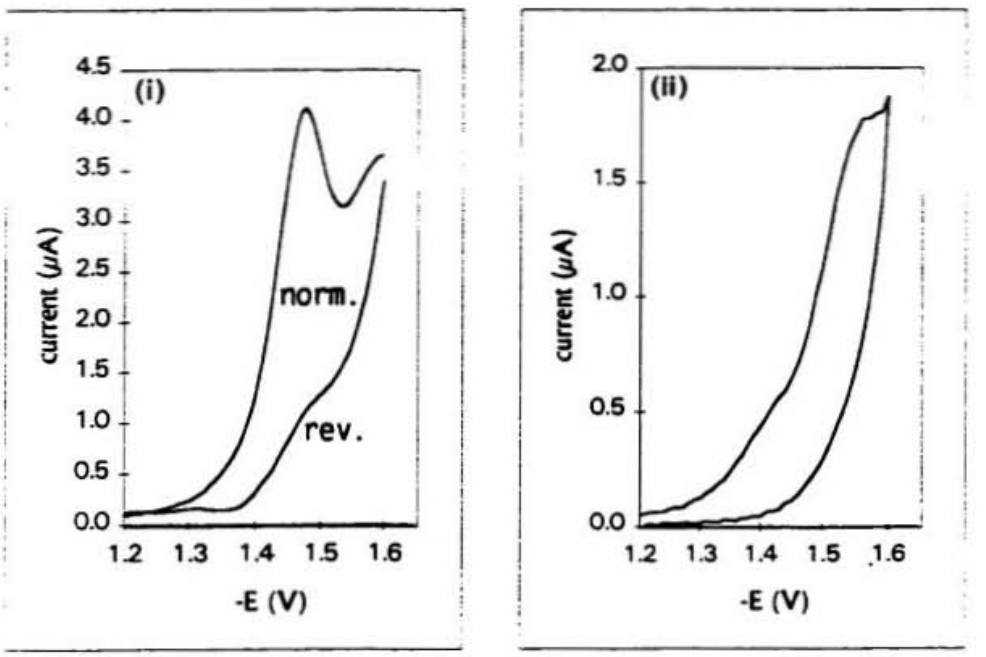

Fig. 4.3(i): SW pseudo-cyclic voltammograms at 200 mV/s. **norm.**: scan from -1.2 to -1.6 V, **rev.**: scan from -1.6 to -1.2 V.
(ii): LS cyclic voltammograms at 200 mV/s scan rate.

After the process was shown to be reversible by pseudo-cyclic voltammetry, the Cr-XO system was investigated further by varying the conditions in the normal linear scan cyclic voltammetry and two important observations were made regarding the occurrence of the anodic peaks.

Results from the cyclic voltammetry of the Cr-XO complex in the absence of NO_3^- showed that the anodic peak is seen only at high scan rates. At the 50 µg/L Cr level, the anodic peak is first observed for a scan rate of about 1 V/s; the anodic peak height, $i_{p,a}$, then increases with increasing scan rates. Fig. 4.4 shows cyclic voltammograms obtained at scan rates of 200, 1000 and 1667 mV/s.

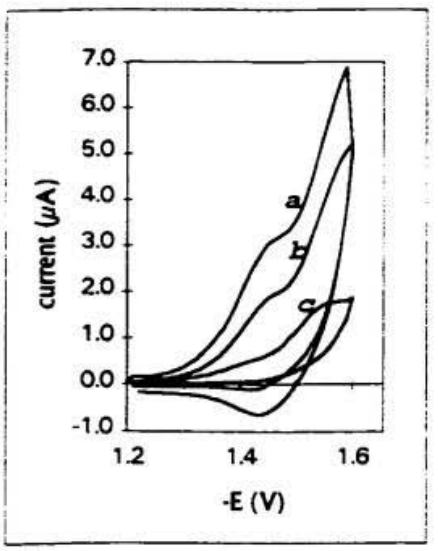

Fig. 4.4: Effect of scan rate on cyclic voltammograms. v = 1667 ***(a)***, 1000 ***(b)*** and 200 mV/s ***(c)***.

Whether an anodic peak is observed or not is also dependent on the switching potential, E_λ; if E_λ is too negative with respect to the cathodic peak potential, $E_{p,c}$, the anodic peak is not seen. This is shown in Fig. 4.5, where under similar scanning conditions, an anodic peak is seen for E_λ = -1.54 V, but not when E_λ = -1.8 V.

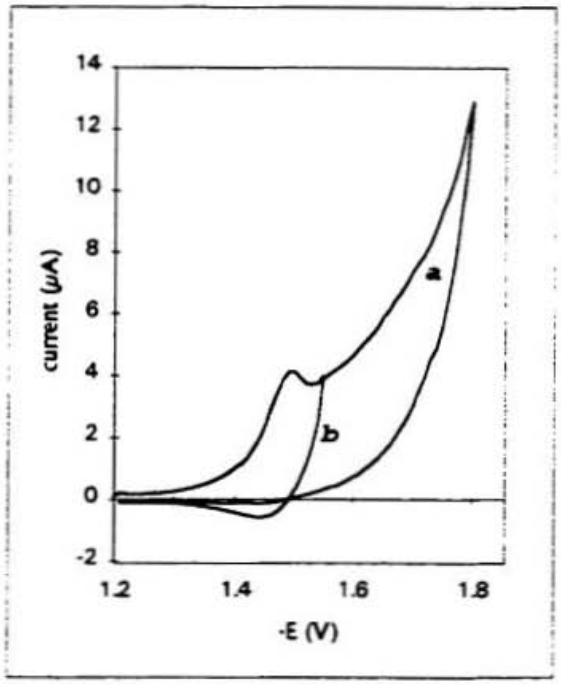

Fig. 4.5: Effect of E_λ on cyclic voltammograms. E_λ = -1800 mV *(a)* and -1540 mV *(b)*.

The effect of E_λ on $i_{p,a}$ is more clearly illustrated in cyclic voltammograms obtained with the Cypress System (see below) in Fig. 4.6. These voltammograms were obtained at 2 V/s for E_λ = -1540, -1600 and -1700 mV. The cathodic peaks are exactly coincident in each case but, as E_λ is made more negative, the decrease in the magnitude of the anodic current becomes distinct.

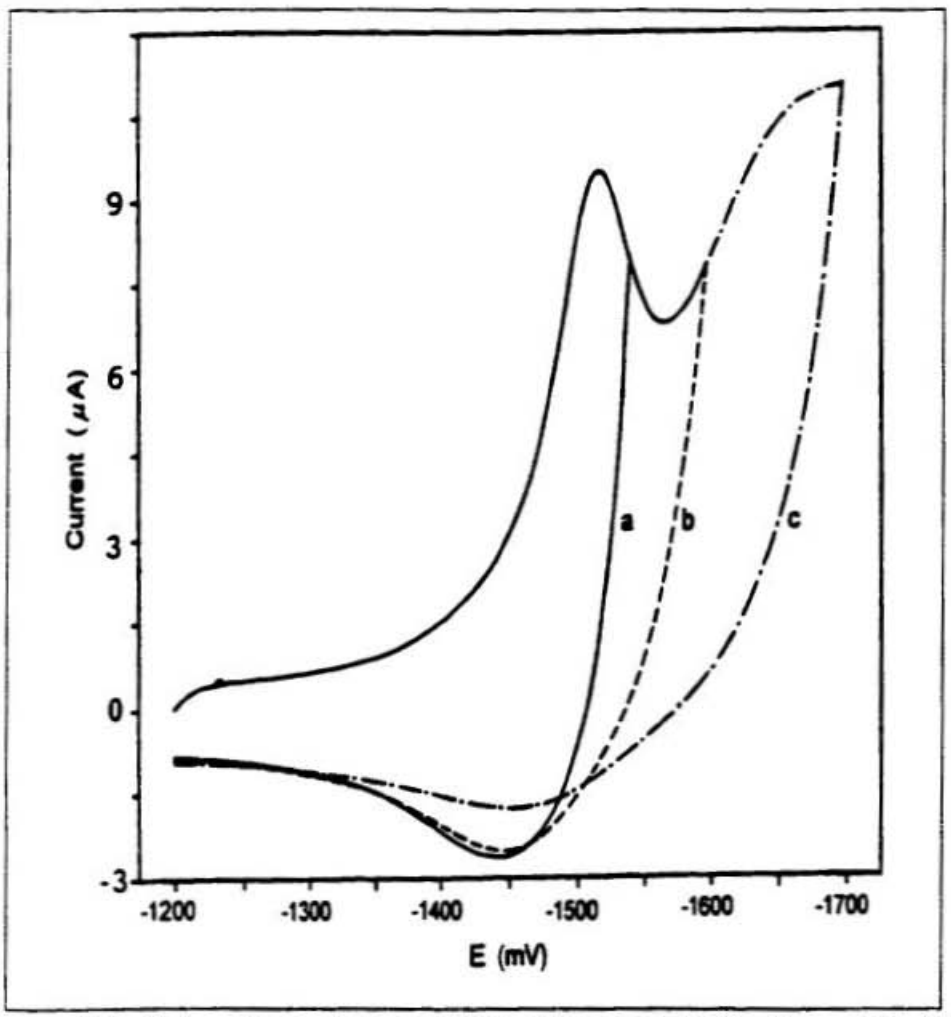

Fig. 4.6: Effect of E_λ on cyclic voltammograms. E_λ = *(a)* -1540, *(b)* -1600 and *(c)* -1700 mV. ν = 2 V/s.

Cyclic voltammograms of the Cr-XO system were also studied as a function of the scan rates, ν. The Model 384B Polarographic Analyzer was found not to be suitable for such a study because it does not provide a great degree of versatility in the choice of the scan rates; theoretically, a maximum rate of 2500 mV/s is

attainable but it was found that in practice, a maximum of only 1667 mV/s could be reached.

The Cypress System was therefore used for a study of the dependence of the anodic and cathodic currents in the cyclic voltammograms of the Cr-XO system. With a view to obtaining appreciably high values of currents, these experiments were done in solutions containing 85 µg/L Cr(VI) and 200 µL, 5 mM XO. At this level of Cr, small anodic peaks were visible for scan rates of 400 mV/s. As before, no anodic peak was seen in the presence on NO_3^-. A typical cyclic voltammogram in the presence of NO_3^- is shown in Fig 4.7.

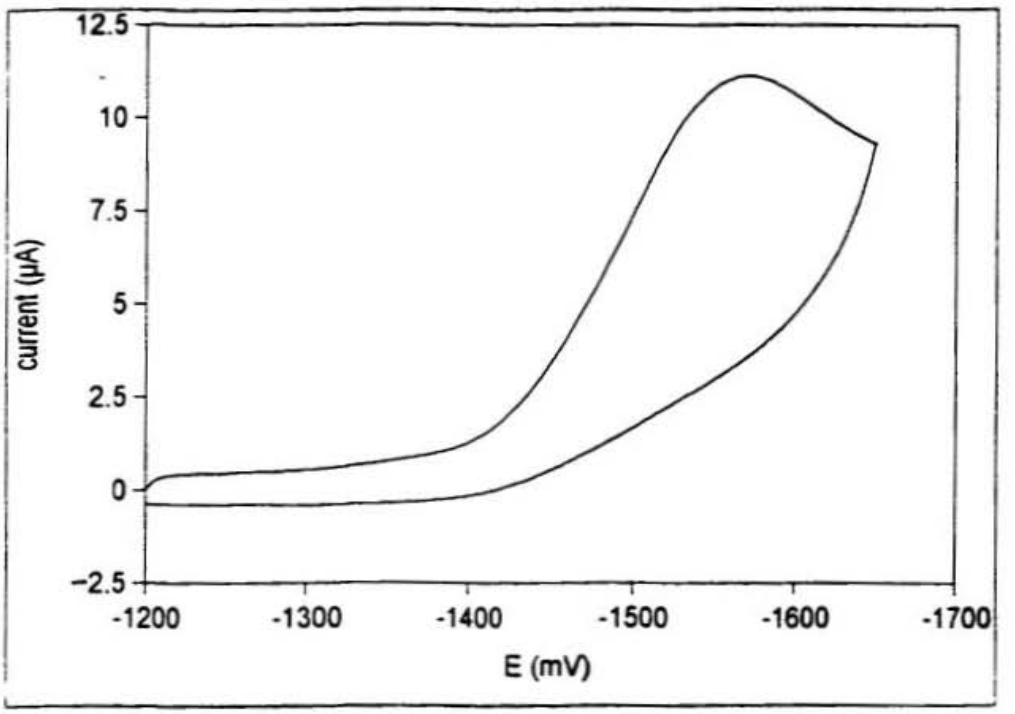

Fig. 4.7: Cyclic voltammogram of Cr-XO in the presence of NO_3^-.

Results obtained for the effect of scan rate on certain parameters of the CV of the Cr-XO system in the absence of NO_3^- are shown in Table 4.1.

It is again emphasized that because of the very high background currents seen, especially as the scan rate becomes faster, the values of the resulting peak currents are only estimates. Fig. 4.8 illustrates the method of estimation of the peak heights as well as the symbols used in Table 4.1.

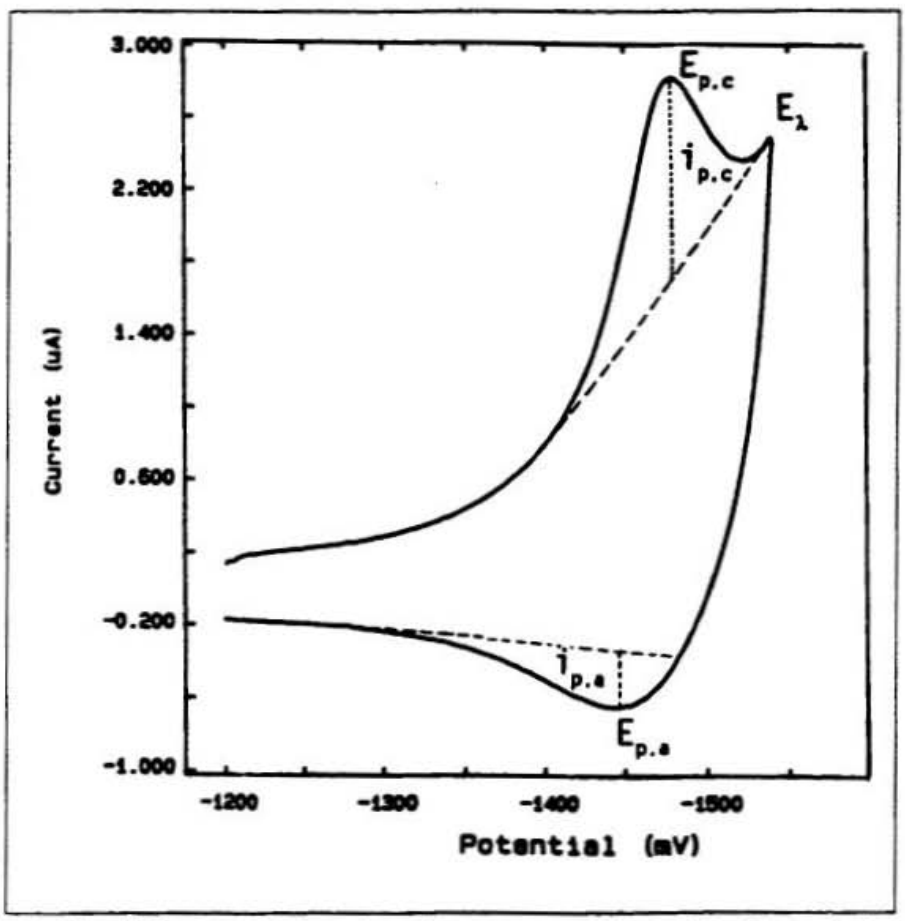

Fig. 4.8: A typical cyclic voltammogram illustrating the symbols used.

It is acknowledged that the method used for the calculation of $i_{p,a}$ is not proper and cannot be used for any rigorous analysis. But the estimated values of $i_{p,a}$ do provide a good qualitative picture of the increase in $i_{p,a}$ with the scan rate. The ratio $i_{p,a}/i_{p,c}$ which is normally a useful quantity in the analysis of cyclic voltammograms seems to be insignificant and will not be used for any conclusion. On the other hand the estimated value of $i_{p,c}$ is considered useful because it has been estimated in a standard manner.

Table 4.1: Effect of the scan rate on the cathodic and anodic peaks

v mV/s	$-E_{p,c}$ (mV)	$-E_{p,a}$ (mV)	ΔE_p (mV)	$-E_p$ (mV)	$i_{p,c}$ (µA)	$i_{p,a}$ (µA)	$i_{p,c}/v^{1/2}$	$10^3 i_{p,c}/v$	$i_{p,a}/i_{p,c}$
200	1438	-	-	-	n.q.	-	-		-
400	1468	1445	23	1457	1.24	0.27	0.06	3.1	0.22
600	1478	1445	33	1462	2.04	0.46	0.08	3.4	0.23
800	1488	1450	38	1469	2.96	0.84	0.10	3.7	0.28
1000	1495	1446	49	1471	3.84	0.92	0.12	3.8	0.24
1200	1498	1448	50	1473	4.40	1.12	0.13	3.7	0.25
1400	1503	1445	58	1474	5.20	1.36	0.14	3.7	0.26
1600	1508	1445	63	1477	6.16	1.60	0.15	3.9	0.26
1800	1512	1442	70	1477	6.96	1.76	0.16	3.8	0.25
2000	1516	1444	72	1480	7.60	1.84	0.17	3.8	0.24
3000	1530	1440	90	1485	10.72	2.72	0.20	3.6	0.25
4000	1543	1438	105	1491	13.44	3.20	0.21	3.4	0.24
5000	1553	1431	122	1492	15.84	4.00	0.22	3.2	0.25
7500	1575	1417	158	1496	20.40	4.80	0.24	2.7	0.24
10000	1592	1413	179	1503	25.60	4.80	0.26	2.6	0.19

ΔE_p: $-(E_{p,c} - E_{p,a})$

E_p: $\frac{1}{2}(E_{p,c} + E_{p,a})$

n.q.: not quantified

From the data in Table 4.1, it is not possible to draw any definite conclusions regarding the electrode processes but the following can be said:

1. the constancy of $i_{p,c}/\nu$ shows that the reduction is occurring from an adsorbed state; for a process occurring from an adsorbed state, $i_{p,c}$ is proportional to ν [190].
2. For 10-fold increases in the scan rate, the following cathodic shifts can be estimated in E_p:

   400-4,000 mV/s: 34 mV

   500-5,000 mV/s: 32 mV

   600-6,000 mV/s: 32 mV

   750-7,500 mV/s: 30 mV

   800-8,000 mV/s: 31 mV

   1000-10,000 mV/s: 34 mV

   This almost constant cathodic shift in E_p is indicative of an EC_{irr} mechanism involving a one-electron reduction. For an EC_{irr}, mechanism, E_p shifts cathodically by 30/n mV for a 10-fold increase in scan rate [191]. However, because of the essentially qualitative value of the cyclic voltammograms, it would not be wise to unequivocally state the existence of an EC_{irr} mechanism.
3. a quasi-reversible reduction or an ECE mechanism can be ruled out because for such processes, $i_{p,c}/\nu^{1/2}$ decreases with increasing ν [192].

This criterion is applicable to diffusion-controlled processes but has also been used for processes where the product is strongly adsorbed [193]. Its applicability in the present process, where the reactant is strongly adsorbed, is assumed.

That the anodic peak vanishes at slow scan rates and when the switching potential is too negative with respect to $E_{p,c}$ is indicative of a consecutive process that very rapidly depletes the reduced species at the electrode under these circumstances. The consecutive process could involve a further, irreversible reduction (an EE_{irr} mechanism) or an irreversible reaction of the reduced species (an EC_{irr} mechanism).

An EE_{irr} mechanism can be formulated as follows. It has been shown (Section 4.1) that the species adsorbed on the electrode is Cr^{III}-XO. Assuming a one-electron charge transfer process, it is possible that at $E_{p,c}$, Cr(III)-XO undergoes a reversible reduction to Cr(II)-XO. The current generated during this reduction constitutes the analytical peak in the Square Wave stripping voltammetry. At a potential E_{irr}, which is only slightly more negative than $E_{p,c}$, the Cr(II)-XO is then rapidly further reduced, irreversibly, to Cr(0) which gets deposited on the electrode as metallic Cr.

$$Cr^{III}\text{-}XO_{ads}(Hg) + e \rightleftharpoons Cr^{II}\text{-}XO_{ads}(Hg)$$

$$Cr^{II}\text{-}XO_{ads}(Hg) + 2e \rightarrow Cr^{0}\text{-}(Hg) + XO_{ads}(Hg)$$

Under such a mechanism, an anodic peak can only be observed if the potential sweep is reversed prior to E_{irr} and if the sweep rate is fast. A switching potential removed from $E_{p,c}$ and/or a slow scan rate will result in a longer time between the generation of the Cr(II) species and the advent of the reverse sweep. During this time interval, the irreversible reduction of Cr(II) can occur and hence no anodic peak will be seen on the reverse sweep. E_{λ} values too negative with respect to $E_{p'c}$ will also enhance the irreversible reduction of Cr(II), resulting in a depletion of the oxidizable species and hence a decrease the anodic current.

The EE_{irr} mechanism hinges on an irreversible 2-electron reduction of Cr(II) to Cr(0) but attempts to locate a peak corresponding to this process were unsuccessful. For this reason, it is thought that the EC_{irr} mechanism is more likely to be occurring at the electrode.

An EC_{irr} process would require an irreversible reaction that rapidly removes the reduced species from the vicinity of the electrode. As in the case of an EE_{irr} mechanism, the time elapsed between the forward sweep and the backward sweep would again explain why the anodic peaks are seen at high scan rates and for E_{λ} close to E_{p}.

One possible irreversible process could involve the reaction of Cr(II) with OH^- in the vicinity of the electrode to form an insoluble film of $Cr(OH)_2$ on the electrode. Such film formation has been shown to occur during the reduction of Cr(III)

complexes of some strongly basic ligands like ammonia or ethylenediammine in neutral unbuffered solutions by Tanaka and Sato [194]. These authors concluded that the reduction product of Cr(III) complexes with basic ligands dissociates to yield Cr(II) species and basic ligands. The liberated ligands make the solution alkaline in the vicinity of the electrode and cause the formation of the $Cr(OH)_2$. Such film formation was found not to occur in acidic solutions or with EDTA complexes, which shows that for such a process to occur, there has to be an excess of basic ligands in the vicinity of the electrode.

Such a process is unlikely to occur with XO as the ligand for several reasons. As seen earlier, the XO remains adsorbed on the electrode after the reduction of the Cr so there is no possibility of excess basicity (derived from the ligand; the products of NO_3^- reduction could in principle lead to extra basicity) in the vicinity of the electrode. Furthermore, although no data exist on the stability of Cr^{II}-XO, it is expected this complex will be very stable, given the extreme versatility of XO as a ligand to form complexes of different geometries (octahedral, tetrahedral and square-planar). The Cr(II)-EDTA complex is very stable in the absence of oxygen and it is believed that the Cr^{II}-XO complex will have comparable stability.

Another possible process responsible for the depletion of the reduced species from the electrode could be the formation of an irreducible polymeric species, $(Cr^{II}\text{-}XO)_n$, on the electrode. Cr(II) is known to form extremely stable polymeric

compounds with Schiff bases, resulting in the formation of compounds whose stability is such that they are insoluble in all common solvents and unusually stable to air oxidation; even on boiling with H_2O_2, oxidation to Cr(III) occurs only slowly [178]. The formation of a polymeric Cr(II)-XO complex would seem to be a natural extension of the capability of XO to form M_2L, ML_2 and M_2L_2 type complexes in solution and such a polymerization process would probably be highly favoured due to the XO being adsorbed on the electrode surface.

4.6 SUMMARY OF ELECTRODE PROCESSES

To summarize the electrode processes involved in the determination of Cr as the Cr-XO complex, it is postulated that the complex deposited on the electrode is Cr^{III}-XO. This complex is formed *in situ* at the electrode, by different mechanisms, depending on the Cr species and the potential used for the deposition, as explained in Section 4.1. For a given Cr species, the amount of Cr deposited under optimized conditions is proportional to [Cr] in the bulk of the solution and on the deposition time. During the stripping step of the CSV, Cr^{III}-XO is reduced reversibly by a one-electron process to Cr^{II}-XO. The current resulting from this step is the analytical parameter measured for the quantification of Cr and is catalytically enhanced by NO_3^-, as explained in Section 4.3.

The one-electron reduction of Cr(III) to Cr(II) is also supported by the fact that a survey of the electrode processes involved in the reduction of Cr(III)) complexes at the mercury electrode [121] shows that most complexes undergo a stepwise reduction, the first step corresponding to the one-electron reduction to the Cr(II) species, followed by the irreversible reduction of the reduced Cr(II) to Cr(0). In fact, no example could be found where the reduction of Cr(II) to Cr(0) occurs reversibly or through a prior one-electron reduction to Cr(I). Hence the analytical peak cannot be due to a process other than a Cr(III)/Cr(II) process.

After the stripping step, the fate of the Cr^{II}-XO is uncertain but of the three possibilities listed in Section 4.5, the EC_{irr} mechanism with the formation of inert polymeric Cr-XO species is thought to be the most probable.

CHAPTER 5

CONCLUSIONS

This research was undertaken following the observation that there was a need for a simple and sensitive method for the chemical speciation of Cr at concentrations prevalent in the aquatic environments, especially in seawater. The accurate determination of Cr species at these levels is fundamental to biogeochemical and geochemical studies of the metal in aquatic systems.

The main objective of this work was therefore to develop a method for the speciation of Cr. Inherent in this objective were requirements of the new method imposed by the environmental chemistry (concentrations and speciation) of Cr. The extremely low concentrations involved meant that

1. the detection had to be sensitive,
2. the overall analytical method should involve the use of a minimum number of additional reagents and analytical steps so as to reduce the risks of contamination and analyte losses,
3. the analytical procedure should be performable in a contamination-free environment.

The need for accurate speciation of Cr meant that the possibility of speciation change during the analysis should be avoided or minimized. Therefore, the method had to be rapid and not include time-consuming pretreatment steps.

The set objective has been achieved by the development of a CSV method described in Chapter 3 of this thesis. The use of XO as the complexing ligand, coupled with the catalytic enhancement due to NO_3^- leads to a highly selective method; the sensitivity attains 65 nA nM^{-1} min^{-1} for Cr(VI) in seawater. This compares extremely favourably with, for example, a reported sensitivity of 5.8 nA nM^{-1} min^{-1} attained with DTPA [101].

Speciation is achieved by the selective determination of Cr(VI) and total Cr as Cr(III) on the basis of the potential at which the analyte complex is deposited on the electrode. The reduction of Cr(VI) requires only SO_3^{2-} at pH 2 and is performed in the voltammetric cell. Hence there is no need for steps like heating/boiling, centrifugation, filtration, solvent extraction etc.; this is a notable asset in trace analysis as contamination risks are greatly lowered.

Some other important attributes of this method are:

1. the method is relatively rapid. A complete analysis for Cr(VI) and Cr(III) can generally be achieved within 1 hour.
2. the method involves almost no prior sample pretreatment and, with the exception of NO_3^- (the purification of which is easily done), only minute amounts of additional reagents are required.
3. the complete analytical procedure is performable on a clean bench.

4. Cr analysis is virtually interference free. Fe^{2+} can potentially interfere but, in seawater, $[Fe^{2+}]$ is too low to affect the determination; in surface waters, the effect of Fe interference can become serious and has to be accounted for.
5. the accuracy and precision of the method are very good. This stems from the fact that the method is electrochemical in nature and is based on the fundamental Faraday's Laws of electrolysis. Measurement of the two parameters that constitute the analytical signal, i.e., current and time (which is a directly related to the potential, the parameter actually displayed), can be made with a great degree of accuracy.

The successful application of this new method to the analysis of Cr in the N.W. Atlantic Ocean samples suggests that its performance is good at the lowest concentration levels likely to be encountered in natural aquatic systems.

Some observations made during the method development process are worthy of further investigation. XO is a very versatile ligand and under the proper experimental conditions, it is believed that it can be very efficient in the CSV determination of many metallic species. It has already been noted that Cu, Pb and Fe reduction peaks are obtained at pH ~ 7 (not optimized). Optimization of the various parameters (especially pH and E_{dep}) could lead to very sensitive methods for the determination of these metal ions.

CSV has now been established as a very sensitive analytical technique and analytical methods have been developed for numerous metal ions. With respect to sensitivity and ease of application, no other technique can compete with CSV. The challenge now facing proponents of CSV would be to develop analytical methods that would allow the simultaneous determination of several metals from the same aliquot sample. Elaboration of such analytical methods would find tremendous applications in environmental trace analysis and would without doubt help in making electroanalytical methods very competitive as compared to, e.g., spectrometric methods, the main asset of which remains their multi-element capability. Making CSV a truly multi-element technique is probably impossible but it is felt that the versatility of complexing ligands like XO could be very beneficially exploited for the simultaneous CSV determination of several elements.

A minor drawback of the method described in Chapter 3 is the interference brought about by Fe^{2+} on the determination of Cr, especially on Cr(VI). Even though, as discussed in Section 3.8.4.2, the interference is negligible in seawater (because of extremely low [Fe]) and in acidic surface waters, it would be worth investigating methods for eliminating this interference. Such an investigation would first need to address the nature of the interaction between Fe^{2+} and Cr, especially Cr(III), in the presence of XO.

In Chapter 4, an attempt is made to understand the mechanism of the processes leading to the appearance of the analytical signal. It has been shown that the adsorbed complex is a Cr^{III}-XO complex and that the analytical peak is due to a 1-electron reduction of this complex. In view of the complexity of the Cr-XO-NO_3^- system and despite the essentially qualitative nature of the arguments presented in Chapter 4, it is felt that, within the scope of this particular work, satisfactory conclusions have been reached. However, a more thorough study of the electrode processes need to be undertaken with a view to identifying the adsorbed species responsible for the analytical peak and the fate of the Cr species after the reduction on the electrode. The scope of such work could be extended to include some fundamental aspects of the voltammetry of systems like the one encountered in this particular case (i.e., cases where an adsorbed species is reduced and the resulting current is catalytically enhanced).

The synthesis of the polymeric Cr(II)-XO species invoked in Section 4.5 should be attempted and its properties investigated. It is believed that this compound will be very stable and inert to oxidation in air, unlike most other Cr(II) complexes.

REFERENCES

1 Wong, C.S.; Boyle, E.; Bruland, K.W.; Burton, J.D.; Goldberg, E.D., (Eds.). *Trace Metals in Seawater;* Plenum Press, New York, **1983**.

2 Moore, J.W.; Ramamoorthy, S. *Heavy Metals in Natural Waters*; Springer-Verlag, New York, **1984**.

3 Salbu, B.; Steinnes, E., (Eds.). *Trace Elements in Natural Waters*; CRC Press, **1995**.

4 Burton, J.D.; Statham, P. *Trace Metals in Seawater*, in Heavy Metals in the Marine Environment, Rainbow, P.S.; Furness, R.W., (Eds.). CRC Press, **1990**.

5 Bruland, K.W. *Trace elements in sea-water*, in Chemical Oceanography, Vol. 8, Riley, J.P.; Chester, R., (Eds.). Academic Press, London, **1983**.

6 Batley, G.E. *Trace Element Speciation: Analytical Methods and Problems*; CRC Press, **1989**.

7 Ure, A.M.; Davidson, C.M., (Eds.). *Chemical Speciation in the Environment*; Blackie, Glasgow, **1995**.

8 Florence, T.M.; Batley, G.E. *CRC Crit. Rev. Anal. Chem.* **1980**, *9*, 219-369.

9 Capodaglio, G.; Scarponi, G.; Toscano, G.; Barbante, C.; Cescon, P. *Fresenius J. Anal. Chem.* **1995**, *351*, 386-392.

10 Dundar, M.; Haswell, S. *Anal. Proc.* **1995**, *32*, 133-135.

11 Florence, T. M.; Batley, G. E. *Talanta* **1977**, *24*, 151-158.

12 Florence, T. M. *Talanta* **1982**, *29*, 345-364.

13 Florence, T. M. *Analyst* **1986**, *111*, 489-505.

14 Florence, T. M. *Analyst* **1992**, *117*, 551-553.

15 Frimmel, F. H.; Gremm, T. *Fresenius J. Anal. Chem.* **1994**, *350*, 7-13.

16 Hill, S.J. *Chem. Soc. Rev.* **1997** *26*, 291-298.

17 Van Loon, J. C.; Barefoot, R. R. *Analyst* **1992**, *117*, 563-570.

18 Donat, J.R.; Bruland, K.W. *Trace Elements in the Oceans*, in Salbu, B. and Steinnes, E. (Eds.), Trace Elements in Natural Waters; CRC, **1995**, page 247.

19 Cotton, F. A.; Wilkinson, G., Eds. *Advanced Inorganic Chemistry*, 3rd ed.; Interscience:, **1972**

20 Katz, S.A.; Salem, H. *The Biological and Environmental Chemistry of Chromium*; VCH, New York, **1994**.

21 Nriagu, J.O.; Nieboer, E. (Eds.). *Chromium in the Natural and Human Environments*; Wiley, **1988**.

22 Ottaway, J.M.; Fell, G.S. *Pure & Applied Chem.* **1986**, *58*, 1707-1720.

23 Farrell, R.A.; Judd, R.J.; Lay, P.A.; Dixon, N.E.; Baker, R.S.U.; Bonin, A.N. *Chem. Res. Toxicol.* **1989**, *2*, 227-229.

24 Bowen, H.J.M. *Environmental Chemistry of the Elements*; Academic Press, **1979**.

25 Fukai, R. *Nature* **1967,** *213*, 84.

26 Elderfield, H. *Earth Planet. Sci. Letts.* **1970**, *9*, 10-16.

27 Pettine, M.; Millero, F. J. *Limnol. Oceanogr.* **1990**, *35*, 730-736.

28 Moffett, J. W.; Zika, R. G. *Mar. Chem.* **1983**, *13*, 239-251.

29 Sperling, M.; Yin, X.; Welz, B. *Analyst* **1992**, *117*, 629-635.

30 Lan, C.R.; Tseng, C.; Yang, M. *Analyst* **1991**, *116*, 35-38.

31 Nakayama, E.; Kuwamoto, T.; Tokoro, H.; Fujinaga, T. *Anal. Chim. Acta* **1981**, *131*, 247-254.

32 Pik, A. J.; Eckert, J. M.; Williams, K. L. *Anal. Chim. Acta* **1981**, *124*, 351-356.

33 Cranston, R. E.; Murray, J. W. *Anal. Chim. Acta* **1978**, *99*, 275-282.

34 Ahern, F.; Eckert, J. M.; Payne, N. C. *Anal. Chim. Acta* **1985**, *175*, 147-151.

35 Vos, G. *Fresenius Z Anal Chem* **1985**, *320*, 556-561.

36 Boughriet, A.; Deram, L.; Wartel, M. *J. Anal. At. Spectrom.* **1994**, *9*, 1135-1142.

37 Peraniemi, S.; Ahlgren, M. *Anal. Chim. Acta* **1995**, *315*, 365-370.

38 Zou, H.; Xu.; Fang, Z. *Atomic Spectrom.* **1996**, *326*, 85-93.

39 de Jong, G. J.; Brinkman, U. A. T. *Anal. Chim. Acta* **1978**, *98*, 243-250.

40 Subramanian, K. S. *Anal. Chem.* **1988**, *60*, 11-15.

41 Beceiro-Gonzalez, E.; Bermejo-Barrera, A.; Barciela-Garcia, J.; Barceila-Alonso, C. *J. Anal. At. Spectrom.* **1993**, *8*, 649-653.

42 Mugo, R. K.; Orians, K. J. *Anal. Chim. Acta* **1993**, *271*, 1-9.

43 Pasullean, B.; Davidson, C. M.; Littlejohn, D. *J. Anal. At. Spectrom.* **1995**, *10*, 241-246.

44 Kubrakova, I.; Kudinova, T.; Formanovsky, A.; Kuz'min, N.; Tsysin, G.; Zolotov, Y. *Analyst* **1994**, *119*, 2477-2480.

45 Inoue, Y.; Sakai, T.; Kumagai, H. *J. Chromatogr.* **1995**, *706*, 127-136.

46 Sperling, M.; Xu, S.; Welz, B. *Anal. Chem.* **1992**, *64*, 3101-3108.

47 Marino, D. F.; Ingle, J. D. *Anal. Chem.* **1981**, *53*, 294-298.

48 Miyazaki, A.; Barnes, R. M. *Anal. Chem.* **1981**, *53*, 364-366.

49 Oktavec, D.; Lehotay, J.; Hornackova, E. *Atomic Spectroscopy* **1995**, *16*, 92-96.

50 Baffi, F.; Cardinale, A. M.; Bruzzone, R. *Anal. Chim. Acta* **1992**, *270*, 79-86.

51 Gammelgaard, B.; Jons, O.; Nielsen, B. *Analyst* **1992**, *117*, 637-640.

52 Isshiki, K.; Sohrin, Y.; Karatani, H.; Nakayama, E. *Anal. Chim. Acta* **1989**, *224*, 55-64.

53 Jen, J.; Ou-Yang, G.; Chen, C.; Yang, S. *Analyst* **1993**, *118*, 1281-1284.

54 Batley, G.E.; Matousek, J.P. *Anal. Chem.* **1980**, *52*, 1570-1574.

55 Vidal, J. C.; Sanz, J. M.; Castillo, J. R. *Fresenius J. Anal. Chem.* **1992**, *344*, 234-241.

56 Trojanowicz, M.; Pobozy, E.; Worsfold, P.J. *Anal. Letts.* **1992**, *92*, 1373-1387.

57 Eaton, A. *Geochim. Cosmochim. Acta* **1979**, *43*, 429-432.

58 Gao, R.M.; Zhou, Z.Q.; Yuan, D.X. *Talanta* **1993**, *40*, 637-640.

59 Pobozy, E.; Wojasinska, E.; Trojanowicz, M. *J. Chromatogr. A* **1996**, *736*, 141-150.

60 Beere, H. G.; Jones, P. *Anal. Chim. Acta* **1994**, *293*, 237-243.

61 Naghmush, A.M.; Pyrzynska, K.; Trojanowicz, M. *Anal. Chim. Acta* **1994**, *288*, 247-257.

62 Beaubien, S.; Nriagu, J.; Blowes, D.; Lawson. *Environ. Sci. Tecnnol.* **1994**, *28*, 730-736.

63 Gaspar, A.; Posta, J.; Toth, R. *J. Anal. At. Spectrom.* **1996**, *11*, 1067-1074.

64 Sule, P.A.; Ingle, J.D. *Anal. Chim. Acta* **1996**, *326*, 85-93.

65 Cespon-Romero, R.M.; Yebra-Biurrun, M.C.; Bermejo-Barrera, M.P. *Anal. Chim. Acta* **1996**, *327*, 37-45.

66 Posta, J.; Berndt, H.; Luo, S.; Schaldach, G. *Anal. Chem.* **1993**, *65*, 2590-2595.

67 Petrucci, F.; Alimonti, A.; Laszity, A.; Horvath, Z.; Caroli, S. *Can. J. Applied Spectros.* **1994**, *39*, 113-117.

68 Manzoori, J.L.; Shemirani, F. *J. Anal. At. Spectrom.* **1995**, *10*, 881-883.

69 Prokisch, J. *J. Chromatogr. A* **1994**, *683*, 253-260.

70 Powell, M.J. *Anal. Chem.* **1995**, *67*, 2474-2478.

71 Lintschinger, J. *Fresenius' J. Anal. Chem.* **1995**, *351*, 604-609.

72 Pantsar-Kallio, M; Manninen, P.K.G. *J. Chromatogr. A.* **1996**, *750*, 89-95.

73 Tomlinson, M.J.; Wang, J.; Caruso, J.A. *J. Anal. At. Spectrom.* **1994**, *9*, 957-964.

74 Pantsar-Kallio, M.; Manninen, P.K.G. *Anal. Chim. Acta* **1996**, *318*, 335-343.

75 van Raaphorst, J.C.; Haremaker, H.M.; Deurloo, P.A.; Beemsterboer, B. *Anal. Chim. Acta* **1994**, *286*, 291-296.

76 Nusko, R.; Heumann, K.G. *Anal. Chim. Acta* **1994**, *286*, 283-290.

77 Rai, D.; Sass, B.M.; Moore, D.A. *Inorg. Chem.* **1987**, *26*, 345-349.

78 Florence, T. M. *Proc. Royal Aust. Chem. Inst.* **1972**, *39*, 211-218.

79 Heyrovsky, J.; Kuta, J. *Principles of Polarography*, Academic Press, New York, **1966**.

80 Bond, A.M. *Modern Polarographic Methods in Analytical Chemistry*, Marcel Dekker, **1980**.

81 Willard, H.H.; Merritt, L.L.; Dean, J.A.; Settle, F.A. *Instrumental Methods of Analysis*, 7th ed.; Wadsworth Publishing Company, Belmont, California, **1988**, page 719.

82 Komarek, K. *Collect. Czech. Chem. Commun.* **1947**, *12*, 399-406.

83 Komarek, K. *Collect. Czech. Chem. Commun.* **1949**, *14*, 469-472.

84 Barker, G.C.; Bolzan, J.A. *Fresenius' Z. Anal. Chem.* **1966**, *216*, 215-238.

85 Pihlar, B.; Valenta, P.; Nurnberg, H. W. *Fresenius Z Anal Chem* **1981**, *307*, 337-346.

86 Fogg, A. G. *Anal. Proc.* **1994**, *31*, 313-317.

87 Wang, J. *Electroanalytical Chemistry*. **1989**, *16*, 1-88.

88 van den Berg, C. M. G. *Analyst* **1989**, *114*, 1527-1530.

89 Bersier, P. M.; Bersier, J. *Analyst* **1989**, *114*, 1531-1544.

90 van den Berg, C. M. G. *Anal. Chim. Acta* **1991**, *250*, 265-276.

91 Kalvoda, R.; Kopanica, M. *Pure Appl. Chem.* **1989**, *61*, 97-112.

92 Paneli, M. G.; Voulgaropoulos, A. *Electroanalysis* **1993**, *5*, 355-373.

93 Princeton Applied Research Corporation. *Application Brief C-2*, **1976**.

94 Tanaka, N.; Ito, T. *Bull. Chem. Soc. Japan* **1966**, *39*, 1043-1048.

95 Zarebski, J. *Chem. Anal. (Warsaw)* **1977**, *22*, 1037-1047.

96 Golimowski, J.; Valenta, P.; Nurnberg, H. W. *Fresenius Z Anal Chem* **1985**, 315-322.

97 Torrance, K.; Gatford, C.; *Talanta* **1987**, *3*, 939-944.

98 Scholz, F.; Lange, B.; Draheim, M.; Pelzer, J. *Fresenius J. Anal. Chem.* **1990**, *338*, 627-629.

99 Sarnaik, K. M.; Palrecha, M. M.; Dhaneshwar, R. G. *Electroanalysis* **1989**, *1*, 469-471.

100 Paneli, M.; Voulgaropoulos, A., V; Kalcher, K. *Mikrochim. Acta* **1993**, *110*, 205-215.

101 Boussemart, M.; van den Berg, C. M. G.; Ghaddaf, M. *Anal. Chim. Acta* **1992**, *262*, 103-115.

102 van den Berg, C. M. G.; Boussemart, M.; Yokoi, K.; Prartono, T.; Campos, M. L. A. M. *Mar. Chem.* **1994**, *45*, 267-282.

103 Boussemart, M.; van den Berg, C. *Analyst* **1994**, *119*, 1349-1353.

104 Wang, J.; Lu, J.; Olsen, K. *Analyst* **1992**, *117*, 1913-1917.

105 Elleouet, C.; Quentel, F.; Madec, C. *Anal. Chim. Acta* **1992**, *257*, 301-308.

106 Gao, Z.; Siow, K. S. *Electroanalysis* **1996**, *8*, 602-606.

107 Sato, H.; Yokoyama, Y.; Momoki, K. *Anal. Chim. Acta* **1977**, *94*, 217-220.

108 CRC Handbook of Chemistry and Physics, 7th ed., CRC Press, **1996**.

109 Bruland, K. W.; Franks, R. P.; Knauer, G. A.; Martin, J. H. *Anal. Chim. Acta* **1979**, *105*, 233-245.

110 Wu, Q.; Batley, G. *Anal. Chim. Acta* **1995**, *309*, 95-101.

111 Abdel-Hamid, R.; El-Sagher, H.; Rabia, M. K. *Can. J. Chem.* **1997**, *75*, 162-168.

112 Korbl, J.; Pribil, R.; Emr, A. *Collection Czechoslov. Chem. Commun.* **1957**, *22*, 961-966.

113 Wilkinson, G; Gillard, R.D.; McCleverty, J. *Comprehensive Coordination Chemistry*, Volume 2. Pergamon Press, **1987**, page 789.

114 Cheng, K. L.; Ueno, K.; Imamura, T., Eds. *Handbook of Organic Analytical Reagents*, 1st ed.; CRC: Boca Raton, 1988.

115 Pribil, R. *Analytical Applications of EDTA and Related Compounds*, Vol. 52 in International Series of Monographs in Analytical Chemistry, Pergamon, **1972**.

116 Bishop, E. *Indicators*, Vol. 51 in International Series of Monographs in Analytical Chemistry, Pergamon, **1972**, page 358.

117 Valcl, O.; Nemcova, I.; Suk, V. *Handbook of Triarylmethane Dyes: Spectrophotometric Determination of Metals*. CRC, Boca Raton, **1985**.

118 Otomo, M. *Bunseki Kagaku* **1972**, *21*, 436-445. Chem. Abst. 76:161776 (in Japanese; as quoted in Ref. 111).

119 IUPAC Chemical Data Series - No. 22. *Stability Constants of Metal-ion Complexes, Part B: Organic Ligands*, Pergamon, **1979,** page 1175.

120 Tonosaki, K.; Otomo, M.; Tanaka, K. *Bunseki Kagaku* **1966**, *15*, 683-686.

121 Niki, K.; Yamada, A.; Tanaka, N.; Itabashi, E.; Hartford, W. H. In *Encyclopedia of Electrochemistry of the Elements*; Bard, A. J., Ed.; M.Dekker: New York, 1986; Vol. IX B, Chapter IXb-4.

122 Tanaka, N.; Kano, T.; Ogino, H.; Yamada, A. *Bull. Chem. Soc. Japan* **1974**, *47*, 3064-3067.

123 Osteryoung, J. G.; Schreiner, G. M. *CRC Crit. Rev. Anal. Chem.* **1988**, *19*(Suppl. 1), s1-s27.

124 Osteryoung, J. G.; Osteryoung, R. A. *Anal. Chem.* **1985**, *57*, 101A-110A.

125 Osteryoung, J.; O'Dea, J. J. In *Electroanalytical Chemistry*; Bard, A. J., Ed.; Dekker: New York, 1986; Vol. 19, pp. 209-308.

126 Skoog, D.A.; Leary, J.J. *Principles of Instrumental Analysis*, 4th ed.; Saunders College Publishing, **1992**, page 556.

127 Harris, D.C. *Quantitative Chemical Analysis*, 3rd ed.; Freeman, New York, **1991**, page 479.

128 Ramaley, L.; Krause.MS. *Anal. Chem.* **1969**, *41*, 1362-1364.

129 O'Dea, J. J.; Osteryoung, J.; Osteryoung, R. A. *Anal. Chem.* **1981**, *53*, 695-701.

130 O'Dea, J. J.; Osteryoung, J. G. *Anal. Chem.* **1997**, *69*, 650-658.

131 O'Dea, J. J.; Osteryoung, J.; Osteryoung, R. A. *J. Phys. Chem.* **1983**, *87*, 3911-3918.

132 Vukomanovic, D. V.; vanLoon, G. W. *Talanta* **1994**, *41*, 387-394.

133 Miyazaki, A.; Barnes, R. M. *Anal. Chem.* **1981**, *53*, 299-304.

134 Stollenwerk, K. G.; Grove, D. B. *J. Environ. Qual.* **1985**, *14*, 396-399.

135 Pavel, J.; Kliment, J.; Suter, O. *Fresenius Z Anal Chem* **1985**, *321*, 587-591.

136 Luther, G. W.; Swartz, C. B.; Ullman, W. J. *Anal. Chem.* **1988**, *60*, 1721-1724.

137 Yokoi, K.; Van den Berg, C. M. G. *Electroanalysis* **1992**, *4*, 65-69.

138 Cosovic, B.; Vojvodic, V. *Limnol. Oceanogr.* **1982**, *27*, 361-369.

139 Van Den Berg, C. M. G. *J. Electroanal. Chem.* **1986**, *215*, 111-121.

140 Quentel, F.; Madec, C. *Anal. Chim. Acta* **1990**, *230*, 83-90.

141 Sharp, J. H. *Mar. Chem.* **1997**, *56*, 265-277.

142 Carlson, C. A.; Ducklow, H. W.; Michaels, A. F. *Nature* **1994**, *371*, 405-408.

143 van den Berg, C. M. G.; Huang, Z. Q. *J. Electroanal. Chem.* **1984**, *177*, 269-280.

144 Lu, J.; Wang, J.; Yarnitzky, C. *Electroanalysis* **1995**, *7*, 79-82.

145 Wang, J.; Mannino, S. *Analyst* **1989**, *114*, 643-645.

146 van den Berg, C. M. G.; Nimmo, M.; Abollino, O.; Mentasti, E. *Electroanalysis* **1991**, *3*, 477-484.

147 Cheng, K. L. *Talanta* **1959**, *2*, 61-66.

148 Landing, W. M.; Bruland, K. W. *Geochim. Cosmochim. Acta* **1987**, *51*, 29-43.

149 Martin, J. H.; Gordon, R. M.; Fitzwater, S. E. *Limnol. Oceanogr.* **1991**, *36*, 1793-1802.

150 Bruland, K. W.; Orians, K. J.; Cowen, J. P. *Geochim. Cosmochim. Acta* **1994**, *58*, 3171-3182.

151 Kemula, W. *Pure Appl. Chem.* **1967**, *15*, 283-296.

152 Wang, J.; Ariel, M. *J. Electroanal. Chem.* **1977**, *85*, 289-297.

153 Sipos, L.; Nurnberg, H. W.; Valenta, P.; Branica, M. *Anal. Chim. Acta* **1980**, *115*, 25-42.

154 Jagner, D. *Anal. Chim. Acta* **1979**, *105*, 33-41.

155 Steeman, E.; Temmerman, E.; Verbinnen, R. *Anal. Chim. Acta* **1978**, *96*, 171-181.

156 Wang, J.; Freiha, B. A. *Talanta* **1983**, *30*, 837-840.

157 Wang, J.; Freiha, B. A. *Anal. Chim. Acta* **1983**, *148*, 79-85.

158 Lazar, B.; Ben-Yaakov, S. *J. Electroanal. Chem.* **1980**, *108*, 143-151.

159 Wang, J.; Dewald, H. D. *Anal. Chem.* **1984**, *56*, 156-159.

160 Djogic, R.; Branica, M. *Anal. Chim. Acta* **1995**, *305*, 159-164.

161 Whang, C.W.; Page, J. A.; vanLoon, G. *Anal. Chem.* **1984**, *56*, 539-542.

162 Kalcher, K.; Jorde, C. *Comput. Chem.* **1986**, *10*, 201-218.

163 Pizeta, I.; Jeren, B.; Aleksic-Maslac, K. *J. Electroanal. Chem.* **1994**, *375*, 169-174.

164 Lanza, P.; Zappoli, S. *Anal. Chim. Acta* **1986**, *185*, 219-228.

165 Wang, J.; Greene, B. *Anal. Chim. Acta* **1982**, *144*, 137-145.

166 Murray, J.W.; Spell, B.; Paul, B. *The contrasting geochemistry of manganese and chromium in the Eastern Pacific Ocean*, in Wong, C.S.; Boyle, E.; Bruland, K.W.; Burton, J.D.; Goldberg, E.D., (Eds.). *Trace Metals in Seawater;* Plenum Press, New York, **1983**. pages 643-669.

167 Campbell, J. A.; Yeats, P. A. *Earth Planet. Sci. Lett.* **1981**, *53*, 427-433.

168 Kieber, R. J.; Helz, G. R. *Environ. Sci. Technol.* **1992**, *26*, 307-312.

169 Grimaud, D.; Michard, G. *Mar. Chem.* **1974**, *2*, 229-237.

170 Cranston, R. E. *Mar. Chem.* **1983**, *13*, 109-125.

171 Jeandel, C.; Minster, J. F. *Global Biogeochem. Cycles* **1987**, *1*, 131-154.

172 Sherrell, R. M.; Boyle, E. A. *Deep-Sea Res.* **1988**, *35*, 1319-1334.

173 Budesinsky, B. W.; Svec, J. *Anal. Chim. Acta* **1972**, *61*, 465-473.

174 Tanaka, N.; Ebata, k. *J. Electroanal. Chem.* **1964**, *8*, 120-126.

175 Bustin, D. I.; Earley, J. E. *J. Am. Chem. Soc.* **1967**, *89*, 1818-1822.

176 Rubel, S.; Golimowski, J.; Wojciechowski, M. *Chem. Anal. (Warsaw)* **1974**, *19*, 41-52.

177 Westheimer, F. H. *Chem. Rev.* **1949**, *45*, 419-451.

178 Wilkinson, G; Gillard, R.D.; McCleverty, J. *Comprehensive Coordination Chemistry*, Volume 3. Pergamon Press, **1987**, page 927.

179 Lanza, P.; Taddia, M. *Anal. Chim. Acta* **1984**, *157*, 37-44.

180 Cantagallo, M.I.C.; De Sousa, M.A. *J. Radioanal. Nuclear Chem.* **1997**, *218*, 117-118.

181 Cantagallo, M. I. C.; Bertotti, M. B.; Gutz, G. R. *Electroanalysis* **1994**, *6*, 1107-1114.

182 Edmonds, T. E. *Anal. Chim. Acta* **1980**, *116*, 323-333.

183 Farias, P.A.M.; Ohara, A.K.; Nobrega, A.W.; Gold, J.S. *Electroanalysis* **94** , *6*, 333-339.

184 Petrovska-Jovanovic, S.; Stojanova, K.; Jakimovic, V. *Anal. Letts.* **1997**, *30*, 1923-1938.

185 Neto, M.M.P.M.; Rocha, M.M.G.S.; Brett, C.M.A. *Talanta* **1994**, *41*, 1597-1601.

186 Quentel, F.; Elleouet, C.; Madec, C. *Electroanalysis* **1994**, *6*, 683-688.

187 Culjak, I.; Mlakar, M.; Branica, M. *Electroanalysis* **1995**, *7*, 64-69.

188 Vega, V.; van den Berg, C. M. G. *Anal. Chem.* **1997**, *69*, 874-881.

189 Nicholson, R. S.; Shain, I. *Anal. Chem.* **1964**, *36*, 706-723.

190 Southampton Electrochemistry Group. *Instrumental Methods in Electrochemistry*; Ellis-Horwood, Chicester, **1985**.

191 Brown, E.R.; Sandifer, J.R. *Cyclic Voltammetry, AC Polarography, and related techniques* , in Rossiter, B.W.; Hamilton, J.F. (Eds.). Physical Methods of Chemistry, Volume 2 - Electrochemical Methods, Wiley, New York, **1986**.

192 Nicholson, R. S.; Shain, I. *Anal. Chem.* **1965**, *37*, 178-190.

193 Wopschall, R. H.; Shain, I. *Anal. Chem.* **1967**, *39*, 1527-1534.

194 Tanaka, N.; Sato, G. *Nature* **1963**, *197*, 176-177.